Aus der Medizinischen Klinik und Poliklinik IV der Ludwig-Maximilians-Universität

München

Direktor: Prof. Dr. med. Martin Reincke

Engineered Mesenchymal Stem Cells In Tumor Therapy: A Comparison Of Three Targeting Strategies

Dissertation

zum Erwerb des Doktorgrades der Medizin

an der Medizinischen Fakultät

der Ludwig-Maximilians-Universität München

vorgelegt von

Anna Maria Hagenhoff

aus München

2018

Mit Genehmigung der Medizinischen Fakultät

der Universität München

Berichterstatter:	Prof. Dr. Peter Jon Nelson
Mitberichterstatter:	PD Dr. Clemens Gießen-Jung
	Dr. Thomas Grünewald
Mitbetreuung durch den promovierten Mitarbeiter:	PD Dr. Dr. med. Irene Teichert-von Lüttichau
Dekan:	Prof. Dr. med. dent. Reinhard Hickel
Tag der mündlichen Prüfung:	26.04.2018

Table of contents

Publications

The results of this doctoral thesis have been featured in the following publications:

Hagenhoff A., Bruns C.J., Zhao Y., von Luettichau I., Niess H., Spitzweg C., Nelson P.J.: **"Harnessing mesenchymal stem cell homing as an anticancer therapy."** *Expert Opinion On Biological Therapy* **16**(9): 1079-1092.

Müller A.M., Schmohl K.A., Knoop K., Schug C., Urnauer S., Hagenhoff A., Clevert D.A., Ingrisch M., Niess H., Carlsen J., Zach C., Wagner E., Bartenstein P., Nelson P.J., Spitzweg C.: "**Hypoxia-targeted 131I therapy of hepatocellular cancer after systemic mesenchymal stem cell-mediated sodium iodide symporter gene delivery."** *Oncotarget* **7**(34): 54795-54810.

Zusammenfassung

Krebserkrankungen rangieren nach wie vor unter den drei häufigsten Todesursachen der Welt. Gleichzeitig steigt die Lebenserwartung in den Industrieländern stetig, sodass die Notwendigkeit besteht neue Therapieansätze zu entwickeln, die einerseits die Überlebensrate verbessern und andererseits die oft erheblichen Nebenwirkungen der Krebstherapie reduzieren. Elementarer Bestandteil dieses Bestrebens ist es die Krebstherapie weiter zu individualisieren. Mesenchymale Stammzellen (MSC) aus dem Knochenmark besitzen eine starke Neigung dazu malignes Gewebe aufzuspüren und das Tumorstroma zu infiltrieren. Daher bieten sie eine Möglichkeit den Tumor gezielt zu attackieren. Durch genetische Manipulation der MSC kann es gelingen jede Tumorart auf eine individuelle Art und Weise anzugreifen.

Das Ziel der vorliegenden Arbeit war es, die MSC mit einem therapeutischen Gen auszustatten, welches sich gezielt gegen das Tumorstroma richtet. Dazu wurden drei verschiedene Strategien untersucht: das inflammatorische Milieu des Stromas speziell anhand der Über-Expression von chemokine-ligand 5 (CCL5/Rantes) anzugreifen, die hypoxischen Areale eines schnell wachsenden Tumors zu nutzen oder letztlich, um einen Weg zu finden das therapeutische Gen in den MSC von extern zu aktivieren, einen Hyperthermie-sensiblen Promoter einzusetzen. Vorangegangene Arbeiten dieser Arbeitsgruppe bewiesen im Mausmodell den Nutzen einer Therapie mit MSC, welche CCL5/Rantes-gesteuert eine Thymidinkinase des Herpes-Simplex-Virus exprimierten. Anfängliche Experimente dieser Arbeit zielten darauf ab diese CCL5/Rantes-Überexpression der das Tumorstroma infiltrierenden MSC zu verstehen. Dabei stellte sich heraus, dass eine Kombination aus mehreren inflammatorischen Zytokinen, in der Hauptsache Tumor-Nekrose-Faktor-α, Interleukin-1β und Interferon-γ, dafür verantwortlich ist, nicht jedoch die in einem wachsenden Tumor vorherrschende Hypoxie. Letztere sorgt lediglich für eine Überexpression des Transkriptionsfaktors HIF-1α (hypoxia-inducible factor 1α) durch MSC. Daher wurde im Folgenden ein Konstrukt entwickelt, welches die Expression eines Reportergens, in diesem Fall die Firefly Luciferase (pGL3-hypxia-luc) beziehungsweise das mCherry Fluoreszenzprotein (pGL3-HIF-Cherry), unter die Kontrolle eines HIF-1α-sensiblen Promoters stellt. Um die Machbarkeit eines solchen Ansatzes in der Therapie mit MSC nachzuweisen, wurden als *in vitro*-Modell Tumorsphäroide aus humanen Leberzellkarzinomzellen herangezüchtet. In Co-Kultur mit MSC, welche zuvor mit dem oben genannten Konstrukt pGL3-HIF-Cherry stabil transfiziert worden waren, zeigte sich, dass letztere die Fähigkeit besitzen in die Tumorsphäroide einzuwandern und im hypoxischen Zentrum das

gewünschte Gen zu exprimieren. Um der Möglichkeit einer externen Aktivierung des Expressionsgens nachzugehen, wurde ein weiteres Konstrukt entworfen, welches anstelle eines HIF-1α-sensitiven Promotors den endogenen HSP70b-Promotor aus der Familie der Heat-Shock-Proteine trägt. Durch Exposition der transfizierten MSC gegenüber einem Temperaturanstieg auf 42° Celsius ließ sich *in vitro* eine deutliche Überexpression des Reportergens erzielen.

Diese Arbeit erbringt den Nachweis, dass die genetische Manipulation mesenchymaler Stammzellen aus dem Knochenmark zum Zwecke eines zielgerichteten Angriffs auf das Tumorstroma eine gute Möglichkeit darstellt, die Tumortherapie weiter zu individualisieren.

Summary

Malignant diseases range among the top three causes of death worldwide. With increasing overall life expectancies, the need for individually tailored, tumor-specific therapies with less detrimental side effects than conventional radio- or chemotherapy is rising. Mesenchymal stem cells (MSC) possess an innate tropism for the tumor microenvironment, which resembles a chronic wound. This has rendered them a flexible, reliable tool for the delivery of therapeutic agents to sites of malignant growth.

The goal of the present study was to study different approaches for the engineering of MSC to specifically induce the expression of transgenes within tumor microenvironments. To this end, three gene promoter systems, that become activated through different mechanisms, were investigated: inflammatory induction of the gene promoter for chemokine ligand 5 (CCL5/Rantes), the transcriptional response to tumor hypoxia using a synthetic promoter, and finally, the induced expression of transgenes via heat-shock responsive gene promoters following the external application of hyperthermia. Previous work by our group has shown the general efficacy of Rantes/CCL5-driven herpes simplex thymidine kinase expressed by MSC infiltrating the tumor stroma. Preliminary experiments revealed that CCL5-expression by MSC in the tumor stroma is triggered by a combination of inflammatory cytokines, especially TNF-α, IL-1β and γ-IFN. Hypoxia, a prominent feature of growing solid tumors, was shown here not to promote CCL5-expression. Hypoxia-inducible factor 1α (HIF-1α) is expressed by MSC in a hypoxia-dependent manner, as confirmed by *in vitro* experiments. Thereupon, a reporter plasmid was designed that contained a HIF-1α-responsive promoter driving a firefly luciferase (pGL3-hypoxia-luc) or mCherry fluorescent protein (pGL3-HIF-Cherry). For proof of concept in this study, an *in vitro* model was developed by establishing tumor spheroids from the human hepatocellular carcinoma (HCC) cell line Huh7. Upon co-culture, MSC stably transfected with the pGL3-HIF-Cherry construct invaded the Huh7 spheroids and expressed the Cherry fluorescent protein once they had reached the hypoxic center of the tumor spheroid. With regards to clinical applicability and incorporation of this novel therapeutic concept into existing treatment regimens, an additional construct was designed such that MSC express a reporter or therapeutic gene using a hyperthermia-responsive promoter, namely, the endogenous HSP70b-promoter. It was strongly induced in MSC exposed to heat shock (42°Celsius) *in vitro.*

This study expands our options for the engineering of MSC to express therapeutic transgenes directed at the tumor microenvironment.

1 Introduction

1.1 Mesenchymal Stem Cells

Mesenchymal stem cells (MSC) have generated scientific interest in recent years. Their role in tissue (re-)generation has led to numerous publications highlighting their therapeutic potential in diverse medical specialties. What has emerged is that MSC possess unique qualities.

MSC are defined by the International Society for Cellular Therapy as plastic-adherent cells that are capable of differentiation into osteoblasts, adipocytes and chondrocytes upon adequate stimulation *in vitro,* and express a set of cell surface markers, including CD105, CD73 and CD90, while simultaneously lacking expression of CD45, CD34, CD14 or CD11b, CD79α or CD19, as well as HLA-DR antigens (Casazza 2014). This combination of expressed proteins can be found on a range of cells and a distinctive surface marker for MSC remains to be identified (Rastegar 2010). MSC have been successfully isolated from almost every type of tissue, including brain, liver, blood and adipose tissue, mostly in the form of resident stem cells. A large source of undifferentiated MSC is found in the bone marrow, although MSC make up as little as 0.001-0.01% of cells (Rastegar 2010) in the average bone marrow aspirate. Numerous study groups have subsequently identified cell surface markers and cytokine receptor profiles for stem cell populations originating from diverse tissues. It was shown that MSC from different tissues can differ in their molecular characteristics (Lazennec 2008, Rastegar 2010, Sivasubramaniyan 2012). What appears common is that MSC lack expression of major histocompatibility complex type II (MHCII)-molecules as well as co-stimulatory ligands CD40, CD80 and CD86 (Rastegar 2010). This aspect of MSC biology is of particular significance, as it renders these cells invisible to immune surveillance by circulating T-cells and thus suitable for allogenic transplantation without the need for immunosuppression (Le Blanc 2005, Chamberlain 2007, Yagi 2010). Interestingly, Le Blanc *et al* (2005) have reported that MHCII can be detected in MSC lysates, suggesting that MSC possess intracellular stores of MHCII that may be mobilized and expressed on to the cell surface (Hagenhoff 2016).

The ability of MSC to escape detection and elimination by the host immune system in the context of allogenic transplantation, has focused interest on their potential role in immunomodulation. A large body of reports has shed light on the often ambivalent functions of MSC in this regard. For example, to tie in with the aforementioned MHCII-expression, it has been established that MHCII surface

expression is generally γ-IFN-dependent. γ-IFN is a proinflammatory cytokine, and while low levels induce MHCII surface expression, high levels of γ-IFN, for example during inflammation, can suppress MHCII expression and may then prevent MSC from functioning as antigen-presenting cells (Chan 2006, Sheng 2008). Furthermore, MSC have been reported to suppress the function of both naïve and memory T-lymphocytes through their secretion of soluble factors (Krampera 2003, Rastegar 2010, Yagi 2010, Klopp 2011). This is supported by numerous publications that describe an immune suppressive effect of MSC in the treatment of Graft-versus-Host-Disease (GvHD) following allogenic stem cell transplantation (Le Blanc 2004, Le Blanc 2008, Wernicke 2011). Other groups have described the influence of MSC on B-lymphocytes and have shown that co-culture leads to cell cycle arrest and reduced expression of chemotactic cytokines in B-cells (Corcione 2006). The overall immunosuppressive effect of MSC is also discussed to play a major role in tumor initiation and preservation (Klopp 2011).

An important trait of MSC is their innate tropism for injured tissue. Through underlying mechanisms that have yet to be fully understood, MSC have the ability to home to sites of injury, including tumors. When injected intravenously or locally in mouse models bearing injuries or tumors, MSC are recruited to the injured tissue with remarkable specificity. Healthy, uninjured tissue does not generally provide the stimuli for MSC to migrate into the tissue, however some tissue specific homing is seen in the heathy mouse. Fluorescently or otherwise labelled MSC, injected intravenously in healthy mice have been shown to accumulate in lymphatic tissue, for example lymphnodes, but also spleen, gut, and skin, as well as the lung. It is assumed that homing to lung and spleen may be mainly due to entrapment of the cells in the microvasculature, while an involvement of chemokine-mediated recruitment is thought to be responsible for their migration to the other tissues potentially as part of normal tissue homeostasis (Studeny 2004, von Luettichau 2005, Chamberlain 2007). The molecular basis of MSC homing is thought to resemble that seen during leukocyte recruitment (Yagi 2010). The CXCR4-SDF1/CXCL12-has been proposed to play a role in MSC recruitment. Stromal-derived-factor 1 (SDF-1) is induced at sites of injury, especially in ischemic tissue in a HIF1-dependent manner (Ceradini 2004). The corresponding chemokine receptor, CXCR4, is expressed on CD34-negative bone marrow-derived progenitor cells. However, reports differ over the extent of CXCR4-expression on the surface of these cells, as several groups have reported low cell surface expression of the receptor combined with high intracellular expression. These findings suggest that CXCR4 is expressed on the cell surface of MSC after

stimulation in situations of injury (von Luettichau 2005, Chamberlain 2007, Yagi 2010). More recent studies suggest that MSC homing to gliomas may also be TGF-β1-dependent (Shinojima 2012).

MSC homing has been identified in various situations of injury and malignant growth. For example, cardiac as well as cerebral ischemic injury can stimulate MSC to migrate towards the damaged tissue. Treatment of patients with myocardial infarction or middle cerebral artery infarcts in clinical trials has led to significantly improved outcome (Rastegar 2010). In paraplegic mouse models, MSC have been found to promote recovery by bridging the injury in the spinal cord and secreting growth factors and other paracrine factors (Hofstetter 2002). Skin defects and chronic inflammatory diseases such as Morbus Crohn have also been targets for treatment with MSC in experimental settings (Mansilla 2005, Chamberlain 2007, Rastegar 2010).

Tumors resemble chronic wounds in certain key aspects (Dvorak 1986). During wound healing, cytokine crosstalk leads to the proliferation of fibroblasts, endothelial and epithelial cells, and the recruitment of MSC to the site of injury leads to tissue regeneration. Tumors are thought to be seen by the body as chronic wounds that drive continuous repair. The body reacts by providing a growth-stimulating environment for the tumor, the tumor stroma (Dvorak 1986, Karnoub 2007, Barcellos-de-Souza 2013). It has been shown that MSC play a key role in this process. They are recruited by signals sent from the tumor microenvironment, migrate towards the tumor and integrate into the tumor stroma (Hall 2007, Spaeth 2009, Kidd 2012). The tumor types shown to actively recruit MSC include gastrointestinal tumors such as colon or pancreatic cancer (Shinagawa 2010, Bao 2012, Shinagawa 2012, De Boeck 2013), gynecological tumors such as breast or ovarian cancer (Karnoub 2007, Dembinski 2013), gliomas (Shinojima 2012) and melanomas (Studeny 2004, Hagenhoff 2016).

The differentiative capacity of MSC, however, is not the only feature that renders these cells vital in wound healing. MSC have been shown to be involved in all three phases of wound healing: inflammation, proliferation and remodeling (Maxson 2012). While anti-inflammatory signaling helps progressing from active to healing wound in an early stage, the secretion of matrix metalloproteases (MMP) and growth factors such as vascular endothelial growth factor (VEGF), platelet-derived growth factor (PDGF) or hepatocyte growth factor (HGF) helps regulate angiogenesis and tissue repair (Gnecchi 2008, Maxson 2012). During formation of tumor stroma, tumor- or cancer-associated fibroblasts (TAF or CAF) have been identified to play a central role. TAF are thought to originate either from the bone marrow or from tissue resident cells (Hall 2007, Spaeth 2009, Quante 2011). Kidd *et al.* have distinguished two types of TAF within the tumor microenvironment: an α-

SMA (α-smooth muscle actin) positive cell type that derives from adipose tissue, and an FAP (fibroblast-activating protein) and FSP (fibroblast-specific protein) positive cell type thought to originate from bone-marrow derived stem cells (Kidd 2012). In addition to their expression of fibroblast markers FSP, FAP and myofibroblast-associated proteins such as α-SMA, TAF are also characterized by expression of MMP-3 and SL-1, and tumor-supportive soluble factors such as IL-6, VEGF, HGF and TGF-β. Growth factors such as HGF, EGF and IL-6 are also thought to be secreted by MSC during their conversion into TAF, suggesting a role for autocrine stimulation (Spaeth 2009). In short, these findings suggest that TAF develop from MSC and promote tumor growth via vascular support, contribution to tumor stroma and immunosuppression. Another aspect of MSC or TAF in tumor biology is their suspected role in metastasis. MSC-secreted CCL5 was suggested to help promote the metastatic potential of breast cancer cells (Karnoub 2007). EMT, epithelial-mesenchymal transition, has been linked to cancer metastasis. MSC have been shown to down-regulate the expression of E-cadherin in favor of N-cadherin in breast cancer cells, a process that is essential to EMT (Klopp 2010, Klopp 2011, Hagenhoff 2016).

The identification of a central role of MSC in tumor biology has led to their development as a tool for cancer therapy. Based on their tropism for tumors, MSC have been exploited as vehicles for the delivery of anti-cancer agents deep into tumor environments (Hagenhoff 2016). A range of strategies have shown efficacy in preclinical models. Studeny *et al* engineered MSC to constitutively express β-IFN, an anti-proliferative cytokine, and injected the engineered cells intravenously into mice bearing melanomas. As a result, the intra-tumor concentration of β-IFN that was sufficient to create an anti-tumor effect was achieved with tolerable serum levels of the cytokine, a clear advantage as compared to systemic β-IFN therapy (Studeny 2002). Sasportas *et al* used MSC expressing TRAIL (tumor necrosis factor related apoptosis inducing ligand), a cytokine that induces apoptosis in cancer cells, to treat mice bearing highly malignant glioblastomas (Sasportas 2009). Miletic *et al* injected MSC secreting herpes simplex virus thymidine kinase (HSV-TK) into the vicinity of tumors in mice (Miletic 2007). HSV-TK is capable of phosphorylating and thus activating ganciclovir, a prodrug that was administered later. When phosphorylated, ganciclovir is a toxic metabolite that induces cell death and kills surrounding cells through a bystander effect (Van Dillen 2002). Previous work by our group focused on evaluation of MSC-based delivery of this suicide gene HSV-TK to solid tumors in a tissue-specific manner, such that expression would be enhanced in MSC that had successfully infiltrated the tumor stroma. To this end, MSC were engineered to express HSV-TK under the control of the Tie-2-promoter/enhancer. This allowed for a selective targeting in

response to the angiogenic state of the tumor stroma, as the MSC respond to angiogenic signals. The Tie-2 gene encodes an angiopoietin receptor tyrosine kinase that is upregulated in growing tumors to promote angiogenesis (Conrad 2011). A slightly different approach focused on use of the CCL5 promoter to drive transgene expression. As was detailed above, CCL5 is upregulated by MSC in the tumor stroma as the cells respond to tumor signals. The CCL5-HSV-TK engineered MSC were shown to infiltrate the tumor stroma, induce expression of the suicide gene and to reduce tumor size in mice bearing metastasized pancreatic carcinoma (Zischek 2009, Hagenhoff 2016). The CCL5 promoter has been subsequently used in a similar experimental setting that relied on use of the sodium iodide symporter (NIS), derived from follicular cells of the thyroid gland, to replace the HSV-TK suicide gene. The engineered MSC express the NIS protein once they reach the tumor stroma and thus allow efficient radioiodine uptake and reduced growth of hepatocellular carcinoma in mice (Knoop 2013).

1.2 Tumor Stroma: Characterization

As detailed above, Dvorak postulated in 1986 that tumors act essentially as chronic wounds (Dvorak 1986). To date, chronic inflammation is seen as one of the main pillars of cancerogenesis (Aldinucci 2014, Borsig 2014). This has led to increased focus on the tissue surrounding the tumor, the tumor stroma. The tumor microenvironment is divided into three compartments: The cancer cells themselves, which reside within a surrounding milieu that acts as a defensive structure with tissue integrity. The second component is comprised of benign cells, mainly fibroblasts, endothelial cells, immune cells and MSC. Finally, the extracellular matrix (ECM) is seen as the third component. The ECM consists of structural proteins like collagen or proteoglycans and specialized proteins like fibronectin and matrix-metalloproteinases (MMP), which are responsible for remodeling the ECM (Bremnes 2011).

The tumor stroma is of vital importance for the progression of solid tumors. Cytokine crosstalk between cancer and non-malignant cells helps dictate a course towards proliferation. The switch from normal tissue stroma to tumor stroma is initiated by the tumor cells. Fibroblasts play a key role in this regard (Bremnes 2011, Borsig 2014). In normal tissues, fibroblasts are usually in a quiescent state. Upon disruption of the tissue equilibrium, as is the case during injury or inflammation, the resident fibroblasts are activated and begin secreting growth factors and producing components of ECM. As soon as the wound has healed, most fibroblasts undergo apoptosis (Desmouliere 1995, Silzle 2004). Correspondingly, tumor stroma is a blur of fibroblast activity but here the fibroblasts do

not undergo apoptosis, but instead develop into TAF (please refer to chapter 1.1) that continue to promote tumor proliferation. TAF release pro-fibrotic growth factors, such as TGF-β (transforming growth factor β), PDGF, FGF-2 (fibroblast growth factor 2) and VEGF. VEGF is a key player in growing tumors, as it helps provide an adequate oxygen supply by inducing neovascularization, and at the same time reinforces the process of fibroblast activation by increasing vascular permeability for plasma proteins such as fibrin, which in turn attracts more fibroblasts and inflammatory cells to the tumor site (Brown 1999, Bremnes 2011). TGF-β is thought to be an important activator of stromal fibroblasts. It is secreted both by cancer cells, and activated fibroblasts, in an autocrine loop that maintains and strengthens TGF-β-induced differentiation of fibroblasts into activated myofibroblasts. Ironically, while TGF-β-signaling has been linked to poor outcome in cancer, it was originally characterized as an anti-proliferative cytokine. One explanation for this paradox is that while cancer cells are able to switch off key components of the anti-proliferative TGF-β pathway, the tumor stroma remains responsive to TGF-β signaling. TGF-β secretion by cancer cells not only results in the activation of resident tissue fibroblasts, but also in the differentiation of bone marrow-derived MSC into TAF. In addition, cancer cell-derived TGF-β is thought to induce MMP secretion by TAF, which is responsible for ECM remodeling and thus enhanced invasiveness of the tumor stroma (Bremnes 2011, Calon 2014).

The tumor stroma is a complex environment where cancer cells communicate with resident tissue cells as well as cells that have been recruited into the stroma. Communication is established by direct cell-cell contact and, more importantly, by secretion of soluble factors. Key players in this cytokine crosstalk include TGF-β, VEGF or PDGF. An active tumor stroma is associated with tumor growth, angiogenesis, invasiveness and metastasis.

Previous work by our group has focused on the biology of chemokines, a class of chemotactic cytokines that induce the directed migration of cells. Chemokines can be produced in response to cytokines such as tumor necrosis factor α (TNF-α) or TGF-β. Cells that possess the necessary chemokine receptors can migrate along a gradient towards the site of increased chemokine expression. These cells include lymphocytes, macrophages, dendritic cells, MSC or resident parenchymal tissues. During inflammation, a set of inflammatory chemokines, such as CCL5 (CC-ligand 5) or CCL2, helps direct leukocyte trafficking towards the site of injury. In lymphoid tissues, homeostatic chemokines, such as CXCL12 or CCL19, are constitutively expressed and help direct the

trafficking and organization of resident leukocytes (Borsig 2014). In tumors, chemokines can act as growth factors, they can help promote angiogenesis and have been linked to metastasis.

1.2.1 RANTES

The RANTES/CCL5 chemokine was first described as a chemokine expressed by T-cells. The name RANTES stands for "regulated on activation, normal T-cell expressed and secreted" (Von Luettichau 1996). Over time, it has become apparent that CCL5 can be expressed by a wide range of cells, including macrophages, fibroblasts and MSC (Nelson 1993, Soria 2008). NF-κB is often involved in CCL5 up-regulation (Nelson 1993). CCL5 is a ligand for the chemokine receptors CCR1, CCR3 and CCR5. CCL5 has been shown to help drive the inflammatory response through recruitment of leukocytes. As inflammation is a hallmark of cancer, investigations focused on a potential involvement of CCL5 in cancerogenesis. While a role for CCL5 in breast cancer has been extensively investigated, other solid and hematological malignancies also show high expression profiles (Aldinucci 2014). In breast cancer, CCL5 is expressed by breast cancer cells, while normal breast epithelial duct cells show minimal expression, suggesting up-regulation of CCL5 during the process of malignant transformation (Soria 2008). Another group found elevated plasma levels of CCL5 in breast cancer patients as well as high expression in operative specimen in these patients to correlate with advanced and progressive disease (Niwa 2001). As a result, CCL5 may serve as a prognostic marker in breast cancer patients, indicating an advanced stage and progressive disease (Yaal-Hahoshen 2006). However, it is not only expressed by the cancer cells themselves, but also by MSC in the surrounding tissue (Luboshits 1999). Karnoub *et al.* showed that CCL5 is highly expressed by MSC when co-cultured with breast cancer cells *in vitro* and that MSC-secreted CCL5 is linked to an increased metastatic potential in a mouse model (Karnoub 2007). As was mentioned earlier, Zischek *et al.* were able to demonstrate CCL5-upregulation in MSC in an orthotopic mouse model of pancreatic cancer. Making use of this biology, MSC were equipped with a CCL5-driven fluorescent protein and administered intravenously three times during a period of 21 days. Fluorescent analysis of the tumors ex vivo showed reporter gene expression, thus showing CCL5 up-regulation in MSC that had infiltrated the tumor stroma (Zischek 2009).

1.2.2 Hypoxia

Tumor hypoxia is an important consideration for cancer therapy. It has been linked to cancer progression, metastasis and outcome. Oxygen diffusion is limited to about 100 to 200µm distance from blood vessels. As a consequence, most rapidly growing tumors show an average oxygen

tension of 0 to 7.5 mmHg, the equivalent of 1% O_2 (Casazza 2014, Mueller 2016). Hypoxia-inducible factors 1α and 2α (HIF-1α and HIF-2α) can be detected in tissue sections from a range of tumors and especially HIF-1α is now established as a prognostic factor for poor outcome in patients with early-stage cancers (Semenza 2009). Hypoxia has also been linked to the resistance of tumors to therapy, especially radiotherapy (Harrison 2002, Harada 2012).

Hypoxia-inducible factor 1 (HIF-1) was discovered almost 30 years ago, when analysis of the 3' enhancer region in the erythropoietin gene revealed a short sequence of five nucleotides, 5'-RCGTG-3', that was later defined as a hypoxia response element (HRE). Later, a dimeric HIF-1 transcription factor was found to bind to the HRE in a hypoxia-dependent manner (Goldberg 1988, Semenza 1991). HIF-1 consists of two subunits: HIF-1α, which is induced in hypoxic conditions and HIF-1β, which is constitutively expressed. Under hypoxia, the two form a heterodimer that translocates into the nucleus, and binds to HRE in the enhancer regions of target genes that need to be regulated in a cellular state of low oxygen tension (Wang 1993). The mechanisms underlying hypoxic induction of the subunit HIF-1α are well-described and have been summarized by Semenza as follows: Under normoxic conditions, the prolyl hydroxylase PHD2, which uses O_2 as a substrate, hydroxylates a proline residue and thus exposes HIF1-α to the von-Hippel-Lindau (vHL) protein, which binds to the hydroxylated proline and marks HIF-1α for ubiquitination and proteosomal degradation. An additional O_2-dependent mechanism for inhibiting HIF-1α during normoxia, is the active hydroxylation of an asparaginyl residue of factor-inhibiting HIF-1 (FIH-1), which undermines co-activation through p300. HIF-1α can also be induced chemically through iron chelators or chemicals like cobalt chloride, that interfere with a divalent iron ion (Fe^{2+}) in the catalytic center of hydroxylases, which leads to intracellular accumulation of HIF-1α (Semenza 2012). Downstream target genes of HIF-1 are generally related to glucose metabolism, angiogenesis, proliferation, pH regulation and, in cancerous cells, genomic instability, radiotherapy resistance, immortalization, immune evasion and metastasis (Semenza 2009). The task of HIF-1 is to help the cell adapt to hypoxic conditions, which includes switching from oxidative to glycolytic metabolism in order to produce energy in the form of adenosine triphosphate (ATP). HIF-1 induces the expression of pyruvate dehydrogenase kinase I (PDKI). This enzyme is capable of inactivating pyruvate dehydrogenase, an enzyme that catalyzes the irreversible conversion of pyruvate to acetyl-CoA, such that pyruvate resulting from glycolysis is not fed into the citrate cycle, but instead converted to lactate (Kim 2006, Papandreou 2006). Another player in this scenario is lactate dehydrogenase A (LDHA), the enzyme catalyzing the aforementioned conversion of pyruvate to lactate (Semenza

1996). Finally, mitochondrial autophagy is also induced by HIF-1 and helps to prevent accumulation of reactive oxygen species (Zhang 2008, Bellot 2009). Another important step in adapting to hypoxia is to reduce proliferation and HIF-1 helps to mediate G1 cell cycle arrest (Semenza 2013). In order to improve oxygen supply, HIF-1 promotes angiogenesis. VEGF, as was explained earlier, assumes a pivotal role in angiogenesis and is also induced via HIF-1-activation (Forsythe 1996).

Oxygen tension varies greatly, not only between cancer types, but also between cells of the same tumor. There is growing evidence for a metabolic symbiosis between those two types of cancer cells, where hypoxic cells accumulate lactate as a waste product of glycolysis, which is in turn utilized by normoxic cells to fire the respiratory chain (Nakajima 2013, Semenza 2013). HIF-1 is assumed to be an important manipulator in this scenario. It induces gene expression of glycolytic enzymes, lactate dehydrogenase A (LDHA) and monocarboxylate transporter 4 (MCT4) in hypoxic cancer cells. Thus, HIF-1 is one of the key players not only in cancer cells themselves, but also in the tumor microenvironment.

Endothelial cells are the principal performers in angiogenesis. The crucial factor initiating migration towards hypoxic areas and promoting the formation of new blood vessels, is a gradient of the growth factors of the VEGF family. VEGF is strongly induced by HIF-1. The over-production of angiogenic factors like VEGF in the stroma of growing tumors can lead to excessive vessel sprouting that can end with a faulty vasculature, where the basement membranes are incoherent, tight junctions are lacking, and supporting pericytes detach from the endothelium (Casazza 2014). Consequently, vessel leakage leads to impaired oxygen supply, high pressure on the surrounding tissue resulting in insufficient delivery of oxygen and other nutrients to the tumor cells (Carmeliet 2011). The role of bone-marrow derived progenitor cells such as MSC in tumor neovascularization has been discussed controversially in the past. What has been established is that MSC have the potential to be mobilized out of their niche in the bone marrow by a range of soluble factors, for example VEGF or SDF-1, via a HIF-1-dependent mechanism (Ceradini 2004, Spring 2005, Kerbel 2008). Hämmerling *et al* describe a multistep process involved in the recruitment of bone marrow-derived MSC, with CC chemokines such as CCL2 or CCL5 attracting circulating progenitor cells to the tumor stroma. These chemokines are described as being secreted by local endothelial cells in an auto- and paracrine fashion. Once incorporated into the tumor stroma, the bone marrow-derived cells begin to secret growth factors like VEGF, PDGF or EGF themselves. Endothelial cells possess receptors for both growth factors and the chemokines CCL2 and CCL5, so that a self-servicing loop is

being established, which launches a so-called angiogenic switch leading to massive neovascularization (Hämmerling 2006). Whether MSC, once they have been incorporated into the tumor stroma, have the capacity to differentiate into endothelial cells themselves remains debatable. Beckermann *et al* report no significant differentiation of MSC exposed to endothelial cell medium containing VEGF into endothelial cells *in vitro* and *in vivo.* However, MSC incorporate into the endothelium of tumor blood vessels in a VEGF-dependent fashion and vessel architecture also includes stabilizing cells such as pericytes and smooth muscle cells (Beckermann 2008). Consistent reports suggest that bone marrow-derived MSC enhance functional vasculature by differentiating into pericytes (Au 2008).

However, as described in chapter 1.1., bone marrow-derived MSC that are recruited into the tumor stroma not only serve to promote angiogenesis, but also make up key components of the tumor microenvironment in the form of TAF, tumor-associated fibroblasts. Once they enter the tumor stroma, the mechanisms that induce the adaption of a TAF-like phenotype are not completely understood. Several groups, however, have shown that HIF-1-dependent lysosomal degradation of Calveolin-1 is one of the key components (Martinez-Outschoorn 2010, Casazza 2014, Hagenhoff 2016).

Tumor hypoxia, or more specifically, positive staining for HIF-1 proteins in tissue sections of tumor specimen, has been identified as a prognostic factor for increased invasiveness, advanced stage of disease and poor outcome in general (Semenza 2009). Increased stage of disease refers to the degree of local progression as well as metastasis to distant organs. HIF-1 protein has been identified as a supporting factor of metastasis in every step of the way. Epithelial to mesenchymal transition (EMT) describes the process of cells losing their polarity and acquiring a mesenchymal phenotype, which enables them to break out of a tight cell compound. Several HIF-1-target genes like SNAIL1 or TWIST are transcriptional repressors of E-cadherin, a transmembrane protein that controls cell-cell adhesions and is required for EMT (Imai 2003, Yang 2008). Degradation of ECM (please refer to chapter 1.2) and disruption of the basement membrane by matrix metalloproteinases (MMP) are prerequisites for an invasive cancer phenotype. MMP-2 and MT1-MMP are up-regulated in hypoxia via a HIF-1-mediated pathway (Krishnamachary 2003, Muñoz-Nájar 2006). Intravasation of cancer cells correlates with increased permeability of the tumor vasculature, mediated by the HIF-1 target genes VEGF, MMP-1 and MMP-2 (Lu 2010). Finally, tumor hypoxia poses a risk for resistance to radio- and chemotherapy. This is partly explained by the fact that the presence of oxygen increases

the amount of free radicals that result from DNA strain breaks. Furthermore, hypoxia and acidity impair the function of DNA mismatch repair, which allows for mutations that can eventually lead to resistance to therapy (Harrison 2002). Now, Harada *et al* were able to show that deeply hypoxic cancer cells at the periphery of a tumor that showed no signs of HIF-1-expression prior to radiation, acquire HIF-1-activity after radiation and subsequently translocate towards blood vessels, thus securing oxygen and nutrient supply required for local recurrence (Harada 2012). These findings suggest that severe tumor hypoxia favors an aggressive and resilient cancer type and is thus worth investigating as a target of cancer therapy.

1.2.3 Heat Shock Proteins and Hyperthermia

The potential importance of heat shock proteins and hyperthermia In the context of resistance of tumors towards radio- and chemotherapy has become a major focus in cancer research over the last years. Heat shock proteins (HSP) are highly conserved proteins involved in the cellular stress response and are either constitutively expressed, or are induced by physiological and environmental stress. In mammalian cells, four families of HSP have been identified that differ in molecular weight. They are designated as HSP90, HSP70, HSP60 and small HSP, a group ranging from 15 to 30 kDa that includes HSP27 (Jego 2010). The main task of the HSP is to save the cell from damage caused by misfolded proteins that result from cellular stress. The stress factors identified include hyperthermia, cellular energy depletion, or shifts in ion and gas concentrations (Feder 1999). The name “heat shock protein” originates from their random discovery by Ritossa and colleagues in the 1960s, when accidental over-heating of *Drosophila* in the laboratory caused a distinct puffing pattern in chromosomes (Ritossa 1962). Since then, decades of research have shed light on the biology of the heat shock response and thus the cellular response to environmental insult. HSP are strongly cytoprotective by acting as chaperones within the cell for misguided proteins. At certain temperatures, proteins begin to denature, which means they lose their tertiary or quaternary structure, and become a threat to the cell. HSP, which typically exhibit a peptide binding site and an ATP-binding site, are able to refold mis- or defolded proteins, or promote their degradation if necessary, and prevent or dissolve the aggregation of proteins and escort proteins on their way for instance to the cell surface (Lindquist 1988, Feder 1999, Garrido 2001). In addition, HSP are directly and indirectly involved in apoptosis: HSP70, the best studied HSP family, is involved in several steps of the apoptotic cascade, mostly showing inhibitory effects on several pro-apoptotic factors, such as apoptotic protease activating factor 1 (Apaf-1) and apoptosis-inducing factor (AIF) (Garrido 2001, Garrido 2006). However, HSP are not only restricted to the cytosol, they can also be encountered as

membrane-bound, or in the extracellular space. Here, they show immunogenic properties and function as chaperones to antigenic peptides that are processed, incorporated into MHC class I molecules and presented to natural killer cells and dendritic cells (Noessner 2002, Srivastava 2002, Schmitt 2007). Furthermore, Multhoff *et al* were able to show that heat shock-induced overexpression of HSP70 on tumor cell surfaces leads to activation of CD94-expressing natural killer cells that subsequently release granzyme B and induce apoptosis of the tumor cells (Multhoff 2007).

The up-regulation of HSP is seen in some cancers, while their healthy equivalent tissue shows little or no expression. These levels can be further increased by additional stress factors, such as hyperthermia, oxidative stress, death receptor ligation or, interestingly, radiation or chemotherapy (Jego 2010). The general assumption is that HSP help tumors survive in adverse environments. Patients undergoing chemo- or radiation therapy for the treatment of solid tumors have been shown to profit from local hyperthermia, in that it reduces both local recurrence as well as distant metastasis (Issels 2010). As reviewed by Jolesch *et al*, this is partly due to an improved immune response mediated by heat-induced expression of HSP70 (Jolesch 2011).

Hyperthermia treatment has also been shown to impair DNA repair on multiple levels. While it induces DNA damage on its own, it also affects DNA damage signaling and cell cycle checkpoint activation (Oei 2015). Thus, hyperthermia has been shown to provide a synergistic effect with certain chemotherapeutic drugs, such as alkylating agents and anthracyclines (Behrouzkia 2016, Seifert 2016). Mild hyperthermia of 40-41°C increases blood perfusion and thus access of anti-cancer drugs to the tumor microenvironment, if applied locally. Increased blood perfusion keeps the tumor microenvironment richly oxygenated, which is known to help radiation therapy (Wust 2002). These examples show that while hyperthermia on its own presents only limited treatment options, its effect combined with that of standard chemo- or radiation therapy protocols holds promise.

To create local hyperthermia in a tumor, energy needs to be deposited precisely and deeply within the body. Emerging technologies that have been used to achieve this include focused ultra-sound - the only non-invasive option - as well as minimally invasive placement of radio frequency electrodes. To control local hyperthermia, magnetic resonance (MR) temperature mapping now represents the method of choice (Rome 2005).

1.3 Hepatocellular Carcinoma

Hepatocellular carcinoma (HCC) is the most common primary liver cancer, and the most lethal malignancy after lung and stomach cancers (Hernandez-Gea 2013). According to the World Health Organization's (WHO) world cancer report of 2014, primary liver cancer is the fifth most common cancer in men, and the ninth most common cancer in women, and accounts for the second highest number of cancer-related deaths worldwide. The vast majority of HCC cases are reported in developing countries of Eastern Asia and sub-Saharan Africa, with Southern Europe and North America showing intermediate incidence (WHO 2014). In areas of high incidence, HCC is diagnosed mostly in patients around 50 to 60 years of age, as opposed to areas of low incidence, where the mean age of diagnosis is as high as 75 years (El-Serag 2012). Prognosis is poor and mirrored in an overall five-year survival below 15%, that improves significantly to over 50% in patients with early-stage diagnosis eligible for surgical treatment (El-Serag 2011, WHO 2014). In Germany, according to the Robert-Koch-Institute's (RKI) cancer report of 2013, roughly 8000 patients are newly diagnosed with primary liver cancer per year, with 65% of them presenting with HCC and 25% with cholangiocellular carcinoma (Robert-Koch-Institut 2013).

The predominant risk factor for development of HCC is liver cirrhosis, with more than 80% of HCC patients presenting with cirrhotic liver disease at the time of diagnosis. Once cirrhosis has become manifest, the overall risk to develop HCC within five years is up to 30% (Fattovich 2004). As reviewed by El-Serag in recent years, chronic hepatitis B (HBV) and hepatitis C (HCV) virus infection can be made out as the underlying cause in more than 80% of HCC patients and geographic distribution of HBV and HCV infection is congruent with that of HCC. Other causes of liver cirrhosis and consequently HCC include chronic alcohol abuse and non-alcoholic fatty liver disease, as well as some hereditary diseases such as hemochromatosis, Morbus Wilson, autoimmune hepatitis and alpha-1-antytrypsine-deficiency (Farazi 2006). The only notable risk factor for HCC without underlying cirrhosis is exposure to aflatoxin-B1, produced by *Aspergillus flavus* fungus, which is associated with a carcinogenic p53-mutation (Bressac 1991).

The high mortality in HCC is a result of several factors. Curative treatment options in HCC therapy are scarce and largely limited to early stages, whereas most patients presenting with HCC have already progressed to advanced stages. To date, with no biomarkers available, diagnosis in early stages relies on frequent and continuous screening of high-risk patients with liver cirrhosis, a

process that requires extensive funding and high patient compliance. Once a cancerous lesion is suspected, further diagnosis includes contrast-enhanced cross-sectional imaging and biopsy.

Treatment options for HCC are evaluated according to local and systemic tumor progress, balanced with remaining liver function (Bruix 2005). In patients with limited local disease and light to moderate liver disease (Child A or B), surgical resection of the tumor represents the best option, if the remaining liver is thought to be functional enough. If that is not the case, and the patient meets certain criteria, they might be eligible for liver transplantation (El-Serag 2011). However, stalling tumor progress until a suitable organ becomes available is vital for treatment success. Common systemic chemotherapeutic agents have proven ineffective in HCC therapy, or contraindicated due to poor liver function. Local ablation techniques have been established that are able to restrain tumor progress in order to either prolong survival in intermediate stages or to downsize to an early stage that allows for curative therapeutic approaches. These techniques include radiofrequency ablation, local intraarterial injection of ethanol and, most importantly, transarterial chemoembolization (TACE) (Llovet 2002, Bruix 2004). For patients with advanced stage HCC, oral chemotherapy with tyrosine kinase inhibitor sorafenib is the treatment of choice and has been shown to prolong survival (Llovet 2008, Villanueva 2011).

As is the case with various types of cancer, the tumor microenvironment is of utmost importance in formation and progression of HCC, which is a multistage process. HBV or HCV infection as well as long-term alcohol abuse and non-alcoholic fatty liver disease pose chronic insults for liver parenchyma, which lead to persistent cycles of necrosis, inflammation and regeneration. In response to liver injury, hepatic parenchyma is activated, mainly in the form of stellate cells. These begin to acquire a myofibroblast phenotype, produce components of ECM and secrete growth factors triggering angiogenesis and fibrosis, much like the afore-mentioned tumor-associated fibroblasts (TAF). This stromal disruption is capable of promoting genetic mutations, which later malignantly transform into early manifestations of HCC (Thorgeirsson 2002, Campbell 2005, Baffy 2012). All in all, hepatocarcinogenesis is a compilation of diverse aetiologies that involve similar molecular mechanisms: p53-mutation is seen in HBV and HCV infection as well as aflatoxin B1 exposure, while chronic inflammation is the common ground of viral hepatitis, lifestyle-induced liver injury like alcoholic cirrhosis and non-alcoholic fatty liver disease as well as hereditary metabolic disorders (Farazi 2006, Hernandez-Gea 2013).

In light of limited treatment options in HCC, that are often a result of underlying liver disease preventing effective therapy as well as promoting new tumor growth after success of treatment, it is necessary to find new therapeutic targets. An overwhelming number of HCC develop on the ground of chronic inflammation, therefore targeted therapies pointing at the tumor microenvironment in primary liver cancer have become an area of scientific focus. This has led to choosing HCC as a tumor model in this study, with the goal to find new treatment options in order to stall tumor growth and to allow for surgical intervention or transplantation.

1.4 Aim of this study

As detailed above, bone-marrow derived MSC possess an innate tropism for injured or inflamed tissue, which has sparked scientific interest in their role as agents in cancer therapy. Previous work by our group has shown that the adoptive administration of MSC engineered to express a therapeutic gene under the control of tissue-specific promoters is a valid approach to treat experimental HCC. It has been demonstrated that the CCL5-promoter is up-regulated by MSC invading the tumor stroma and thus can be used to help enhance tumor selective transgene expression in response to the inflammatory milieu within the tumor setting. One aim of this study was to better characterize the activation of CCL5 in this environment, but in addition, to explore other potential means of focusing transgene expression in the context of malignant tissue using various engineered versions of MSC. The general goal was to help create new potential angles for attacking the tumor, and potentially allow a wider range of tumor entities to be included in this therapeutic approach, and at the same time, reduce potential side effects of MSCs that are recruited to normal tissues. Thus, under the precondition of limiting damage to non-malignant tissue, the following targeting strategies were examined:

Tumor hypoxia was investigated in this study as a potential means to trigger transgene induction in engineered MSC. We hypothesized that MSC invading the tumor stroma should respond to hypoxia. MSC engineered with a gene controlled by a hypoxia-sensitive promoter should be able to induce expression of the transgene once they have reached the hypoxic areas of the tumor microenvironment. The potential feasibility of this approach was tested with the help of an *in vitro* model of hepatocellular carcinoma.

Finally, we sought to evaluate the potential activation of transgene expression in MSC within tumors using externally applied processes. To this end, we examined whether MSC could activate transgene

expression in response to hyperthermic treatment, similar to that currently used for hyperthermic adjuvant therapy. If so, cancer patients undergoing hyperthermia treatment of afflicted body regions could in theory be treated with MSC engineered to express therapeutic genes under the control of heat-sensitive promoters.

1.5 Design of this study

To help address the specific aims of this study, the following experimental steps were performed:

- Reporter constructs containing firefly luciferase were designed with the respective promoters in order to examine expression of CCL5, HIF-1 and HSP70b by MSC under various experimental conditions *in vitro.* Induced CCL5 expression was further tested in MSC in response to various inflammatory cytokines, while HIF-1 and HSP70b-mediated transgene expression was analyzed by adjusting cell culture conditions to hypoxia or hyperthermia, respectively.
- Reporter constructs containing Cherry fluorescent protein were designed with hypoxia-responsive and heat shock-responsive promoters in order to examine expression by MSC using fluorescent microscopy.
- A spheroid model was established using the Huh7 cell line in order to study hepatocellular carcinoma *in vitro*. It was further used to develop an invasion assay as a means to examine whether bone-marrow derived MSC invaded the tumor spheroids *in vitro.*
- Immortalized, bone-marrow derived MSC were stably transfected with a reporter construct containing Cherry fluorescent protein under the control of a hypoxia-sensitive promoter.
- These stably transfected MSC were used in an invasion assay with Huh7 spheroids to demonstrate activation of a hypoxia-sensitive reporter gene within the hypoxic areas of the spheroid.

2 Materials and Methods

2.1 Materials

2.1.1 Cell Culture

2.1.1.1 Medias and supplements

Media

DMEM	Life Technologies, Carlsbad
RPMI 1640	Life Technologies, Carlsbad
HAM-F12	Life Technologies, Carlsbad
OptiMEM	Life Technologies, Carlsbad

Supplements

Fetal calf serum (FCS)	Biochrom AG, Berlin
Human serum	PAA Laboratories, Pasching
Penicillin/Streptomycin (P/S), 100x	PAA Laboratories, Pasching
Platelet concentrate	Blood bank, Klinikum Schwabing, München
Na-Heparin	Ratiopharm, Ulm
Blasticidin S HCL	Life Technologies, Carlsbad

Others

Dimethylsulfoxide (DMSO)	Merck, Darmstadt
Dulbecco's PBS (no Ca^{2+} or Mg^{2+}), 1x/10x	PAA Laboratories, Pasching
Trypan blue	Sigma Aldrich, Taufkirchen
Trypsin-EDTA in PBS, 1x	PAA Laboratories, Pasching

2.1.1.2 Cell lines and primary cells

Cell line	Comments	Media	Supplements	Source
L87	Immortalized (SV40) Mesenchymal Stem Cells (human bone marrow) *Thalmeier et al, 1994*	RPMI 1640	10% FCS 1% P/S	Institut für Pathologie, LMU Munich
Alex-2	Immortalized (SV40) Mesenchymal Stem Cells (human bone marrow)	DMEM	10% FCS 1% P/S	Alexandra Wechselberger, in-house
Huh7	Hepatocellular Carcinoma	DMEM/HAM-F12 (1:1)	10% FCS 1% P/S	AG Spitzweg, LMU Munich
hBMSC	Mesenchymal stem cells	DMEM	1000IE Na-	Deutsche

	(human bone marrow), isolated according to standard protocol for plastic adherence (Alexandra Wechselberger)	Heparin 5% platelet concentrate 1% P/S 10% human serum	Knochenmarkspende Bayern (DKB), Gauting

2.1.2 Bacteria

Type	Genotype	Source
E.coli DH5α	*sup*E44, Δ*lac*U169 (Φ80 *lac*ZΔM15) *hsd*R17 *rec*A1 *end*A1 *gyr*A96 *thi*-1, *rel*A1	In-house
E.coli One Shot® Mach1™-T1R	F-φ80(*lac*Z)ΔM15 Δ*lac*X74 *hsd*R(r_{κ}-m_{κ}^{+}) Δ*rec*A1398 *end*A1 *ton*A	Life Technologies, Carlsbad

2.1.3 Buffers and solutions

If not stated otherwise, volume percentage specifications are referring to ultra-pure H_2O.

2.1.3.1 Western blot

Prepared in-house

Ammoniumpersulfate (APS)	10% APS w/v
Blocking solution	5% skim milk powder (w/v) in TBST
Electrophoresis buffer	1.9M Glycine 0.25M Tris 1% SDS (w/v)
Laemmli Buffer 3x	150mM Tris/HCl, pH 6.8 (rt) 30% Glycerine (v/v) 6% SDS (w/v) 0.3% bromphenol blue (w/v) 7.5% β-mercaptoethanol (v/v)
Sodiumdodecylsulfate (SDS), 10%	10% SDS (w/v)
Tris, 1M, pH 6.8	1M Tris, pH 6.8 (rt)
Tris 1.5M, pH 8.8	1.5M Tris, pH 8.8 (rt)
Tris-buffered saline (TBS), 10x	1.5M NaCl 100mM Tris 10mM NaN_3
Tris-buffered saline with Tween (TBST)	0.05% Tween20 (v/v) in 1x TBS

Commercially available

Acrylamide/Bisacrylamide solution, 30%	Roth, Karlsruhe
ECL-substrate for western blot	Pierce, Rockford
NuPAGE LDS sample buffer, 4x	Life Technologies, Carlsbad
NuPAGE transfer buffer, 20x	Life Technologies, Carlsbad

RIPA buffer

Tris/HCl pH 7.4	50mM
NaCl	150mM
EDTA	1mM
Triton X 100	1%
Natriumorthovanadat	1%
SDS	0.1%
$CoCl_2$	1mM
Protease inhibitor	1 tablet/50ml

Separation gels

1.5M Tris, pH 8.8	5ml
10% SDS	200µl
10% APS	200µl
Tetramethylethylendiamine (TEMED)	20µl
Acrylamide/Bisacrylamide mix, 30%	5.3ml (8%), 4.0ml (6%), 3.3ml (5%)
H_2O	Ad 20ml

2.1.3.2 Molecular biology

Prepared in-house

Loading buffer, 6x	0.25% Bromphenol blue (w/v) 0.25% Xylen-Cyanol FF (w/v) 30% Glycerin (w/v)
Tris-borate-EDTA (TBE) buffer, 1x	90mM Tris 2mM boric acid 0.01M EDTA pH 8.0 (rt)

Commercially available

DNA restriction enzyme buffers, 10x	NEB, Ipswich
dNTP *Set*	Thermo Fisher Scientific, Waltham
Phusion HF buffer for *Phusion* polymerase, 5x	NEB, Ipswich
UltraPure Agarose	Life Technologies, Carlsbad

2.1.3.3 Microbiology

Prepared in-house

Agar, 2x	3% Agar (w/v) (autoclaved)
Ampicillin solution	50 mg/ml Ampicillin (in 70% ethanol, w/v)

$CaCl_2$ solution	60mM $CaCl_2$ 15% Glycerin (v/v) 10mM PIPES (piperazine-N,N'-bis(2-ethanesulfonic acid), pH 7 (rt) (sterile filtered)
Freezing medium, 10x	132.3 mM KH_2PO_4 21 mM Sodiumcitrate 3.7 mM $MgSO_4$*7 H2O 68.1 mM $(NH)_2SO_4$ 459.3 mM K_2HPO_4*3 H_2O 35.2% Glycerin (w/v) (autoclaved)
LB medium	2% Bacto Tryptone (w/v) 342 mM NaCl 1% yeast extract (w/v) pH 7.2-7.3 (rt) (autoclaved)

2.1.3.4 ELISA

Assay buffer	1% BSA (in 1x PBS, w/v, prepared in-house)
OptEIA substrate solution for ELISA	Commercially available; BD Biosciences, Bedford
PBS, 20x	2.74M NaCl 129.2 mM Na_2HPO_4 * 2 H_2O 54mM KCl 29.4mM KH_2PO_4
Wash buffer	0.05% Tween20 (in 1x PBS, v/v)

2.1.3.5 Histology and immunohistology

Vectamount mounting medium (DAPI)	Vector laboratories, Burlingame
Shandon Formal-Fixx formalin	Thermo Fisher Scientific, Waltham

2.1.4 Antibodies

Antibody	Source	Application
Alexa Fluor® 594 Donkey Anti-Mouse IgG	Life Technologies, Carlsbad	Immunofluorescence
Anti-Pimonidazole (mouse IgG1)	Hypoxiprobe, Burlington	Immunofluorescence
Purified Mouse Anti-Human HIF-1α (mouse IgG1)	BD Biosciences, Franklin Lakes	Western Blot

2.1.5 Enzymes

Restriction enzymes *BamH*I, *Bgl*II	NEB, Ipswich
Phusion polymerase	NEB, Ipswich

Alkaline phosphatase	NEB, Ipswich
T4 DNA Ligase	NEB, Ipswich

2.1.6 Human recombinant proteins

γ-IFN	PeproTech, Hamburg
IL1-β	PeproTech, Hamburg
IL-6	PeproTech, Hamburg
IL-10	PeproTech, Hamburg
TGF-β1	PeproTech, Hamburg
TNF-α	PeproTech, Hamburg
VEGF	PeproTech, Hamburg
Wnt5α	R&D Systems, Minneapolis

2.1.7 Size standards for electrophoresis

1 kb DNA ladder	Life Technologies, Carlsbad
MagicMark™*XP* western protein standard	Life Technologies, Carlsbad

2.1.8 Primers

For PCR primers used in the context of recombinational cloning, please refer to table 3 in chapter 2.2.3.2 on page 36. All primers were designed using the *Clone Manager* software and produced by Life Technologies.

2.1.9 Plasmids and vectors

Plasmid	Comments	Resistance gene	Source	Application
pCMV-Bsd	Contains a blasticidin resistance gene driven by a CMV-promoter inbetween two multiple cloning sites	Ampicillin	Life Technologies, Carlsbad	Blasticidin resistance for pGL3-hypoxia-luc
PGL3-Basic	Contains a multiple cloning site followed by firefly luciferase	Ampicillin	Promega	Cloning of pGL3-HSE and pGL3-HSP70b

pN3-BAR-Gluc	Contains Gaussia luciferase	Ampicillin	Anke Fischer, Department of Clinical Biochemistry, LMU Munich, AG Nelson	Template for amplification of Gaussia luciferase
pCAG-Kosak-Cherry	Contains mCherry fluorescent protein	Ampicillin	Dr. Rosemann, Helmholtz Center Munich, German Research Center for Environmental Health, Germany	Template for amplification of mCherry fluorescent protein
PGL3-RFL	PGL3-Basic (Promega) vector that carries a CCL5 promoter (Rantes Full Length) in the multiple cloning site	Ampicillin	Christoph Zischek, Department of Clinical Biochemistry, LMU Munich, AG Nelson	Transient transfections of MSC
PGL3-RaPro-TK	PGL3-Basic (Promega) vector that carries a CCL5 promoter driving thymidine kinase	Ampicillin	Christoph Zischek, Department of Clinical Biochemistry, LMU Munich, AG Nelson	Template for amplification of thymidine kinase
PGL3-6xHRE-tk	PGL3-Basic (Promega) vector that carries a hypoxia-responsive promoter in the multiple cloning site.	Ampicillin	Prof. Dr. Grässer, Universitätsklinikum des Saarlandes, Homburg, Germany)	Transient transfections of MSC; Template for amplification of 6xHRE-tk
pHSE-SEAP	Contains secreted alkaline phosphatase (SEAP) controlled by three tandem copies of HSE consensus sequence fused to a TATA-like promoter.	Ampicillin	Clontech (provided by Prof. Manfred Ogris, Department of Pharmacy, LMU Munich)	HSE-promoter for pGL3-HSE
PGL3-HSE	PGL3-Basic (Promega) that carries the HSE-promoter in the multiple cloning site	Ampicillin	Sylke Rohrer, Department of Clinical Biochemistry, LMU Munich, AG Nelson	Transient transfections of MSC; Template for amplification of HSE

pHSP70b-SEAP	Contains secreted alkaline phosphatase (SEAP) controlled by the endogenous HSP70b promoter	Ampicillin	Prof. Manfred Ogris, Department of Pharmacy, LMU Munich)	HSP70b-promoter for pGL3-HSP70b
PGL3-HSP70b	PGL3-Basic (Promega) that carries the HSP70b-promoter in the multiple cloning site	Ampicillin	Sylke Rohrer, Department of Clinical Biochemistry, LMU Munich, AG Nelson	Transient transfections of MSC; Template for amplification of HSP70b
pcDNA6.2PLITRBlasti-Dest	pcDNA-vector that carries two ITR-sites for transposition, attR1 and attR2 sites for recombination with a *ccdB*-gene in between, as well as a blasticidin resistance gene	Ampicillin	Carsten Jäckel, Department of Clinical Biochemistry, LMU Munich, AG Nelson	Destination vector for all Multisite Gateway cloning projects in this study

2.1.10 Kits

DuoSet CCl5 ELISA development kit	R&D Systems, Minneapolis
Endofree Plasmid Maxi kit	Qiagen, Hilden
Innuprep Plasmid Mini kit	Analytik Jena, Jena
MultiSite Gateway Pro Plus kit	Qiagen, Hilden
Quant-it DNA assay kit, broad range	Life Technologies, Carlsbad
Quant-it DNA assay kit, high sensitivity	Life Technologies, Carlsbad

2.1.11 **Other laboratory equipment**

CM3000 cryotome	Leica, Wetzlar
Developing machine for autoradiography films	Agfa, Morsel
E.coli Pulser	Bio-Rad, Hercules
Electroporator (for cell-culture use)	Bio-Rad, Hercules
Fluorescence activated cell scanner/sorter *FACSAriaIII*	BD Biosciences, Franklin Lakes
Fluorometer *Qubit*	Life Technologies, Carlsbad
Inverted fluorescence microscope *DMIL*	Leica, Wetzlar
Photo camera for Leica DMIL	Jenoptik, Jena

PCR cycler	Eppendorf, Hamburg

2.1.12 Chemicals

Aqua ad injectabilia	Braun, Melsungen
EDTA (ethylenediaminetetraacetic acid)	Merck, Darmstadt
EGTA (ethyleneglycoltetraacetic acid)	Sigma-Aldrich, Taufkirchen
Ethanol	Merck, Darmstadt
Ethidiumbromide 1%	Merck, Darmstadt
Glycerin	AppliChem, Darmstadt
Isopropanol	Roth, Karlsruhe
Methanol	Merck, Darmstadt
TRIS (trishydroxymethylaminomethane)	Merck, Darmstadt
β-Mercaptoethanol	Roth, Karlsruhe

2.1.13 Disposables

96-well microtiter plate, flat bottom	TPP AG. Trasadingen
96-well ELISA Maxisorb plate	Nunc, Roskilde
4mm electroporation cuvettes	PeqLab, Erlangen
Amersham *Hyperfilm ECL* autoradiography film	GE Healthcare, Uppsala
Cell culture dishes (3cm, 6cm, 10cm)	TPP AG. Trasadingen
Cell culture flasks ($75cm^2$, $150cm^2$)	TPP AG. Trasadingen
Cell scrapers	TPP AG. Trasadingen
Falcon tubes (15ml, 50ml)	BD Bioscience, Heidelberg
Pipette tips	Greiner Bio-One, Kremsmünster
Reaction tubes (0.5ml, 1.5ml, 2ml)	Eppendorf, Hamburg
Serological pipettes	TPP AG. Trasadingen
Superfrost Ultra Plus adhesion slides	Thermo Fisher Scientific, Waltham

2.1.14 Software

Clone Manager (PCR primer design)	Scientific & Educational Software, Morrisville
FlowJo (FACS data analysis)	TreeStar Inc., Ashland
Prism 6 (graphic program, statistical analysis)	GraphPad Software, La Jolla
ProgRes Capture (imaging at Leica DLIM)	Jenoptik, Jena
SnapGene Viewer (plasmid map design)	GSL Biotech LLC, Chicago

2.2 Methods

2.2.1 Cell culture

2.2.1.1 Day-to-day handling of cells

All cells indicated as grown under normoxic conditions have been kept in incubators set to 37°C, 21% O_2 and 5% CO_2. For hypoxic conditions, an incubator was used that allowed to adjust the oxygen level by insufflation of a gaseous mixture of 95% N_2 and 5% CO_2. For all *in vitro* experiments that required hypoxic conditions, the oxygen level was set to 2%. Alternatively, cells were incubated in the normoxic incubator, but under the influence of $CoCl_2$, an inorganic compound, that is able to prevent HIF1α-degradation and thus simulates cellular hypoxia. For these *in vitro* experiments, $CoCl_2$ was added to the culture media in a concentration of 300µM.

For passaging and further use, the cells were kept in a laminar flow hood that helped to avoid contamination. All reagents were heated to 37°C in a water bath prior to use. First, cells were rinsed with PBS to remove all traces of culture media, especially serum. Then, a small amount of Trypsin-EDTA that just about covered the surface of the culture dish was applied and cells were incubated for up to 10 minutes, until they began to detach from the plastic. Subsequently, culture media was added to the Trypsin-EDTA in a 3:1-ratio, in order to deactivate the latter. After rinsing the surface of the culture dish a couple of times to ensure detaching of cells, the suspension was aspirated in a pipette and transferred to a 50ml-tube, which was then centrifuged at 200xG for three minutes. After decanting of the supernatant, the resulting cell pellet was re-suspended in culture media, in order to be redistributed among culture dishes at the desired ratio.

For performance of luciferase assays, the *Dual Luciferase Reporter Assay System* was used, that allowed to measure both Firefly and Renilla luciferase. If Renilla luciferase was not co-transfected, the *Luciferase Assay System* was used. To begin, culture media was removed and the cells rinsed with PBS. Afterwards, a lysis buffer was applied and the lysate was either analyzed at once, or stored at -20°C. The assay was performed according to the manufacturer's instructions, using the provided reagents and a luminometer for signal detection.

2.2.1.2 Freezing and thawing of cells

To freeze cells that were currently not used for experiments, a part of the cell suspension after centrifugation was not re-distributed, but instead added to a freezing tube the size of 2ml in a 1:1-

ratio with a previously composed freezing medium. The latter contained culture medium and DMSO in a 4:1-ratio. The tubes were stacked in a box containing isopropanol before storage at -80°C, to prevent the cells suffering damage from rapid freezing. After cooling down overnight at -80°C, the tubes were transferred to a liquid nitrogen tank. From there, the tubes were removed if cells were needed and could be rapidly thawed in the water bath. After adding the thawed cell suspension to fresh media in a culture dish, the cells could be placed in the incubator overnight and received fresh media the next day to remove all traces of DMSO.

2.2.1.3 Counting cells

For certain *in vitro* experiments, the cells needed to be counted. To this effect, the cells were suspended in a particular volume and a small amount of the suspension was mixed with Trypan blue solution (0.4%), a marker for dead cells, at a 1:1-ratio. The resulting mix could be applied to a Neubauer counting chamber, which is only able to hold a certain volume. It was then possible to deduct the number of cells per ml in the original suspension from the mean number of viable cells counted in each of the four fields within the chamber, by multiplying the latter by 10^4.

2.2.1.4 Creation and handling of spheroids

For the creation of spheroids, a multitude of different approaches has been developed in the past. For this study, the spheroids needed to be as precisely rotund as possible, as oxygen gradients within the spheroid played a key role. To achieve this, it was agreed to try and grow spheroids from single cells, rather than pressing cells into a composite by for example centrifugation.

Polyhydroxyethylmethacrylate, referred to from here on in as polyHEMA, is a hydrophilic polymer that can be used to reduce the adherence of cells to the surface of a culture dish to a minimum. Dissolved in 96%-ethanol to a concentration of 120mg/ml and mixed overnight on a magnetic twirler, it formed a liquid that could be stored at 4°C. To be used for the coating of culture dishes, it was further diluted in 96%-ethanol in a 1:10-ratio. For a 10cm culture dish, 3-4ml of this dilution was added to the surface and the dish subsequently placed under the laminar flow hood for it to dry with the help of a drain of air and without fear of contamination. After a couple of hours, the polyHEMA-coat had dried and provided a clean surface for cells to be placed upon but not attach to.

The polyHEMA-coated culture dish was filled with culture media and a very small number of cells were added to the media. The dish was then placed in an incubator for several days and over the course of time, with the cells not having a surface to attach to, they started growing in spheroids.

Depending on the cell line, different sizes of spheroids could be seen after a certain time. For Huh7 cells, typically after 6-10 days, the spheroids had grown to the desired size between 400 and 600 µm. Every couple of days, to supply the spheroids with fresh media, it was partly exchanged. By rotating the dish on a flat surface, spheroids assembled in the middle of the dish and the media could be aspirated at the periphery without accidentally gathering up spheroids. The same technique was applied to purposely extract spheroids from the dish.

2.2.1.5 Spheroid invasion assay

In order to investigate whether MSC could invade a tumor spheroid under these *in vitro* conditions, the first invasion assays were conducted with a simple experimental design. Primary MSC, obtained from a bone marrow aspirate, were stained with 10µM CMFDA, a green fluorescent marker, and added to the culture media in a dish that already contained tumor spheroids that had been growing for a week and had reached the desired size of 400 to 600 µm. After 72 hours of incubation, the spheroids were extracted from the dish, prepared for and cryo-sectioned as detailed above. For fluorescent microscopy, the slides were stained with DAPI, a blue fluorescent marker of cell nucleuses, and mounted with 50%-glycerin-0.2%NPG-PBS.

To get an idea of the distribution of oxygen within the spheroids, a pimonidazole staining was added to the method. Pimonidazole is a 2-nitroimidazole that is reductively activated in hypoxic cells and subsequently forms stable complexes with thiol-groups in other molecules that can be detected by immunohistochemistry (Franko 1986). Pimonidazole reagent and antibody were used according to the manufacturer's instructions (*Hypoxyprobe*).

After demonstrating that the primary MSC invaded the Huh7 tumor spheroids, the experimental design was further refined. One goals was to control the number of MSC that were added, and to isolate the spheroids for the purpose of the assay, so that every spheroid plus the MSC added to the culture media of the respective spheroid became an experimental unit. To achieve this, the MSC were stained with CMFDA (10µM), harvested and counted. 25 000 CMFDA-labelled MSC were re-suspended in 25µl culture media and added to a 1.5ml-tube, that already contained a tumor spheroid, also gathered up in 25µl culture media. The tubes were then placed on a roller plate for 2 hours. During that time, all the tubes were stacked together in a 50ml-tube and assembled in a way that made sure, none of them were positioned upside down during the process of rolling, with the danger of the spheroid attaching to any surface. After rolling, the tubes were carefully dislodged and the spheroids were gathered up in a pipette tip and transferred to the well of a 96-well-plate, each

spheroid again on their own. Subsequently, the culture media was exchanged three times, so as to wash away all remaining MSC that had been unable to attach to the spheroid. In the end, spheroids were cultured in 100µl media for the duration of 48 hours at 37°C. Afterwards, the spheroids were extracted from the wells, prepared for and cryo-sectioned as detailed above. For fluorescent microscopy, the slides were processed as detailed in chapter 2.2.5.3.

2.2.2 Molecular Biology

2.2.2.1 Freezing and thawing of bacteria

All plasmid constructs were transformed into *E.coli* strains (DH5α or for Multisite Gateway cloning, Mach1). Long-term storage was achieved by adding 100µl of a previously composed freezing medium to 900µl of an overnight culture and storing the mix at -80°C. In order to restart culture from that vial in stock, a small amount of frozen bacteria was scratched away from the surface and dispersed on an agar plate with a thinning streak. The plate was then cultured at 37°C overnight and a single colony was picked the next day, of which a liquid culture could be started.

2.2.2.2 Preparation of agar plates

Agar plates were prepared regularly with the desired selective antibiotic. Here, a 3% Agar solution was heated in a microwave and mixed with an equal volume of 2x LB medium. For DH5α bacteria, 100µg/ml Ampicillin was added, Mach1 bacteria required a higher concentration of 150µg/ml. The mixture was poured into petri dishes, which were then set out to cool down and dry under a laminar flow hood. For storage purposes, the plates were all packed and sealed in plastic bag and kept at 4°C.

2.2.2.3 DNA restriction digests

For restriction digests of DNA, either to cut out fragments or to verify correct internalization of fragments into destination vectors, the following experimental set-up was applied: 1µg of DNA was digested with 1 unit of restriction enzyme in the span of 1 hour. For larger DNA amounts, either more of the restriction enzyme was used or the reaction time was extended. In case of the former, reaction volume was increased accordingly, so that the enzyme volume never surpassed one tenth of the total volume. Another tenth of the reaction volume was taken up by the respective restriction buffer that had been supplied by the manufacturer. All reactions, if not indicated otherwise by the manufacturer, took place at 37°C in a table top shaking device at 300rpm.

2.2.2.4 Separation of DNA fragments by electrophoresis

Agarose gel electrophoresis was applied either for diagnostic tests on DNA fragments in terms of size or correct restriction digests, or in order to isolate and prepare said DNA fragments, for example after amplification by PCR. Agarose concentration varied between 0.6% and 2%, depending on the expected size of the fragment in question. Typically, for a fragment larger than 1000 base pairs a concentration of 0.6% would suffice, whereas a fragment smaller than 1000 base pairs required a 2% agarose gel. The gel consisted of 0.5xTBE buffer, containing ethidium bromide in a concentration of 100ng/ml, mixed with the desired amount of agarose powder, which was subsequently dissolved by heating the mix in a microwave until it turned transparent. The heated agarose gel was dispersed in an appropriate electrophoresis chamber. Before applying them to their allocated slots, DNA samples were mixed with blue 6x loading buffer in a 5:1-ratio. Next, the chamber was topped with the aforementioned 0.5x TBE buffer and a voltage of 120 was applied. The gels were observed and documented under a UV lamp and, if necessary, fragments were cut out and subsequently extracted from the gel using a commercial kit (*QIAquick Gel Extraction Kit*).

2.2.2.5 Determination of DNA concentrations

In order to determine DNA concentrations, the *Qubit* fluorometer was utilized, along with commercially available reagents (*Quant-iT*) supplied by the same manufacturer. All assays have been performed according to the instructions of the manufacturer.

2.2.2.6 Dephosphorylation and ligation of DNA ends

In order to avoid religation of single-cut DNA ends in ligation reactions, an additional step in between restriction digest and ligation was necessary. This step involved the dephosphorylation of two ends of a fragment that had been cut out or linearized by digest with a single cutting restriction enzyme. Without the phosphate, the DNA molecule was not able to re-ligate with itself. To this effect, one of the two DNA molecules that were supposed to be ligated in the following reaction, typically the plasmid, was incubated for another hour at 37°C with a commercially available calf intestine alkaline phosphatase (CIP) that catalyzes the dephosphorylation of both the 5’ and the 3’ end. Subsequently, the DNA molecule had to be purified again, using a commercially available kit (*QIAquick PCR Purification Kit*).

For the ligation of vector and insert DNA fragments, both were included in a reaction containing a ligation enzyme, in this case a commercially available T4 DNA ligase. According to laboratory protocol, four different reactions were prepared. Two of these reactions contained both fragments,

vector and insert, in a 1:3- and 1:10-ratio of molar weight, respectively. A third reaction contained the uncut plasmid and served as positive control, while a potential fourth reaction contained the cut and "CIP-ed" plasmid and served as a negative control. 1µl T4 DNA ligase was added to the mix in a concentration of 400 U/µl, along with 2µl of a 10x ligase buffer (supplied by the manufacturer) and the reaction volume was topped up to 20µl with water. After 1 hour incubation at room temperature, typically one tenth of the total reaction volume was transformed into competent bacteria.

2.2.2.7 Preparation and transformation of competent E.coli DH5α and Mach1

Competent DH5α bacteria were prepared according to a standard laboratory protocol with the help of a calcium chloride ($CaCl_2$) solution. To this effect, a 4ml overnight liquid culture of *E.coli* DH5α was added to 400ml fresh LB medium and incubated at 37°C and 250rpm. During that time, the optical density was reassessed every couple of minutes by absorption spectroscopy of a culture sample. Once an OD_{600nm} of 0.375 was reached, the bacterial culture was aliquoted in 50ml tubes, kept on ice for 5 minutes and centrifuged at 4°C and 1600xG for 7 minutes. Afterwards, the supernatant was discarded and the bacteria in each aliquot re-suspended in 10ml of an ice-cold $CaCl_2$ solution. 30 minutes incubation on ice were followed by another centrifugation step identical to the previous one. Now, the bacteria in each aliquot were re-suspended in 2ml of an ice-cold $CaCl_2$ solution and re-dispersed in smaller aliquots of 200µl. These aliquots were then snap-frozen by immersing them in a bath of ethanol and dry ice, before storing them at -80°C. Competent *E.coli* Mach1 bacteria were obtained from *Invitrogen.*

For transformation of both *E.coli* DH5α and Mach1 bacteria, one tenth of the ligation reaction volume was added to a tube containing 50µl of rapidly thawed bacteria and kept on ice for 10 minutes. Subsequently, the tubes were stacked into a table-top heater and exposed to 42°C heat for exactly 45 seconds. Afterwards, the bacteria were re-suspended in pre-warmed LB medium and incubated for another 45 minutes at 37°C and 300rpm. This suspension was then plated on agar plates containing the desired selective antibiotic and incubated overnight at 37°C. The next morning, single colonies could be picked from the plate and seeded into a liquid culture.

2.2.2.8 Isolation and analysis of plasmid DNA from transformed bacteria

In order to analyze plasmid DNA from transformed bacteria, the latter had to be lysed and the DNA isolated from the lysate. For this step, a commercially available kit was used, depending on the size of the overnight culture (*Innuprep Plasmid Mini Kit* for cultures up to 1.5ml, *Endofree Plasmid Maxi*

Kit for culture up to 100ml) and according to the manufacturer's instructions. For analysis, diagnostic restriction digests were performed and evaluated by gel electrophoresis.

2.2.2.9 Polymerase chain reaction (PCR)

Polymerase chain reaction (PCR) was used in this study to amplify the desired inserts for the Multisite Gateway cloning and at the same time add the relevant attB-recombination sites. To this effect, primers that contained both the necessary short nucleotide sequences for recombination as well as the complement nucleotides that were able to attach to the DNA that was to be amplified, were designed using the *Clone Manager* software. For all reaction mixtures, the same protocol was adhered to (see table 1). PCR settings can be observed in table 2. For primer sequences please turn to chapter 2.1.8. The inserts were amplified and purified by gel electrophoresis and extraction.

	volume (µl)
dNTP	4
fw-primer	1
rv-primer	1
***Phusion* Polymerase**	1
***HF*-buffer**	5
Target DNA (5-10ng/µl)	1
H_2O	12

Table 1: Standard reaction mixture for PCR. DNA was diluted to a concentration between 5 and 10 ng/µl before use, one reaction mix always adding up to a volume of 25µl in total. To amplify the insert sufficiently, 5 PCR reactions were performed at the same time. Afterwards, they were pooled together and dispensed across the slots of an agarose gel.

	6xHRE-tk (412bp)	**HSP70b (590bp)**	**mCherry (821bp)**	**Gaussia (633bp)**	**TK-pA (1801bp)**
Template	PGL3-hypoxia-luc (6401bp)	PGL3-HSP70b (5268bp)	pCAG-Cherry (7100bp)	pN3-BAR-Gluc (4200bp)	PGL3-RaPro-TK (6800bp)
Initial denaturation	95°C 5 min	95°C 5 min	95°C 5 min	95°C 5 min	95°C 5 min
Denaturation	95°C 30 sec	95°C 30 sec	95°C 30 sec	95°C 30 sec	95°C 30 sec
Annealing	61°C 30 sec	61°C 30 sec	58°C 30 sec	64°C 30 sec	63°C 30 sec
Elongation	72°C 3 min	72°C 2.5 min	72°C 3.5 min	72°C 2 min	72°C 3.5 min
Cycles	30x	30x	30x	30x	30x
Final elongation	72°C 10 min	72°C 10 min	72°C 10 min	72°C 10 min	72°C 10 min

Table 2: PCR settings. Elongation time was chosen depending on template size (30 sec per 1000bp).

2.2.2.10 Sequencing of DNA

Sequencing of DNA was performed by GATC Biotech, Konstanz. Primers used in the process of sequencing that are not standard primers are listed in chapter 2.1.8.

2.2.2.11 Transient Transfections in L87 and primary MSC

Transient transfection of L87 cells were either conducted by lipofectamine or electroporation. For both methods, the plasmids were isolated and suspended in sterile H_2O. In most experiments, an additional plasmid carrying a Renilla luciferase driven by a CMV-promoter was added in a 1:50-ratio.

In the case of lipofectamine, a commercially available kit (*Lipofectamine*) was used and concentrations as well as cell numbers and incubation times were applied according to the manufacturer's instructions. After transfection, culture medium was exchanged after 4 to 6 hours and cells were left in the incubator over night before starting stimulation. For primary MSC, lipofectamine was the only transfection method applied in the course of this study.

For electroporation, L87 cells were seeded out to reach an 80% density overnight, to ensure they had entered a logarithmic growth phase on the day of transfection. The plasmid DNA was re-suspended in sterile, endonuclease-free water to a concentration of 1-3µg/µl. The cells were counted and re-suspended in culture medium containing 10% FCS but no antibiotics to a concentration of one million cells per 100µl. A disposable electroporation cuvette with a 4mm gap was filled with 200µl of cell suspension and 4µg plasmid DNA (plus a potential 0.08µg pRL-CMV) was added to the mix. The cuvette was kept on ice for 10 minutes before electroporation, which was performed at 960µF and 230V. Afterwards, the cuvette was kept on ice for another 10 minutes. To transfer the cells from the cuvette to the culture dish, the cuvette was flushed with 200µl culture medium. If a higher number of transfected cells than 2 million were required, electroporation was performed in several identical steps and the cell suspension was pooled again after transfection, to be distributed across multiple wells.

2.2.2.12 Stable Transfection of L87

Stable transfection of L87 with the pcDNA-ITR-HIF-Cherry construct in this study has been achieved using a sleeping beauty-based transposon system. The vector backbone carried two indirect terminal repeats (ITR), flanking the promoter and transgene as well as the selective marker, in this case a blasticidin resistance. The sleeping beauty transposon system requires a transposase (SB100X) to be co-transfected with the plasmid. The ratio between pcDNA-ITR-HIF-Cherry and the

plasmid carrying the SB100X-transposase was 1:3. After transfection, the transposase facilitated excision of the transposon from the plasmid and inserted it into the genome of the cell at TA dinucleotides.

In the course of this study, L87 cells were transfected with pcDNA-ITR-HIF-Cherry (20µg) and SB100X (60µg) by using electroporation. Experimental parameters were the same as detailed above regarding transient transfection, except for DNA concentrations. A total of 3 million cells were transfected and transferred into a 10cm culture dish afterwards. 48 hours after transfection, the culture medium was removed and replaced by fresh medium containing 6µg/ml blasticidin. During the next 14 days, selective medium was exchanged every 72 hours.

2.2.3 Cloning strategies

2.2.3.1 Construction of pGL3-hypoxia-luc

For *in vitro* studies of hypoxia in MSC, a plasmid was obtained from Prof. Grässer of Saarland University, Bad Homburg, that carried the hypoxia-sensitive 6xHRE-tk-promoter inserted in the multiple cloning site. The foundation of this vector is the commercially available pGL3-Basic vector (*Promega*). To be able to use this plasmid in a potential stable transfection experiment, a selective marker for human cell culture had to be integrated into the backbone. To this effect, pCMV-Bsd (*Life Technologies*), also a commercially available plasmid, was examined for mutual restriction sites. In the end, the blasticidin resistance gene that is driven by a human CMV-promoter was excised from the vector by restriction digest with *BamH*I and *Bgl*II. At the same time, the aforementioned pGL3-Basic vector carrying the 6xHRE-tk-promoter, was linearized by restriction digest with *BamH*I alone and incubated with an alkaline phosphatase to dephosphorylate both ends. Subsequently, the CMV-blasticidin insert was ligated into the *BamH*I-site, with the possibility of a clockwise or counterclockwise integration. The new vector would lose one of the *BamH*I ends to ligation with *Bgl*II and contain once again a single cutter *BamH*I site on the other end of the insert. To verify correct integration and orientation, the resulting clones were digested with *Xba*I and *EcoR*I. *Xba*I represented a single cutter in the original pGL3-Basic vector, while *EcoR*I only cutting in case of correct integration of the insert. The length of the fragment excised out of the newly-constructed pGL3-hypoxia-luc in the course of this control digest depended on insert orientation and either came up as short as 300 base pairs (counterclockwise) or 1600 base pairs (clockwise). For the following *in vitro* studies, the clockwise orientation was preferred.

2.2.3.2 Construction of pcDNA-ITR-HIF-Cherry and pcDNA-ITR-HSP70b-Cherry

Originally, MSC were transfected with a construct similar to pGL3-hypoxia-luc that had the firefly luciferase replaced by a red fluorescent protein. However, after various efforts to stably integrate the transgene into MSC, a new strategy was devised. As the efficiency of plasmid integration into the MSC genome was identified as a key problem, a system was devised that assured higher transfection efficiency. To achieve that the promoter and the reporter gene were integrated into a vector containing two inverted terminal repeats (ITR), which are needed for transfection with the Sleeping Beauty transposon system. These nucleotide sequences are crucial for transposition, as they are identified by the transposase and lead to excision of the transposon.

For the new construct, the commercially available *Multisite Gateway Pro Plus* kit was applied. With the help of this recombinational cloning tool, several new vectors could be produced in a short time span. This method is referred to several times throughout this study and is outlined in the following.

The Gateway cloning system is based upon site-specific recombination between the lambda bacteriophage and *E.coli* bacteria. In short, bacteriophageal enzymes, the recombinases, are able to attach to certain nucleotide sequences, the attachment or *att* sites, in both strands and recombination takes place as the flanking regions of matching att sites are interchanged. There is no nucleotide gain or loss in the process, instead new att sites are created that are hybrids with nucleotides from both donor strands. The Gateway cloning system makes use of proteins from both bacteriophage and *E.coli* that catalyze the recombination reactions (BP and LR reaction) and uses the same 15 base pair core regions within the original att sites. These core regions are flanked by additional nucleotides that help the recombinases attach to the DNA.

Recombinational cloning speeds up the process, because it merges several conventional cloning steps into one. It allows cloning all modules, promoters as well as expression genes, into the destination vector at the same time. Correct integration in the right order is guaranteed by equipping PCR products with the respective att sites. Figure 1 is a schematic outline of the different stages of recombinational cloning with the Gateway system. AttB sites have to be integrated into PCR primers before amplification of the insert, whereas pDONR-vectors are supplied by the manufacturer and already contain the matching attP sites. PCR primers were designed using the *Clone Manager* software. Table 3 shows primer sequences and highlights template-specific nucleotides and att sites. The amplicons containing the promoters were flanked by an attB1 site on the 5’ end and an attB5r site on the 3’ end. The reporter genes were flanked by attB5 and attB2,

respectively. In the following BP reaction that represents the lysogenic pathway of recombination between bacteriophage and *E.coli*, the promoters were integrated into pDONR-221-$P_2P_{5r,}$ whereas the reporter genes were integrated into pDONR-221-P_5P_2. The donor vectors as well as the destination vector carry a *ccdB*-gene between att sites. The *ccdB*-gene is a bacterial toxin originating from the *E.coli* genome that leads to death of transformed bacteria, if it is not replaced by the gene of interest during recombination, and therefore serves as a control for correct process of recombination. For plasmid maps of the entry clones please turn to chapters 3.2.3.1 and 3.3.3 (Jaeckel 2016).

With both promoters, 6xHRE-tk and HSP70b, as well as expression genes, Gaussia luciferase, mCherry fluorescent protein and thymidine kinase, integrated into entry clones, six new plasmids could be generated at the same time in a system of mix and match. The destination vector in this study, pcDNA6.2PLITRBlasti-Dest, was kindly provided by Carsten Jäckel. It contains the necessary attR1 and attR2 sites with the *ccdB*-gene in between as well as the desired ITR sites for sleeping beauty transposition and a blasticidin resistance gene. In the following LR reactions that represent the lytic pathway of recombination between bacteriophage and *E.coli*, the six new plasmids evolved, namely pcDNA-ITR-HIF-Cherry (see chapter 3.2.3.1) and pcDNA-ITR-HSP70b-Cherry (see chapter 3.3.3) (Jaeckel 2016).

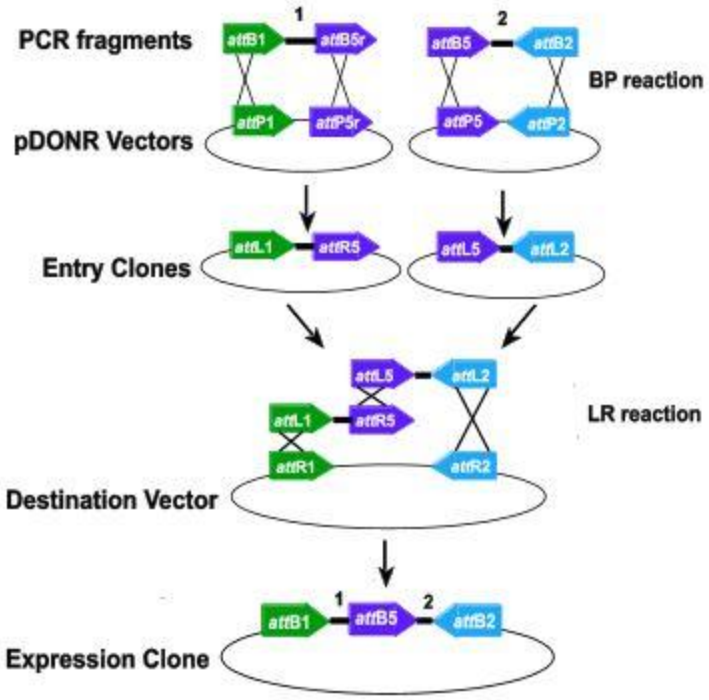

Figure 1: Schematic outline of the Gateway technology. AttB sites always recombinate with attP sites in a BP reaction, while attL sites always recombinate with attR sites in an LR reaction. Source: MultiSite Gateway Pro® User Guide.

Att-sites	Insert	Fw/ Rv	Sequence
B1 B5r	6xHRE-tk/ HSP70b	Fw	GGGGACAAGTTTGTACAAAAAAGCAGGCTTAATAGGTACCGAGCTCTTACG
		Rv	GGGGACAACTTTTGTATACAAAGTTGTTACCAACAGTACCGGAATGC
B5-B2	mCherry	Fw	GGGGACAACTTTGTATACAAAAGTTGTAGCAGCCACCATGTCTAG
		Rv	GGGGACCACTTTGTACAAGAAAGCTGGGTTGCCTTCACAAAGATCCTCTA
	Gaussia-luciferase	Fw	GGGGACAACTTTGTATACAAAAGTTGTAATCCAGCCACCATGGGAGTC
		Rv	GGGGACCACTTTGTACAAGAAAGCTGGGTTGGCCGCTTAGTCACCACC
	Thymidine kinase	Fw	GGGGACAACTTTGTATACAAAAGTTGTACAGCCTCTCCCACAGGTAC
		Rv	GGGGACCACTTTGTACAAGAAAGCTGGGTTTAAAACGACGGCCAGTGC

Table 3: Primer sequences. Att sites are highlighted in yellow, template-specific sequences in blue. Primers for 6xHRE-tk and HSP70b promoters have the same template-specific sequence, as they are both integrated into pGL3-basic.

2.2.4 Protein-based methods

2.2.4.1 Western blot

In order to measure HIF1α protein expression in MSC by western blot, proteins had to be extracted from the cells. Unfortunately, as mentioned before in the introduction, HIF1α is dismantled rather quickly once cells find themselves in a normoxic environment. To avoid this, a special extraction buffer had to be composed, that was based on several publications on the topic as well as previous protocols from other laboratory members. For all buffers mentioned in this section, compilations

are listed in chapter 2.1.3.1. In short, the buffer applied in this study served to extract a whole cell lysate and contained cobalt chloride to a concentration of 1 mM. Cells were washed in 4°C PBS and subsequently scraped off the culture dish with RIPA buffer, transferred to a reaction tube and kept on ice for one hour. Centrifugation at 13000rpm and 4°C for 20 minutes followed and the supernatant was aliquoted and stored at -20°C.

A polyacrylamide gel was prepared with an acrylamide concentration gradient increasing from 5% to 8%, with an additional 6% step in between. This way, both HIF1α at 140 kDa and α-tubulin at 52 kDA could be accommodated and separated at the optimal gel concentration. SDS-PAGE was performed according to Laemmli (Laemmli 1970). Extracts were mixed with Laemmli reducing buffer and heated at 95°C for five minutes before loading them on the gel along with a MagicMark size standard for molecular weight control. Electrophoresis was started at 80V and continued at 120V once all samples had visibly entered the gel.

Western Blot was performed according to Towbin (Towbin 1979). At the end of electrophoresis, the gels were blotted onto polyvinylidene fluoride (PVDF) membranes and the proteins transferred in *NuPage* buffer at 30V for one hour (wet blot technique). The membranes were then blocked with a blocking solution (5% skim milk powder in TBST) for either 1 hour at room temperature or overnight at 4°C and washed twice in water before application of the primary antibody. The primary antibody, a mouse anti-human HIF1α, was diluted in a 1:1000-ratio in TBST and applied either for 2 hours at room temperature or again at 4°C overnight. Four washings with TBST at 10 minutes each followed, before adding the secondary antibody, in this case rabbit anti-mouse IgG, diluted 1:5000 in TBST with 5% skim milk powder. To avoid high background, incubation with the secondary antibody was limited to 1 hour. To conclude, four washings with TBST at 10 minutes each and two additional rounds of TBS for 5 minutes ensued. The membrane was then soaked in 4ml ECL solution for 1 minute, exposed to radiography and the resulting film processed in a developing machine.

2.2.4.2 ELISA

ELISA was applied for quantification of CCL5 in cell culture supernatants. The supernatants were collected and stored at -20°C and subjected to ELISA at various dilutions. For the assay, a commercially available sandwich ELISA (*DuoSet*) for CCL5 was used, according to the manufacturer's instructions. Chromogenic development was achieved by adding OptEIA substrate solution.

2.2.5 *In vitro* experiments

2.2.5.1 Fluorescence activated cell scanning (FACS)

FACS analysis and sorting of stably transfected L87-HIF-Cherry was done in collaboration with Dr. Josef Mysliwietz and Prof. Dr. Elfriede Nößner of the Helmholtz Zentrum Munich, Institut für Molekulare Immunologie. The FACS machine, a BD FACSAria III, is equipped with a 561nm-laser that is able to excite (587nm) and detect (610nm) the mCherry red fluorochrome at near-optimal wavelengths. Analysis and sorting both relied on ordinary L87 cells as negative control in order to establish sorting gates. After detection, mCherry-positive cells were released directly into a 1.5ml reaction tube that was filled with culture medium and 30% FCS.

2.2.5.2 Fluorescence microscopy of cells

To verify expression of the mCherry red fluorochrome in transfected L87-HIF-Cherry, cells were analyzed with an inverted microscope and the necessary fluorescence filters.

2.2.5.3 Immunofluorescent staining and microscopy of spheroids

Spheroids were analyzed following cryosection and fluorescence microscopy. For analysis, the spheroids needed were embedded in OCT compound, a transparent gel at room temperature, and cut with a cryotome. To this effect, the spheroids were gathered from the dish and transferred into a 1.5ml tube. Spheroids quickly descended to the bottom of the tube, so that the excessive culture media could easily be removed with a pipette. The spheroids were pipetted on to the OCT compound along with a miniscule remnant of media, which could be removed fully once the spheroids had begun to subside into the gel. The goal was to transfer the spheroids into a cassette filled with OCT compound with as little media as possible, to limit the amount of H_2O, which tends to ruin the chances of attaining a clean slice with the cryotome later on. The cassettes were then frozen and stored at -20°C for further processing. 16 to 18µm thin slices were obtained at the cryotome and gathered up on slides immediately. The slides were left outside the cryotome at room temperature to air-dry for a couple of minutes, before immersing them in a container with 4°C cold formalin for fixation. If the spheroids had been exposed to pimonidazole before, pimonidazole antibody was applied according to the manufacturer's instructions (0.6µg/ml). As a second antibody and in order to allow for the pimonidazole stain to be analyzed by fluorescence microscopy, red fluorescent AlexaFluor594-labelled anti-donkey-IgG was used (3.75µg/ml). For fluorescent microscopy, the slides were stained with DAPI, a blue fluorescent marker of cell nucleuses, and mounted with 50%-glycerin-0.2%NPG-PBS.

3 Results

The aim of this study was to better characterize CCL5-based engineered MSC, and to evaluate new targeting strategies. Herein, the study focused on tumor hypoxia and externally applied hyperthermia. To this end, three different targeting strategies were examined for genetically engineered MSC: using gene promoters based on CCL5, HIF1α HSP70b biology.

3.1 Rantes/CCL5 is activated in MSCs in tumor stroma via inflammatory cytokines

3.1.1 IL1-β, TNF-α and γIFN appear to be responsible for CCL5 activation in tumor stroma

As was previously shown in the work of Christoph Zischek and colleagues, CCL5 biology can be used to enhance the specificity of genetically engineered MSC. CCL5 is up-regulated in MSC that have infiltrated tumor stroma. When adoptively applied MSC invade growing tumor stroma, a CCL5-driven reporter or therapeutic gene can become activated specifically in the desired area.

What was largely unknown, was which factors present in the tumor stroma lead to the up-regulation of CCL5 seen in MSC. As we know from previous studies, CCL5 serves as a stress response signal. As a first step, immortalized MSC (Alex-2) were used for in vitro experiments to measure CCL5 protein production in the supernatant via specific ELISA, in response to treatment with a range of cytokines associated with tumor inflammation and the stress response, namely IL-6, VEGF, TNF-α, IL-10, Wnt5a, IL-1β, γ-IFN and TGF-β1. These cytokines are thought to be present in the tumor microenvironment and thus may influence the ability of cells to respond to inflammatory signals. As detailed in chapter 1.1, both IL-6 and TGF-β1 are involved in recruitment, activation and differentiation of tumor-associated fibroblasts within the tumor microenvironment. Wnt5a is thought to have both tumor-suppressive and tumor-promoting effects, for instance through enhanced differentiation of tumor-associated fibroblasts (Endo 2014). VEGF is responsible for increasing oxygen supply to the tumor stroma by inducing angiogenesis (see chapter 1.2) and Voronov *et al* were able to show similar effects of IL-1β (Voronov 2003). TNF-α has been previously shown to be a potent activator of CCL5 expression in some, but not all cell types (see chapter 1.2.1). IL-10 is thought to reduce inflammation and could thus potentially limit CCL5 expression (Sabat 2010). Last but not least, γ-IFN has been shown to recruit immune-modulating cells to the scene of inflammation, as was detailed in chapter 1.1.

The results provided in Figure 2-B show a ten-fold increase in CCL5 expression after 24h incubation with TNF-α at various concentrations. A five-fold activation was provoked by stimulation with IL-1β. Only a moderate effect was seen with stimulation by γIFN. A combined and more powerful effect was seen through double stimulation, for example with TNF-α and γ-IFN. While the effect of γ-IFN alone on CCL5 expression was not significant, the combination of TNF-α and γ-IFN created a more than additive effect than that seen with TNF-α alone. TGF-β1 has been proposed to activate CCL5 expression in tumor fibroblasts (Borczuk 2008). However, the experiments here showed that treatment with TGF-β1 was not able to induce expression of CCL5 by MSC. In subsequent ELISA experiments, the potential interplay of TNF-α, IL1-β and γ-IFN was examined in more detail. Figure 2 shows again that stimulation through γIFN does not produce a significant effect. However, a combination of TNF-α and γIFN was able to enhance CCL5 expression more than with TNF-α alone. The biggest effect was achieved by stimulating CCL5 expression with all three cytokines at once. This suggests that the activation of CCL5 in MSC that have invaded tumor stroma is to a great extent regulated by an inflammatory milieu.

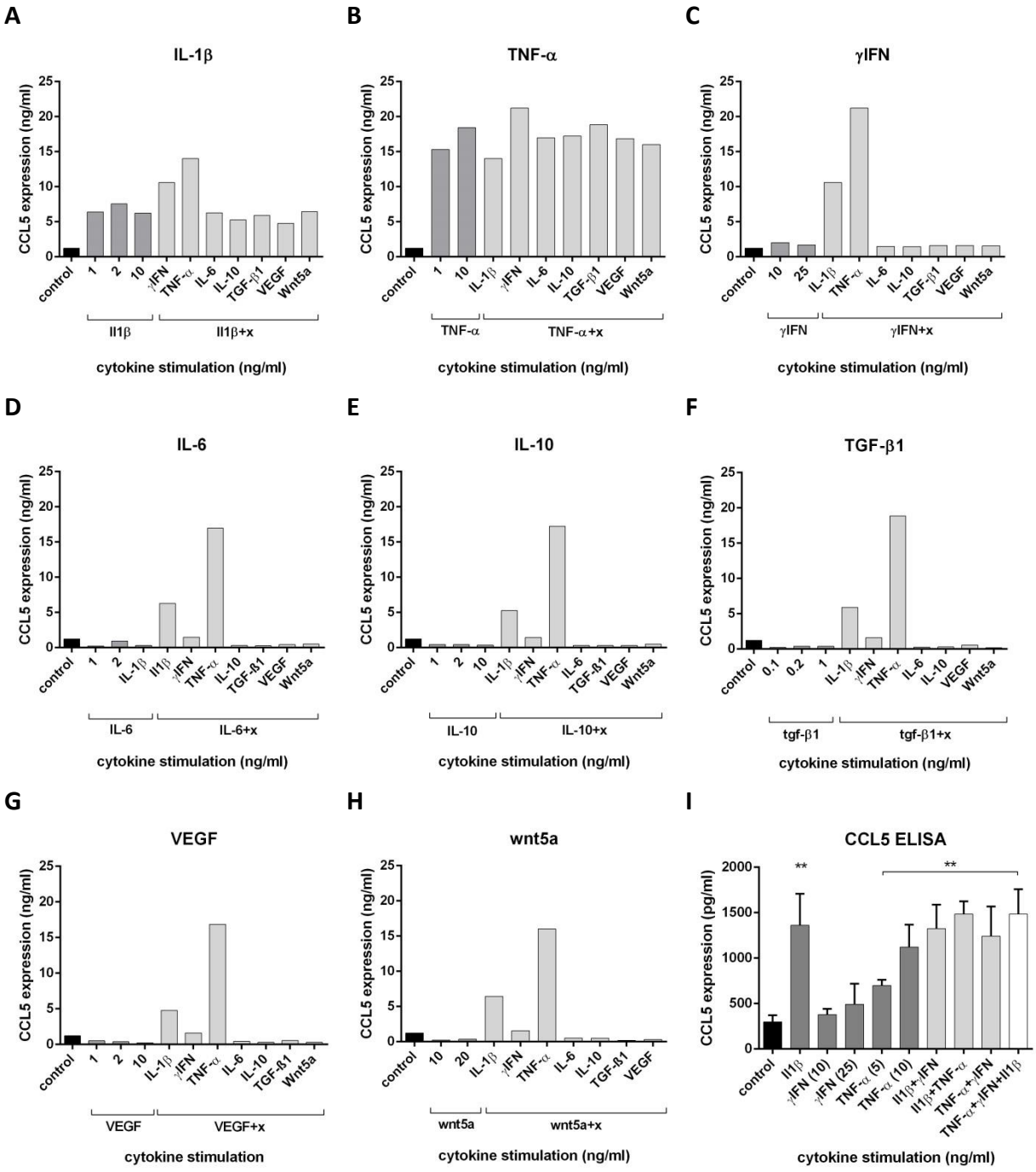

Figure 2: *In vitro* stimulation of CCL5 expression (ELISA). (A-H) Cells (Alex-2) were seeded in 96-well plates and cytokines added six hours later. After 36h incubation, the supernatant was harvested and immediately stored at -20°C. ELISA was performed with a 1:100 dilution of the supernatant. Recombinant human cytokines (commercially available) were used. Concentrations in single cytokine assays (n=1) as indicated within the graphs for the respective cytokine, concentrations for additional cytokines (n=2) as follows: IL1-β=1ng/ml, γIFN=10ng/ml, IL-6=1ng/ml, IL-10=1ng/ml, TGF-β1=0.1ng/ml, VEGF=1ng/ml, Wnt5a=10ng/ml. **(I)** Cells (Alex-2) were seeded out the previous day. Human recombinant cytokines were added along with reducing fetal calf serum (FCS) content to 5% instead of 10%. After 24h incubation, the supernatant was harvested and immediately stored at -20°C. Concentrations in single cytokine assays as indicated, concentrations for double or triple cytokine assays as follows: IL1β=1ng/ml, TNF-α=5ng/ml, γIFN=10ng/ml. Statistical analysis was performed by applying Mann-Whitney-U-Test (n=5, P=0.0079). Stimulation with γIFN alone yielded no significant result.

Measuring protein secretion was a good means of screening for factors that could induce native CCL5 production in MSC. To then determine if these effects could translate to moderation of CCL5 promoter activity, a -971-upstream region of the human CCL5 gene promoter was cloned into an expression vector, and the construct was transiently introduced into two human MSC-lines (using either lipofectamine for Alex-2 or electroporation for L87), and the ability of the cells to respond to specific signals was monitored using firefly luciferase assays. To control for transfection efficiency, the control plasmid pRL-CMV was co-transfected at a 1:50-ratio and the firefly luciferase values were normalized to renilla luciferase. After transfection and overnight incubation, the cells were incubated for an additional 24h with recombinant human TNF-α or TGF-β1 added to cell culture media. Afterwards, the cells were lysed and the lysate subjected to a dual light luciferase assay. As demonstrated in figure 3, the addition of TNF-α causes a low but statistically relevant effect on luciferase activity. TGF-β1, on the other hand, produced no such effect, confirming the ELISA assays.

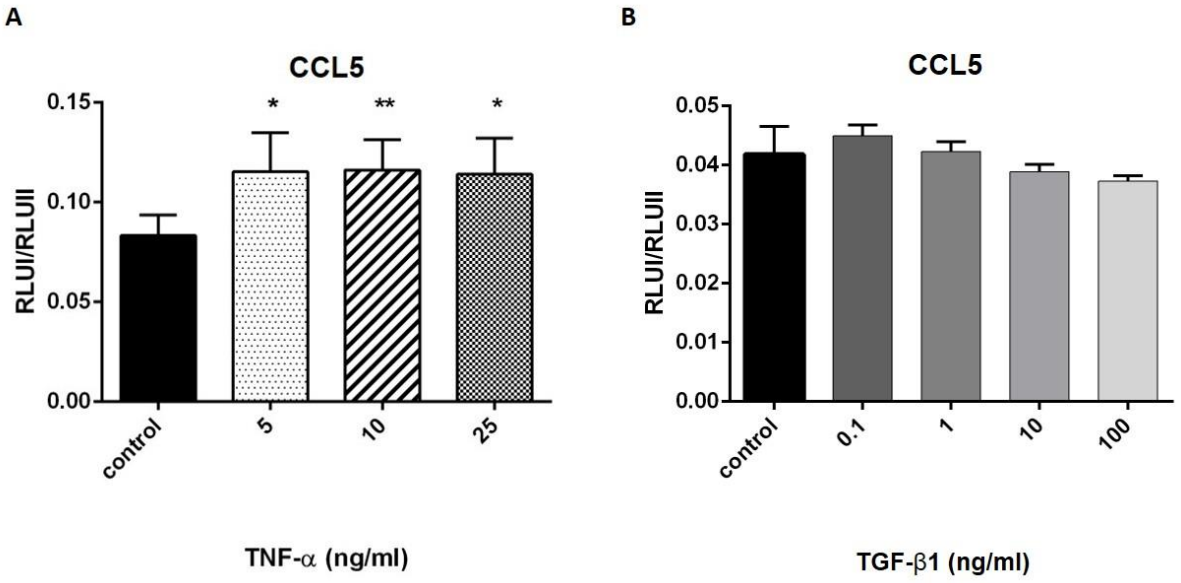

Figure 3: *In vitro* stimulation of CCL5 expression (luciferase assay). (A) Cells (Alex-2) were seeded out in 96-well plates (n=5) and transiently transfected with PGL3-RFL using lipofectamy according to protocol. Six hours after transfection culture media was changed along with adding human recombinant TNF-α at indicated concentrations. After 24h incubation under normoxic conditions cells were lysed and luciferase activity was determined according to protocol. Statistical analysis was performed by using the Mann-Whitney-U-Test (**: P=0.0079, *: P=0.0159). The experiment was repeated several times to the same effect. **(B)** Cells (L87) were harvested and transiently transfected with PGL3-RFL using electroporation (230V; 1 million cells in 100µl culture media without antibiotic along with 4µg pGL3-RFL and 0.08µg pRL-CMV per electroporation cuvette) before being seeded out in 96-well plates (n=5) and incubated at normoxia. Addition of human recombinant TGF-β1 followed after overnight incubation. 24h later, cells were lysed and luciferase activity was determined according to protocol. Statistical analysis was performed by applying Mann-Whitney-U-Test and yielded no significant result. The experiment was repeated several times to the same effect.

3.1.2 CCL5 is not stimulated by heat shock

To further investigate the potential effect of heat shock, or hyperthermia on CCL5 transcription, immortalized MSC (L87) were transiently transfected, using lipofectamine, with the very same plasmid construct that has already been used for the previous experiments. After 24 hours incubation, the cells were exposed to hyperthermia using a water bath, with the temperature adjusted to 42°C. Exposure time was set to 30 minutes, after which the cells were returned to the standard incubator (37°C) for another 24 hours of incubation. Subsequently, the cells were lysed and the lysate tested for luciferase activity. The result of the luciferase assay is demonstrated in Figure 4-A. No significant effect of heat shock on CCL5 expression can be noted. The experiment was repeated several times, to the same effect.

3.1.3 CCL5 is not stimulated by hypoxia

The expression of CCL5 is generally thought to be a response to stress. Tissue hypoxia poses a threat to the cell and the promoter region for CCL5 contains potential transcription factor binding sites for the HIF-1 factor (Nelson 1993). To test if hypoxia also potentially contributes to CCL5 promoter activity, MSC (L87, Alex-2) were transiently transfected with the CCL5 and control expression constructs. They were then placed in a hypoxic incubator, set to an oxygen level of 2% via insufflation of a gaseous mixture (95% nitrogen, 5% carbon dioxide), for a further 24h incubation. As shown in figures 4-B and 4-C, no significant effect on reporter activity was seen in response to hypoxic conditions. Because hypoxia is known to be a key player in tumor growth and prognosis, we then sought to determine if the general response of MSC to hypoxia could potentially act as an additional strategy for the activation of transgenes in engineered MSC.

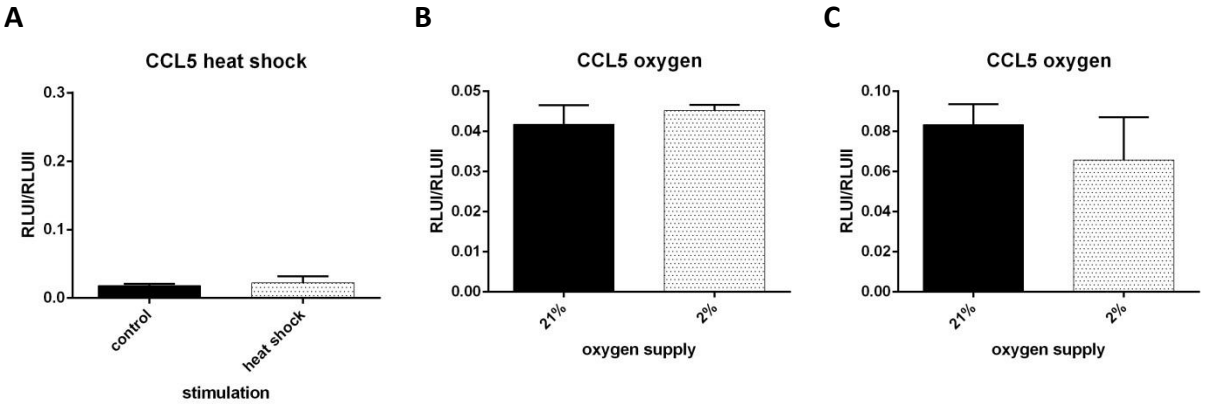

Figure 4: *In vitro* stimulation of CCL5 expression by heat shock or hypoxia (luciferase assays). (A) Cells (L87) were seeded out in 96-well plates on day 1. On day 2, transient transfection with PGL3-RFL was performed by using lipofectamy according to protocol. 6 hours after Transfection, culture media was exchanged and cells were incubated for 24 hours at 37°C. On day 3, cells were subjected to heat shock for 30 minutes by using a 42°C water bath. Cells were subsequently

returned to the 37°C incubator and incubated for another 24 hours, before being analysed for luciferase activity. The experiment was repeated several times and yielded no statistically significant result. **(B)** Cells (L87) were harvested and transiently transfected using electroporation (230V; 1 million cells in 100µl culture media without antibiotic along with 4µg pGL3-RFL and 0.08µg pRL-CMV per electroporation cuvette) before being seeded out in 96-well plates. Cells were then incubated at 21% oxygen overnight before one of the plates was being moved to a hypoxic incubator set to an oxygen level of 2%. After another 24 hours incubation, cells were lysed and luciferase activity was determined according to protocol. The experiment was repeated several times and yielded no statistically significant result. **(C)** Cells (Alex-2) were seeded out in 96-well plates (n=5) and transiently transfected with PGL3-RFL using lipofectamy according to protocol. Six hours after transfection culture media was changed and one plate was moved to a hypoxic incubator set to an oxygen level of 2%. After another 24 hours incubation, cells were lysed and luciferase activity was determined according to protocol. The experiment was repeated several times and yielded no statistically significant result.

3.2 HIF1α is stabilized in MSC in hypoxic areas of solid tumors

3.2.1 pGL3-hypoxia: Hypoxia-responsive synthetic promoter comprised of six HIF1α-responsive elements driving a minimal promoter

As detailed earlier, HIF1α is constantly expressed, but rapidly turned over in normoxic cells. The protein becomes stabilized under hypoxic conditions, and then acts as a transcription factor. One goal of this study was to develop a system where hypoxia in MSC could be easily detected through a promoter-reporter construct. The reporter construct used here was based on the idea that HIF1α, as a transcription factor, binds to specific short sequences of nucleotides within the promoter region of a gene in order to up-regulate gene expression. These consensus sequences for HIF1α-responsive elements (HRE) consist of five core nucleotides: A or G followed by CGTG. The promoter used in this study (which has been kindly provided by Prof. Dr. Grässer of Saarland University, Bad Homburg, Germany) contains six of these short sequences driving a minimal promoter based on the thymidine kinase (TK) promoter, as shown in figure 5.

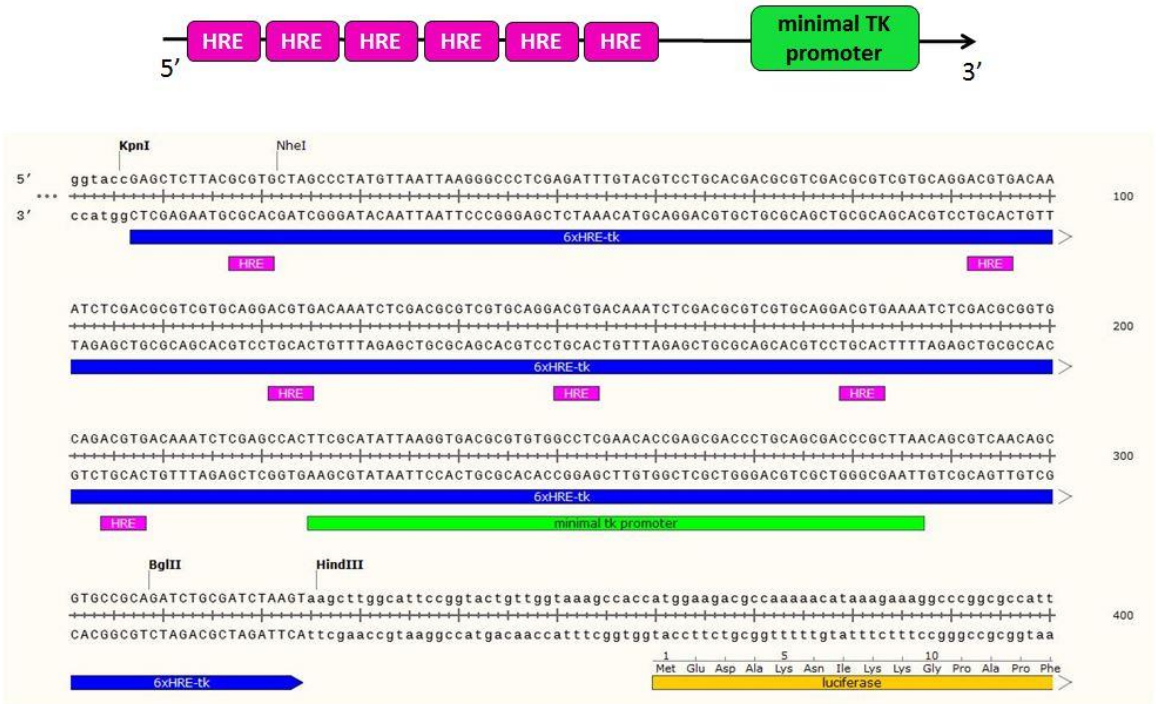

Figure 5: HIF1α-responsive elements (HRE) lined up on the 5'-end of a TK minimal promoter.

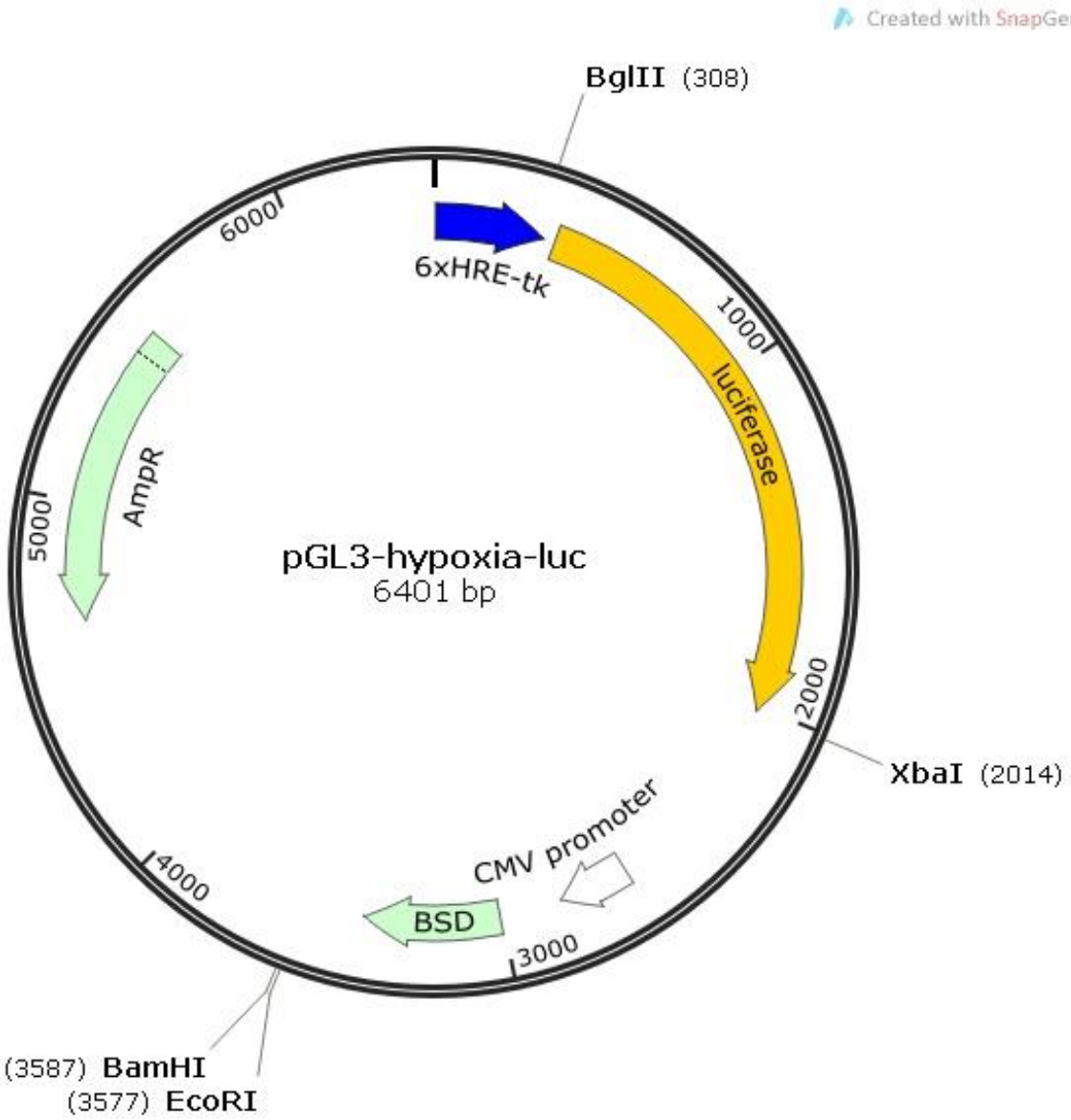

Figure 6: Plasmid map of pGL3-hypoxia-luc. A construct based on the pGL3-Basic by ProMega®, with the 6xHRE-promoter inserted in the multiple cloning site and a Blasticidin resistance inserted into the backbone. The latter was achieved by introducing CMV-Bsd at the BamHI site in the pGL3-vector.

3.2.2 *In vitro* HIF1α-stabilization in MSC using cobalt chloride treatment or a hypoxic incubator

For *in vitro* studies in cell culture, HIF1α can be stabilized and thus studied, either by creating hypoxic conditions, for example by using a hypoxic incubator or a chamber system, or by artificially stabilizing HIF1α through chemical treatment, in this case by adding cobalt chloride to the culture media. Preliminary experiments revealed an astonishing robustness of MSC towards hypoxia. The oxygen level for experimental hypoxia used in this study was usually 2%. Cobalt chloride has been described in the literature as a potent HIF1α-stabilizer. Preliminary experiments regarding cobalt chloride concentrations suggested that 300µM represents an optimal concentration for the MSC experiments (data not shown). Cobalt chloride and the hypoxic incubator were directly compared with regards to HIF-1 activity in MSC. As observed in figure 7, hypoxic incubation of immortalized MSC (Alex-2) led to an increase of HIF1α protein concentration as determined by western blot. The next step was to transiently transfect immortalized MSC with the pGL3-hypoxia-luc (along with pRL-CMV as positive control) and to quantify luciferase activity in response to either hypoxia (hypoxic incubator) or cobalt chloride. Similar results were obtained for both stimuli (Figure 8). Stimulation resulted in a ten-fold increase of luciferase activity. For transient transfections, pGL3-hypoxia-luc served as a good system. However, stable transfection would provide a more robust platform for subsequent experiments. To this end, it became necessary to optimize transfection efficiency and generate stable cell lines.

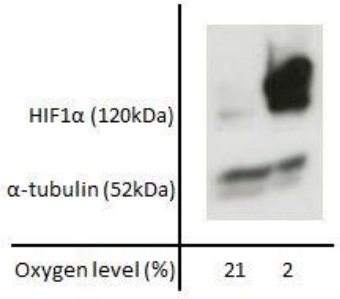

Figure 7: HIF1α-stabilization in MSC *in vitro* through hypoxia. Cells (Alex-2) were plated out in 6cm culture dishes at 75% density and incubated overnight at the indicated conditions. Afterwards, cells were rinsed in PBS and extracts for western blot analysis were obtained by adding a pre-conditioned RIPA-buffer (see chapter 2.1.3.1 for more information). The cell lysate was subsequently incubated on ice for one hour, centrifuged and the supernatant stored at -20°C for future analysis. Exposure time: 5'.

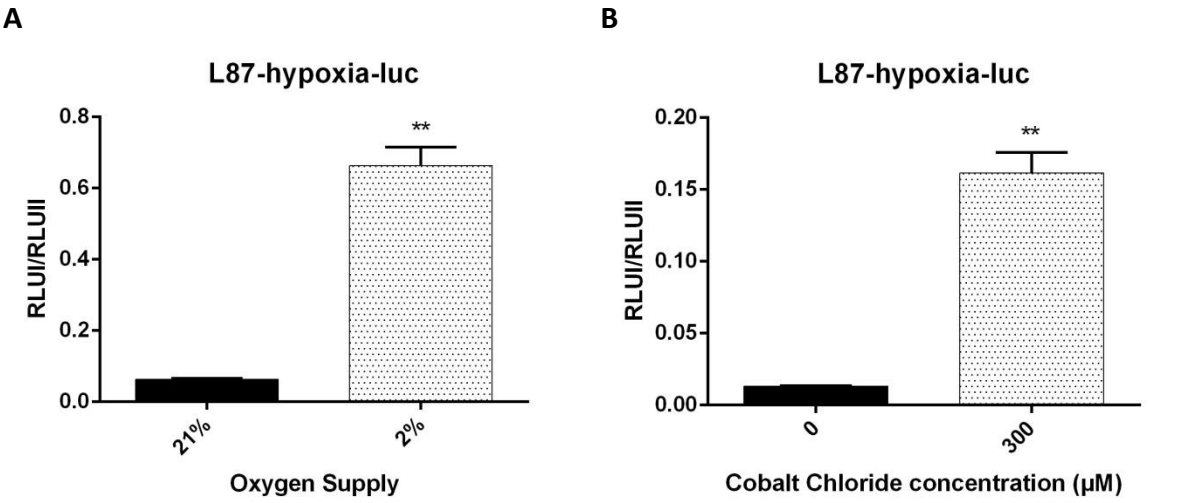

Figure 8: HIF1α-induced transcription in MSC *in vitro* through hypoxia or cobalt chloride. (A)+(B) Cells (L87) were transiently transfected using electroporation (230V, 1 million cells per 100µl culture media without antibiotics, 4µg pGL3-hypoxia plus 0.08µg pRL-CMV per cuvette) and incubated for 48 hours at the indicated conditions. Subsequently, cells were lysed and luciferase activity was determined according to protocol. For statistical analysis Welch-corrected t-test was applied (P=0.0024).

3.2.3 pcDNA-ITR-HIF-Cherry/Gaussia/TK: integrating *Sleeping Beauty* into the backbone of the reporter vector enhances the efficiency of stable transfection in MSC

3.2.3.1 Gateway Cloning

In order to maximize the stable transfection efficiency of plasmid vectors, it was decided to make use of a Sleeping Beauty Transposon system. To this end, a plasmid was designed that had two ITR (inverted terminal repeats) sites flanking the region containing the promoter and the gene of interest, thus forming a transposon. For stable transfection, the cells were co-transfected with a plasmid containing the transposon and a second expression plasmid carrying the Sleeping Beauty transposase (SB100X). The transposase SB100X excises the transposon from the original plasmid and integrates it into the DNA of the host cells at specific TA dinucleotide sites (Jaeckel 2016).

The general cloning strategy was also based on the *Multisite Gateway Pro Plus* kit, a commercially available kit. As was already mentioned in chapter 2.2.3.2, the kit allows to clone plasmids in a short time by applying a mix and match strategy. For this project, two different types of entry vectors (pENTR) were designed that could be integrated back to back into a destination vector (pDEST), forming a new plasmid, called an expression vector. The entry vectors contained either a promoter, in this case the hypoxia-sensitive 6xHRE-tk-promoter, or a reporter gene, either mCherry or Gaussia-luficerase. For future experiments, an entry vector that contained thymidine kinase, a therapeutic gene, was designed simultaneously.

To create the entry vectors, the promoters and genes of interest had to be “copied” out of their original vector and amplified via PCR. To this end, primers were designed that could be used to duplicate the desired amplicon from the template, and at the same time, add the specific nucleotides at either end of the amplicon, that were needed to generate the sequences for the entry vector and expression vector.

Forward and reverse primers were designed using the *Clone Manager* software under consideration of size and temperature and avoiding dimers. The attB recombination sites were added according to the manufacturer’s instructions. The amplicon containing the promoter was thus flanked by an attB1 site on the 5’ end and an attB5r site on the 3’ end. The reporter genes were flanked by attB5 and attB2, respectively. For primer sequences please turn to chapter 2.1.8. The PCR products were then integrated into the entry vectors by performing the BP reaction (Figure 9). The resulting DNA constructs were checked for correct integration of the PCR products by restriction digest and sequencing (done by GATC).

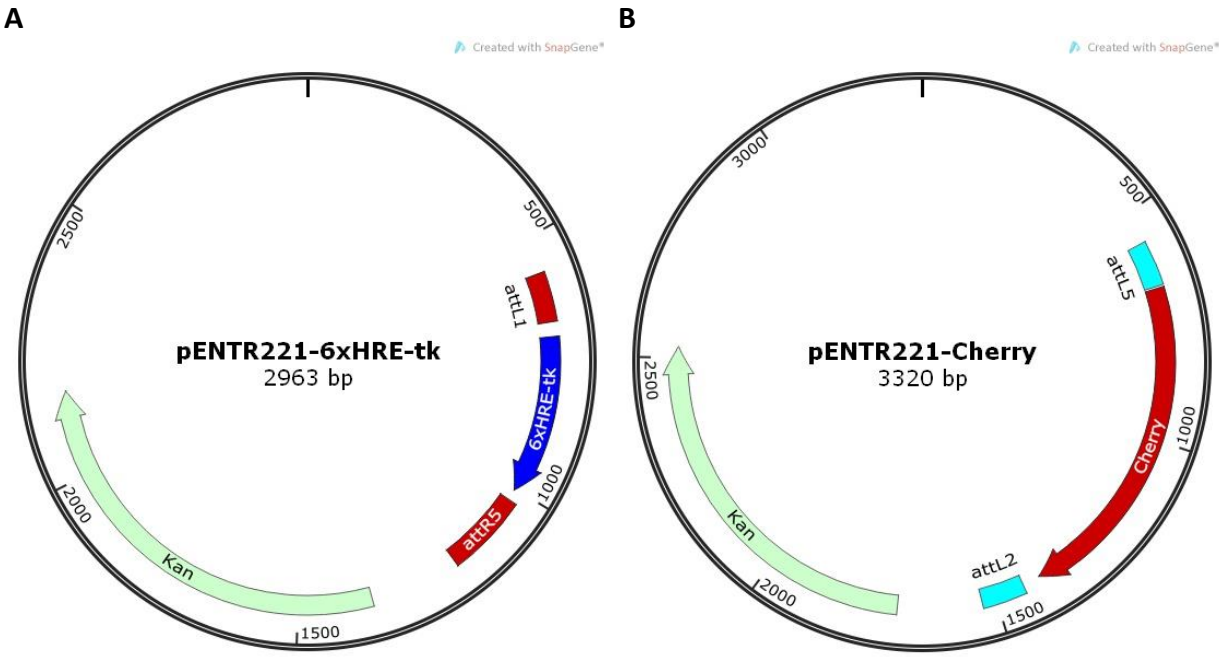

Figure 9: pENTR221-vectors. (A) Entry vector containing the hypoxia-responsive promoter 6xHRE-tk now flanked by attL1 and attR5 recombination sites (highlighted in red). **(B)** Entry vector containing the reporter gene mCherry now flanked by attL5 and attL2 recombination sites (highlighted in blue). AttR5 and attL5 recombination sites will later merge and create a new attB5 site.

In the following LR reaction, recombination took place between the two entry clones and a destination vector, in this case pcDNA6.2PLITRBlasti-Dest, a plasmid provided by Carsten Jäckel that contains two Sleeping Beauty transposition sites framing the Gateway cloning site and a Blasticidin

resistance gene in the backbone (for a plasmid map, turn to chapter 2.2.3.2). The resulting expression vector pcDNA-ITR-HIF-Cherry contains the hypoxia-responsive promoter 6xHRE-tk followed by the reporter gene mCherry, flanked by the transposition sites, and an additional Blasticidin resistance in the backbone (Figure 10). Again, the resulting clones were checked for correct gene integration by restriction digest and sequencing (done by GATC).

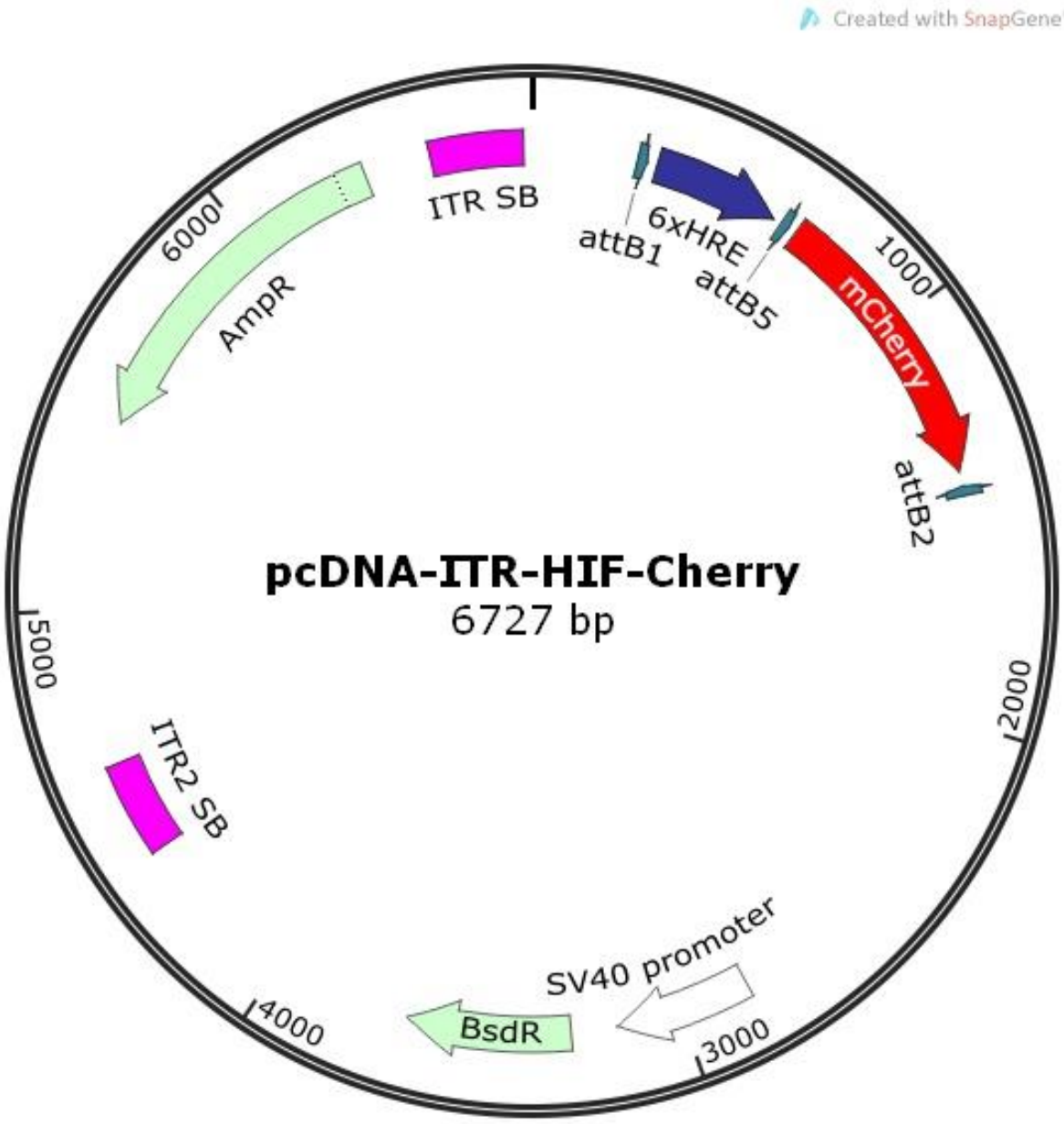

Figure 10: pcDNA-ITR-HIF-Cherry plasmid map. Sleeping Beauty transposition sites are highlighted in pink, att recombination sites are highlighted in yellow.

3.2.3.2 Creating a stable MSC cell line using pcDNA-ITR-HIF-Cherry

The plasmid pcDNA-ITR-HIF-Cherry was subsequently used for stably transfecting MSC lines. The L87 MSC cell line was used, as it could be passaged over a long period of time without ceasing to proliferate, while still maintaining key stem cell characteristics. For stable transfection, the pcDNA-ITR-HIF-Cherry was added to the electroporation mix along with pCMV-SB100X, the plasmid containing the Sleeping Beauty transposase, in a 1:3-ratio. 48 hours after electroporation, selective media containing Blasticidin was added. After a fortnight, cells were ready to be passaged for the first time and simultaneously checked for plasmid expression.

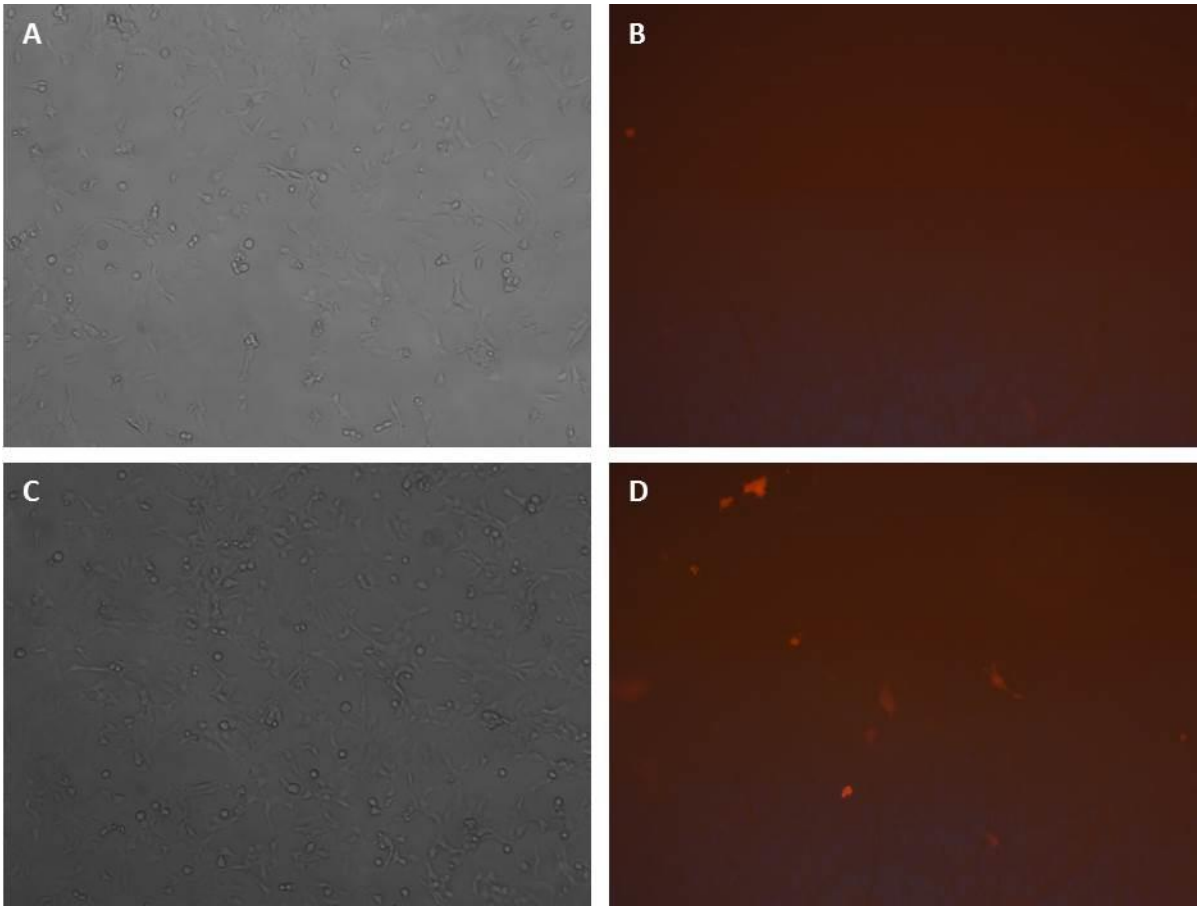

Figure 11: mCherry-expression in L87-HIF-Cherry. Images were taken after 24h incubation at 21% oxygen **(A+B)** or 2% oxygen **(C+D).** After comparison of the two in bright field **(A+C)** and fluorescent **(B+D)** microscopy, it becomes evident that there is good activation of the transgene. However, transfection efficiency is mediocre. Images were taken in ten-fold magnification with overall identical exposure time.

As can be observed in figure 11, activation of the transgene is visible under the fluorescent microscope. However, transfection efficiency was still not sufficient for the cells to be included in further experiments, as in case of a negative result it is uncertain whether this was due to a poor

expression rate or due to an actual lack of hypoxia. To resolve this, it was decided to subject the transfected cells to FACS analysis and eventually sorting for expression of the transgene. This was done in collaboration with the Insititut für Molekulare Immunologie, Helmholtz Zentrum Munich (Dr.rer.nat. Dipl-Biol. J.J. Mysliwietz, Prof. Dr. rer.nat. E.Nössner). At the time, the transfected cells were analyzed by FACS, only 1.1% expressed the transgene under normoxia, and 2.7% under hypoxia (see figure 12). Subsequently, cells were expanded in 300cm^2 flasks to a total number of 15 million and subjected to FACS sorting two weeks after the initial analysis. For the sort, cells were not incubated in hypoxia beforehand as the aim was to select cells with the highest transfection efficiency and expression rate. With an expression rate of 0.9%, 13.000 cells remained that expressed the transgene (see figure 13). These cells were plated out on 96-well plates, applying limited dilution aiming for single clones. After a few more days, cultured in selective medium, the cells began to grow out in wells and were tested for transgene activation by incubating them at 2% oxygen for 24 hours. Fluorescence microscopy of the clones resulted in two of them, B12 and C10, being transfected to a satisfactory result (see figure 14).

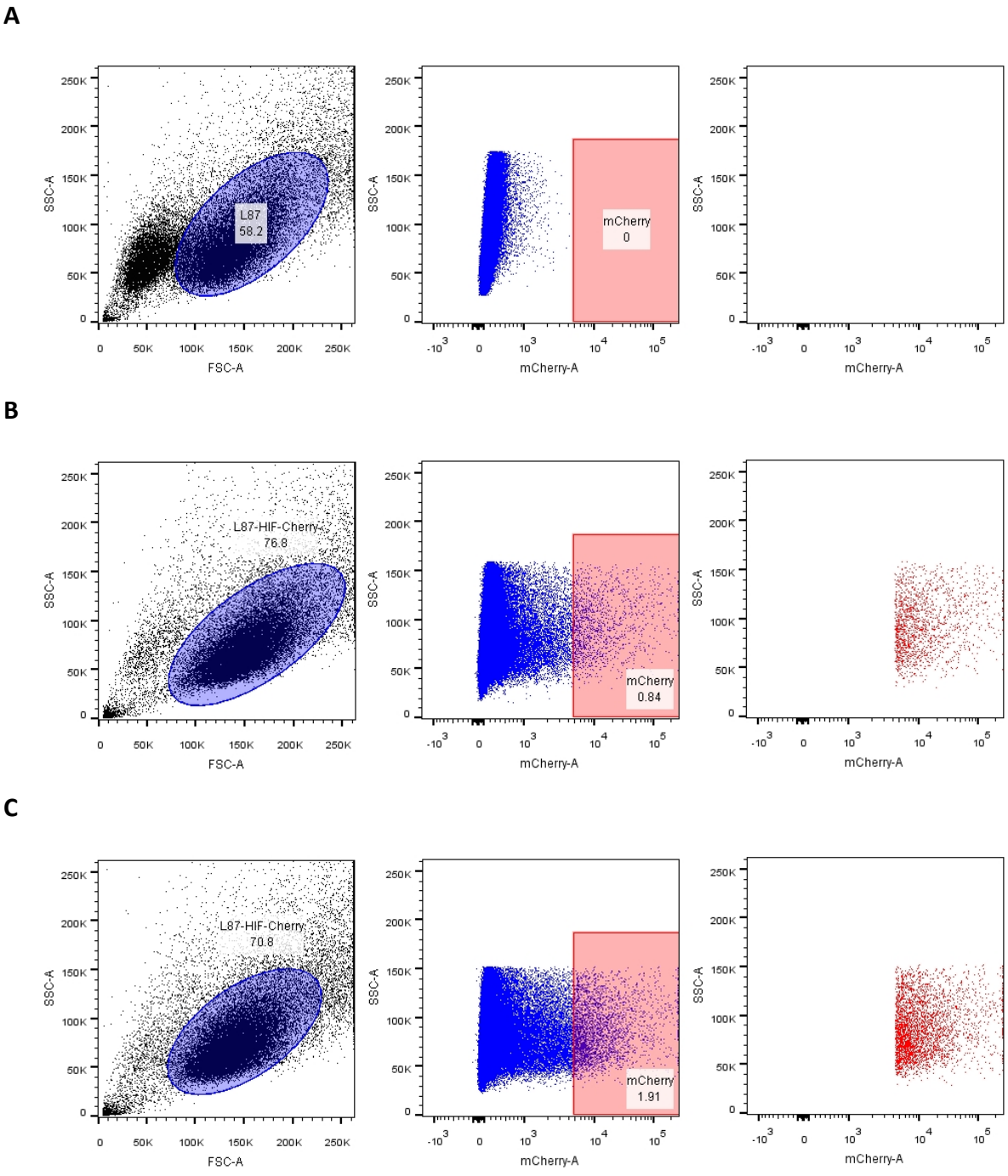

Figure 12: Transgene expression in L87-HIF-Cherry, analyzed by FACS. (A) Empty L87 cells were used as a negative control in order to set the gate for mCherry expression. **(B)** L87-HIF-Cherry incubated under normoxic conditions were analyzed by FACS using the same settings established by analysis of empty L87. 1.1% of the cells identified as viable before came up in the gate set for mCherry expression. **(C)** L87-HIF-Cherry incubated under hypoxic conditions (2% oxygen) were analyzed by FACS using the same settings established by analysis of empty L87. 2.7% of the cells identified as viable before came up in the gate set for mCherry expression.

A

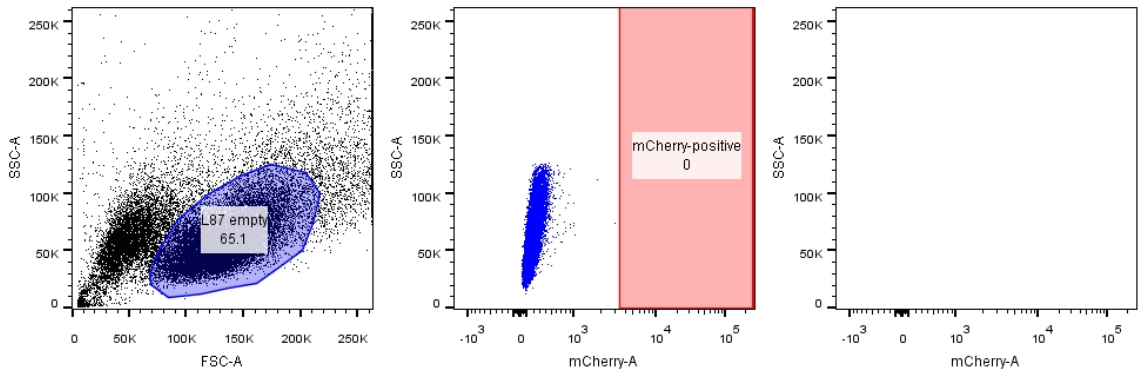

B

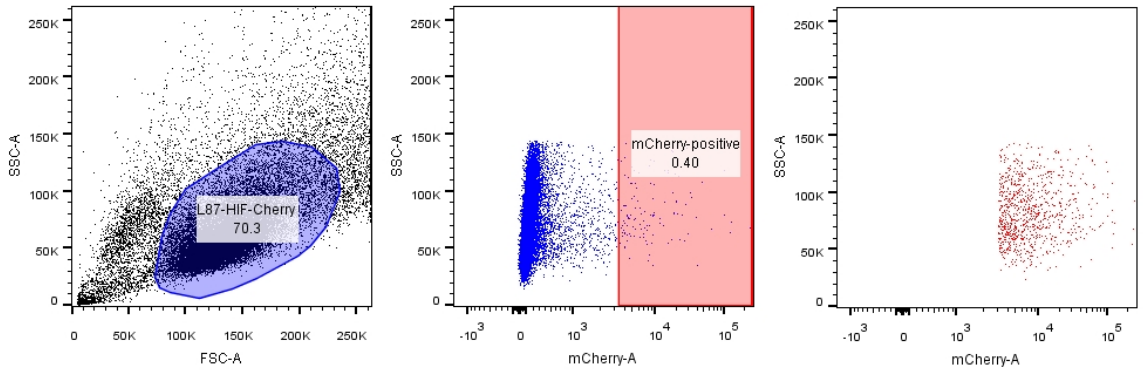

Figure 13: Selection of cells with sufficient transgene expression by FACS. (A) FACS analysis of empty L87 cells in order to set the gate for mCherry expression. **(B)** L87-HIF-Cherry that were incubated under normoxic conditions were analysed and sorted by FACS for transgene expression. Cells coming up in the SSC-A/mCherry-window made up 0.6% of all cells earlier identified as viable. These cells were collected in a 1.5ml-tube containing culture media with 20% FCS and immediately stored on ice for transport.

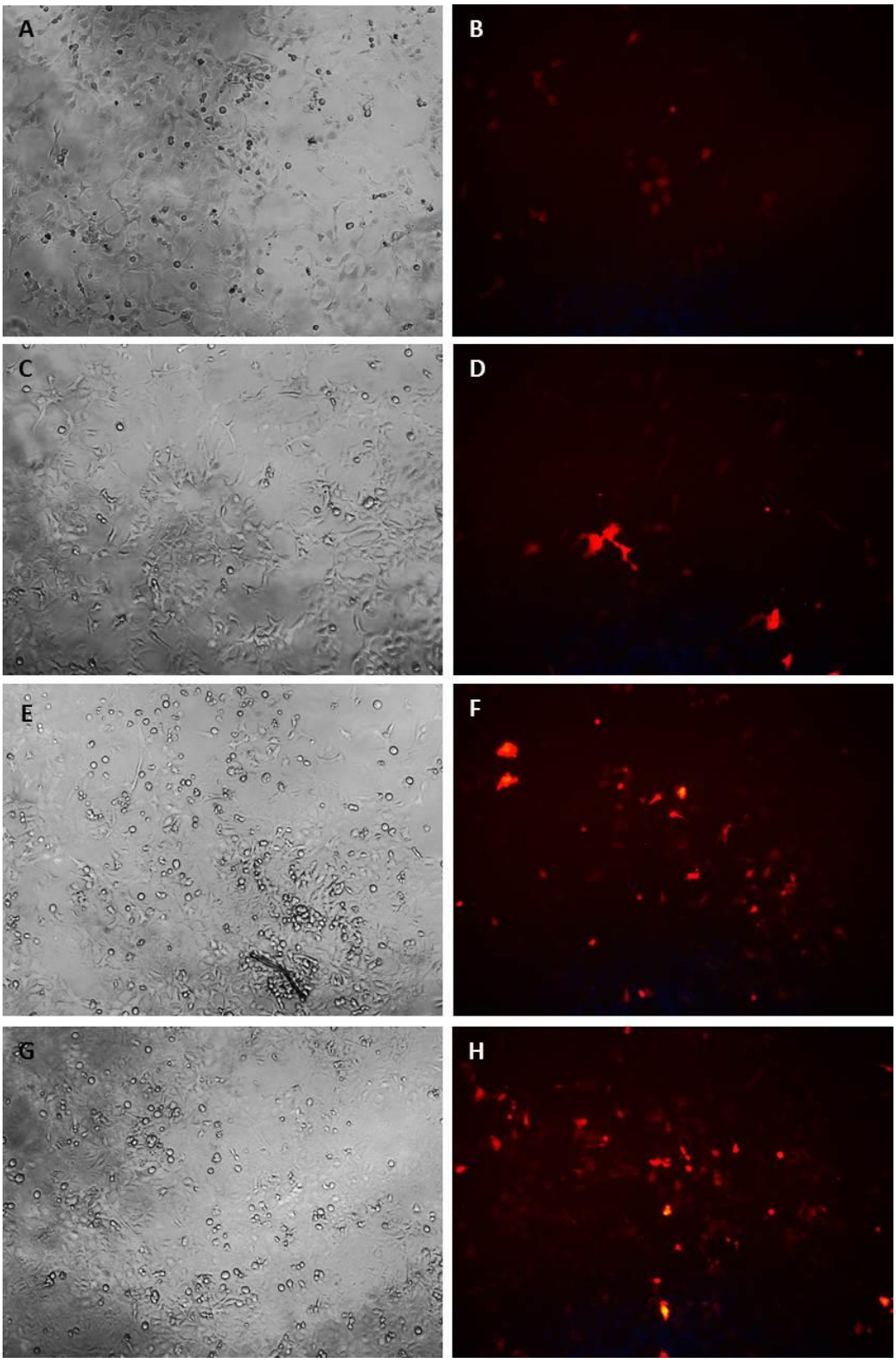

Figure 14: Clones B12 and C10 in light and fluorescence microscopy: All images were taken in ten-fold magnification with identical exposure times. **(A)+(B)** Clone B12 incubated in 21% oxygen for 24 hours. **(C)+(D)** Clone C10 incubated in 21% oxygen for 24 hours. **(E)+(F)** Clone B12 incubated in 2% oxygen for 24 hours. **(G)+(H)** Clone C10 incubated in 2% oxygen for 24 hours.

3.2.4 Creation of spheroids from Hepatocellular Carcinoma Cells and MSCs

To study the behavior of MSC in experimental settings that more closely resemble tumors, a system was established that was able to render a reproducible *in vitro* tumor model. To this end, a series of preliminary experiments (data not shown) was performed to generate spheroids from the hepatocellular carcinoma (HCC) cell line Huh7. To grow spheroids, the Huh7 cells were distributed in culture dishes that had been coated with polyHEMA (see chapter 2.2.1.4). Thus, they were unable to attach to the plastic, but instead grew into spheroids from single cells. After 6 to 10 days in culture, spheroids made from Huh7 cells typically reached a size of 400 to 600 µm.

3.2.4.1 Huh7- and L87-spheroids merge in co-culture

The first experiments investigated the potential interaction between Huh7 and MSC, by co-culture experiments with spheroids. To this effect, spheroids were grown from both Huh7 and MSC (L87) that had been stained with CMTMR and CMFDA, respectively, to distinguish them using fluorescent microscopy. After 24 hours of co-culture, the spheroids had grown into a single larger spheroid that contained both CMTMR- and CMFDA-stained cells (see figure 15).

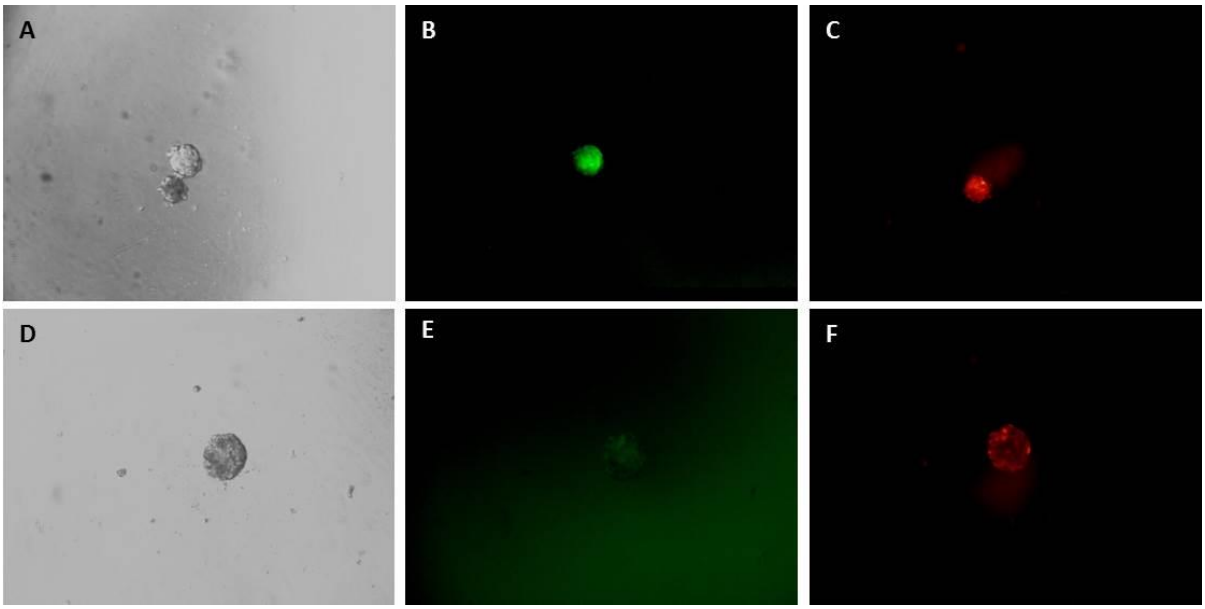

Figure 15: Spheroids from Huh7 and L87 in co-culture. Huh7 and L87 cells were harvested, stained with fluorescent markers CMTMR (Huh7, orange) and CMFDA (L87, green) and plated out in limited dilution in 96-well plates coated with polyHEMA on day 1. On day 2, most wells contained a single spheroid, which could easily be extricated. A new 96-well plate was populated with one Huh7- and one L87-spheroid each. Images **(A)-(C)** all show the same well and were taken shortly afterwards. On day 3, after 24 hours in co-culture, images **(D)-(E)** were taken, which all show the same well again.

3.2.4.2 CMFDA-labeled MSC invade Huh7-spheroids in vitro

As a next step, MSC invasion of tumor spheroids was studied. The Huh7 spheroids were co-cultured with primary human bone-marrow-derived MSC. The primary MSC were stained with the fluorescent marker CMFDA. Huh7 spheroids were grown as described above using polyHEMA-coated culture dishes. CMFDA-stained MSC were added to the media and the spheroids incubated for 72 hours before being embedded and sectioned using a cryotome. Figure 16 shows images taken with the sections viewed under a fluorescent microscope. The results show an efficient invasion of the primary MSC directly into the core of the spheroid.

In the next set of experiments, Huh7 spheroids were incubated with pimonidazole and cryosections were stained with a pimonidazole complex antibody and a fluorescent secondary antibody. Pimonidazole is a 2-nitroimidazole that is reductively activated in hypoxic cells and subsequently forms stable complexes with thiol-groups in other molecules that can be detected by immunohistochemistry (see chapter 2.2.1.4). It is used as a marker for cellular hypoxia. The complexes do not dissociate when the cells become reoxygenated, as may be the case with HIF1α. Figure 17 shows strong pimonidazole staining of the center of a Huh7 spheroid along with invasion by CMFDA-labelled primary MSC.

These experiments show that tumor spheroids serve as a good system to investigate invasion by MSC and can be relied on in further studies involving MSC stably expressing a reporter transgene.

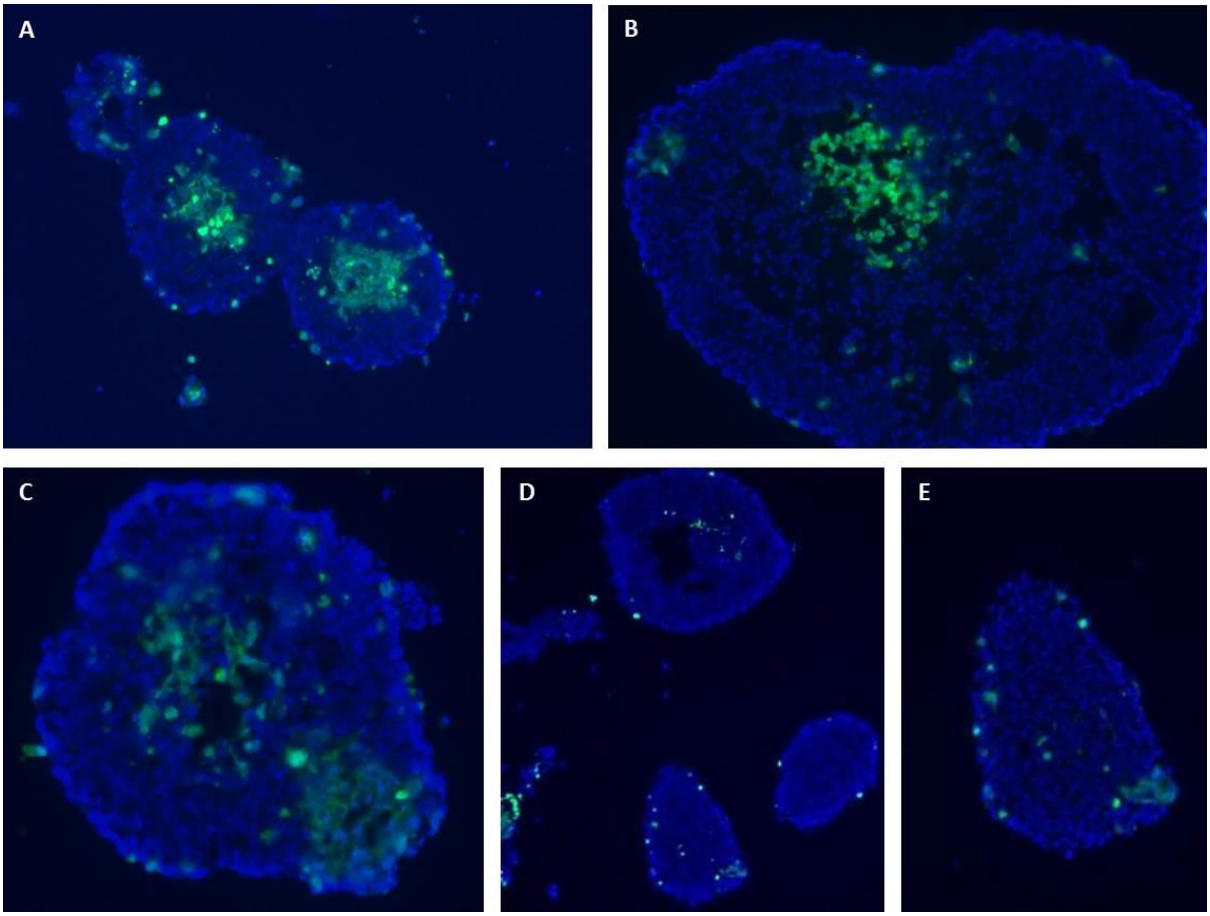

Figure 16: Immortalized MSC invading Huh7 spheroids in co-culture. Spheroids from Huh7 have been grown for eight days in polyHEMA-coated culture dishes. For an additional three days, spheroids were co-cultured with CMFDA-stained immortalized MSC (green). For analysis, spheroids were fixed with formalin and embedded in OCT compund for cryo-sectioning. 18µm-cryoslides were stained with DAPI (cell nucleuses, blue) for fluorescence microscopy.

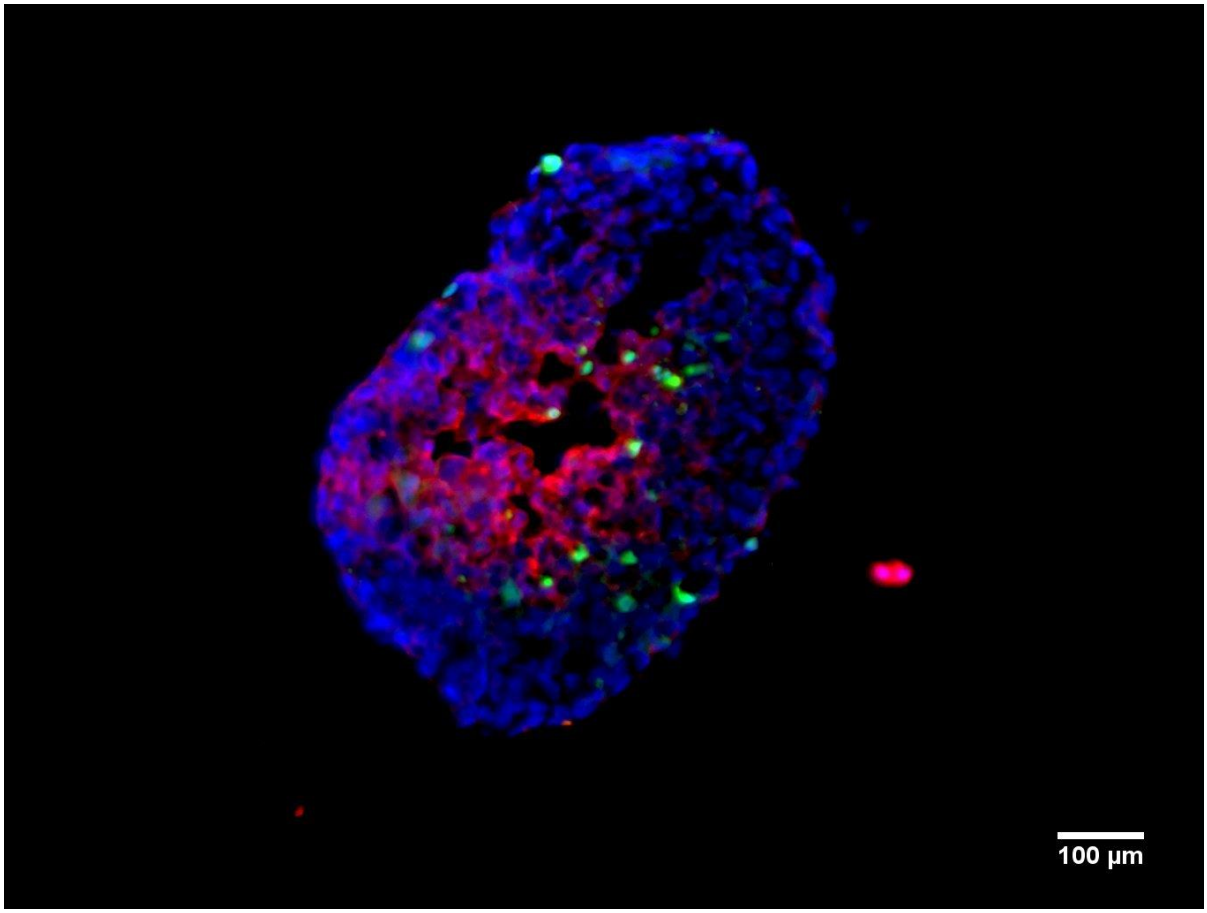

Figure 17: Immortalized MSC invading pimonidazole-labelled Huh7 spheroids in co-culture. Spheroids from Huh7 have been grown for eight days before adding pimonidazole-HCl to the media. For an additional five days, spheroids were co-cultured with CMFDA-stained immortalized MSC (green). For analysis, spheroids were fixed with formalin end embedded in OCT compound for cryo-sectioning. 18µm-cryoslides were stained with pimonidazole-antibody overnight and Alexa Fluor® 594 (red) as secondary antibody as well as DAPI (cell nucleuses, blue) for fluorescence microscopy.

3.2.5 Invasion assay with Huh7-spheroids and CMFDA-labelled L87-HIF-Cherry

When a system for producing and analyzing experimental tumor spheroids, as well as a MSC line engineered with a reporter gene under the influence of a hypoxia-responsive promoter had been established, the two tools were combined to determine if the HIF-responsive MSC induced the reporter gene in response to spheroid invasion. For this experiment, the L87-HIF-Cherry clone B12, as described in chapter 3.2.3.2, was used as the basis for MSC-based control spheroids. As observed in figure 18, the L87-HIF-Cherry formed spheroids that showed activation of the transgene in the MSC cells that were in the center, hypoxic regions of the spheroid.

The next stage of experiments used spheroids grown from the Huh7 cell line incubated with the established L87-HIF-Cherry cell line. For this experiment, the L87-HIF-Cherry clone C10, (3.2.3.2) was used. Huh7 spheroids were grown and then transferred to 1.5ml tubes filled with culture media. Next, the L87-HIF-Cherry, previously stained with CMFDA, were added to the tubes and the latter were placed on a roller plate for two hours for distribution and attachment of MSC to the surface of the spheroids. Afterwards, the spheroids were transferred back into 96-well plates, with one spheroid per well, and incubated for 72 hours. For analysis, spheroids were embedded and sectioned using a cryotome. Figure 19 shows images taken with the sections viewed under a fluorescent microscope. It can be observed, that L87-HIF-Cherry efficiently invade the tumor spheroids, and also activate the hypoxia-responsive promoter and thus the transgene mCherry once they encounter hypoxia within the spheroid. The L87-HIF-Cherry cells that do not activate the transgene, appear green under the fluorescent microscope, while the ones activating the transgene appear orange/red.

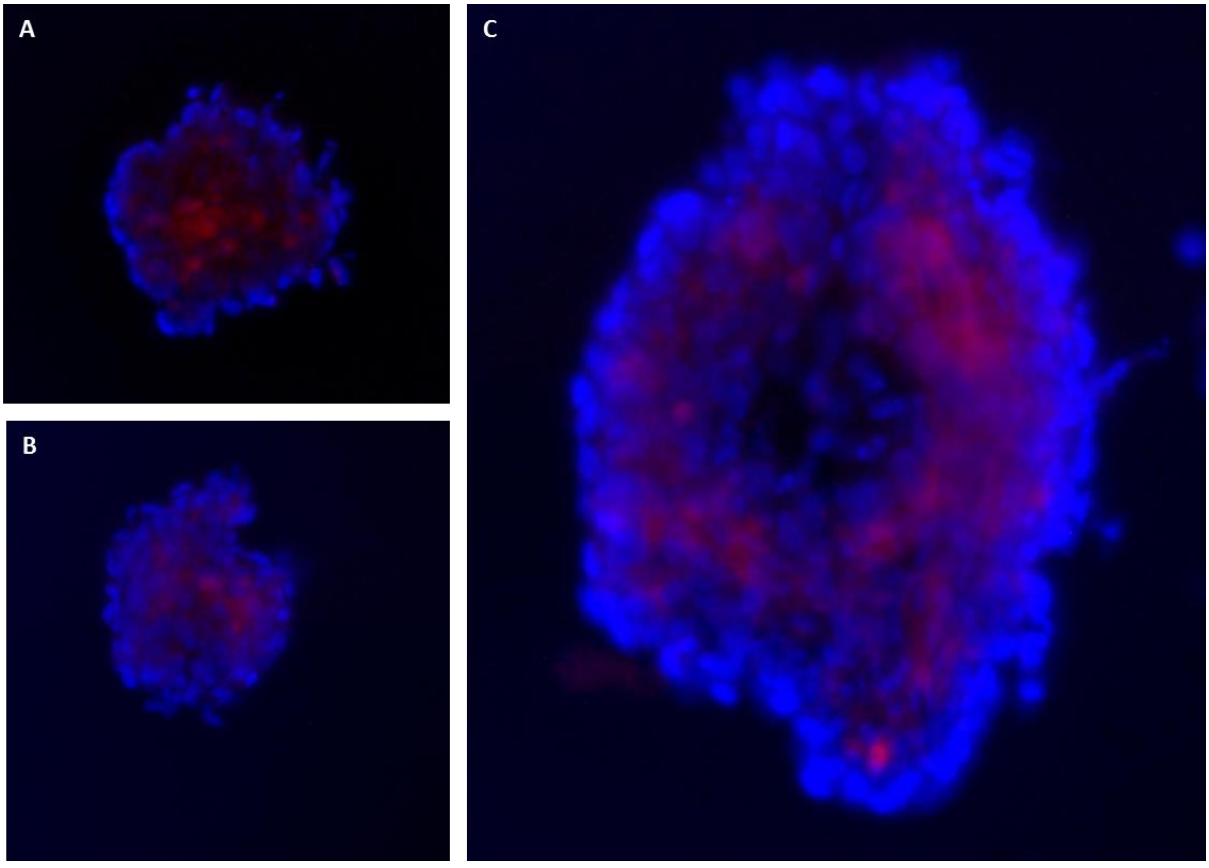

Figure 18: Spheroids from L87-HIF-Cherry. Spheroids were grown for x days before being fixed in formalin and embedded in OCT compound for cryo-sectioning. 18µm-cryoslides were stained with DAPI (cell nucleuses, blue). Red fluorescence indicates activation of the transgene mCherry within the spheroid and thus cellular hypoxia.

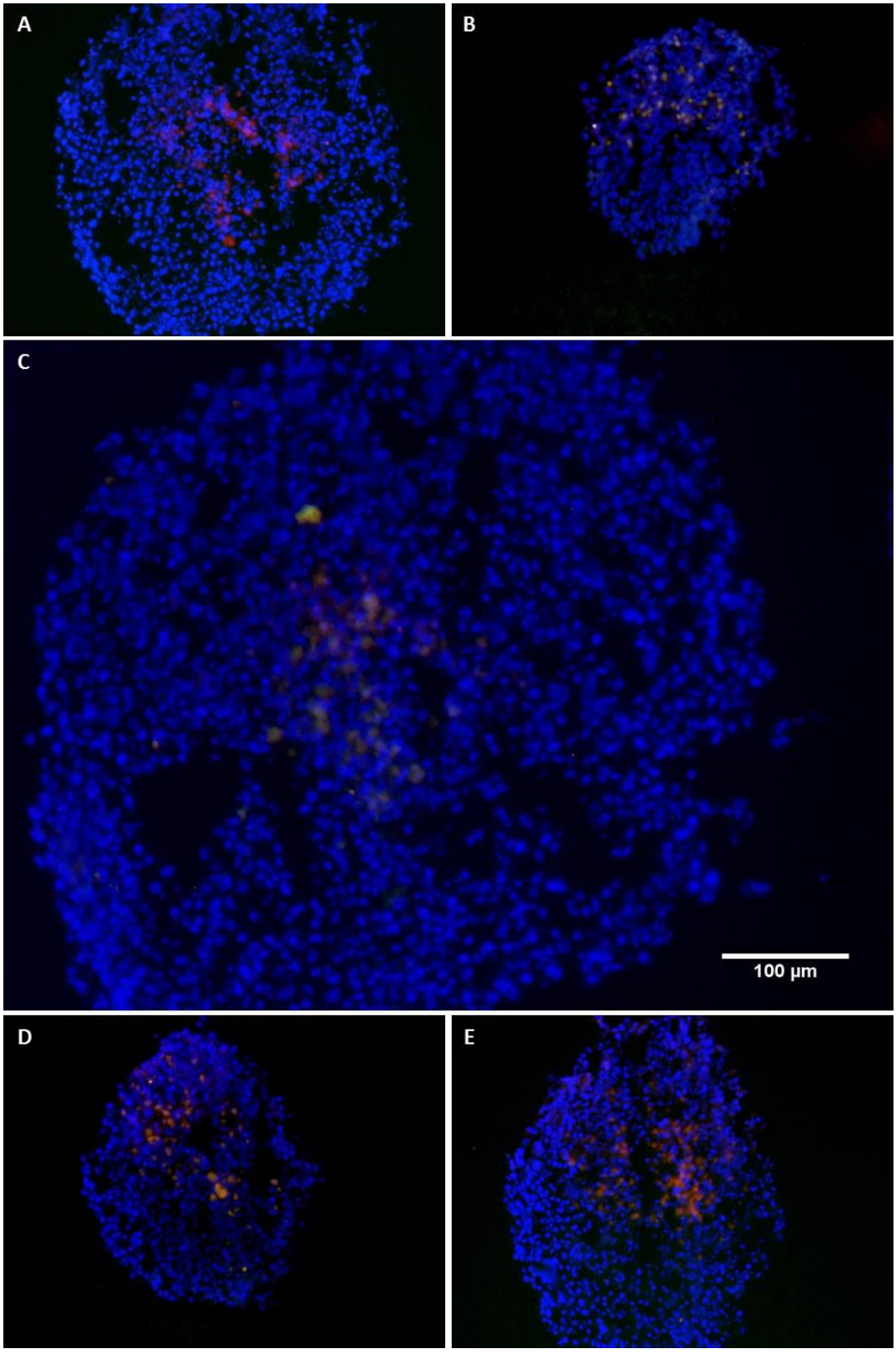

Figure 19: L87-HIF-Cherry invading Huh7 spheroids in co-culture. Huh7-spheroids were grown for 8 days in a polyHEMA-coated culture dish. For the invasion assay, Huh7-spheroids were singled out and transferred to a 1.5ml-tube filled with

culture media. L87-HIF-Cherry were harvested, labelled with 10µM CMFDA and added to the tube at a fixed cell number of 25.000 cells per tube, to a total amount of 50µl of culture media. The tubes were then placed on a roller plate for two hours. Afterwards, the culture media, along with L87-HIF-Cherry unable to attach to the spheroid, was carefully removed from the tubes and replaced by fresh media. This washing procedure was repeated three times. The spheroids were then gathered in a pipette tip with 100µl culture media and transferred into a single well of a 96-well-plate for incubation at 37°C for 48 hours. After that time, all spheroids were transferred in a single 1.5ml-tube, in order to be embedded together in OCT compound for further processing. Cryotome cassettes were stored at -20°C. 16µm slices were cut with a cryotome and after formalin fixation the slides were stained with DAPI (blue) for cell nucleuses. For analysis, the slides were mounted in 50%-glycerin-0.2%NPG-PBS and observed under the fluorescent microscope. **(A)-(E)** all show L87-HIF-Cherry have invaded the spheroid and are expressing the transgene mCherry. **(C)** Shows a single cell of the CMFDA-stained L87-HIF-Cherry cell line that appears not to be expressing the transgene and is therefore of a rather green than red fluorescence. It is located further away from the center of the spheroid than the red L87-HIF-Cherry. Spheroid size has been measured using a scaling tool and amounts to 574µm.

3.3 Heat Shock Protein 70b (HSP70b) can be activated by hyperthermic treatment

Hyperthermia is under development as an adjuvant treatment strategy for some solid cancers by creating localized hyperthermia in the region of the tumor (see chapter 1.2.3). We sought to determine if externally applied hyperthermia could be used to activate transgenes in engineered MSC. If so, the general principle could be used for the controlled regional expression of MSC-based therapy transgenes in the context of hyperthermic treatment.

3.3.1 Design of two different heat shock responsive promoters: endogenous HSP70b and HSP70b-responsive

To this end, a gene promoter was needed that would work in a similar manner to that seen for the hypoxia-responsive promoter detailed above. The hypoxia-responsive promoter contains six binding sites for the HIF1α transcription factor. A similar synthetic promoter was obtained that contained heat-shock-responsive elements upstream of a minimal promoter (pHSE-SEAP by Clontech®). It was provided by Prof. Manfred Ogris (Department of Pharmacy, LMU Munich). He also provided a second potential vector that used the endogenous HSP70b-promoter (pHSP70b-βgal by StressGen®). Both promoters were cloned into a pGL3-Basic expression vector (Promega®), which uses firefly luciferase as a reporter gene. Figure 20 shows the design of both these plasmids.

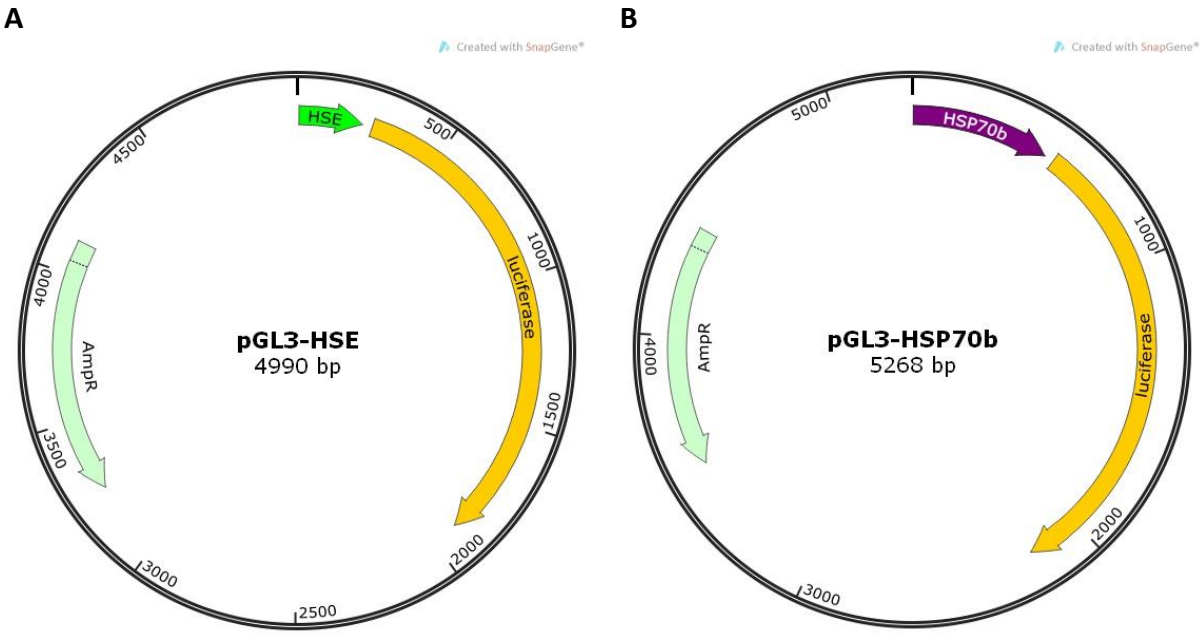

Figure 20: Plasmid maps of pGL3-HSE and pGL3-HSP70b. These plasmids represent two different approaches to heat response. **(A)** PGL3-HSE carries a heat shock responsive promoter that is made of three consecutive heat shock response elements (HSE) and a TATA-like promoter (P_{TAL}) region from the Herpes simplex virus thymidine kinase (HSV-TK) promoter. **(B)** PGL3-HSP70b carries the endogenous HSP70b-promoter that is directly activated by heat.

3.3.2 In vitro stimulation in a 42°C waterbath: The endogenous HSP70b-promoter responds more efficiently

The two potential heat-responsive promoters were compared by transiently transfecting MSC (L87 cells) using lipofectamine and pGL3-HSE or pGL3-HSP70b vectors. pRL-CMV was co-transfected at a 1:50-ratio to control for transfection efficiency. The following day, the transfected cells were subjected to heat shock for 30 minutes, using a 42°C water bath. Afterwards, the plates were returned to the 37°C-incubator and incubated for a further 24 hours, before lysis and analysis of luciferase expression. Figure 21 shows the results. Both promoters showed a statistically significant increase in luciferase activity following heat shock, however, the endogenous HSP70b-promoter yielded a much more promising result showing a ten-fold induction of the reporter gene, as compared to a three-fold induction obtained with the HSE-promoter. Therefore, the HSP70b-based vector was used for subsequent experiments.

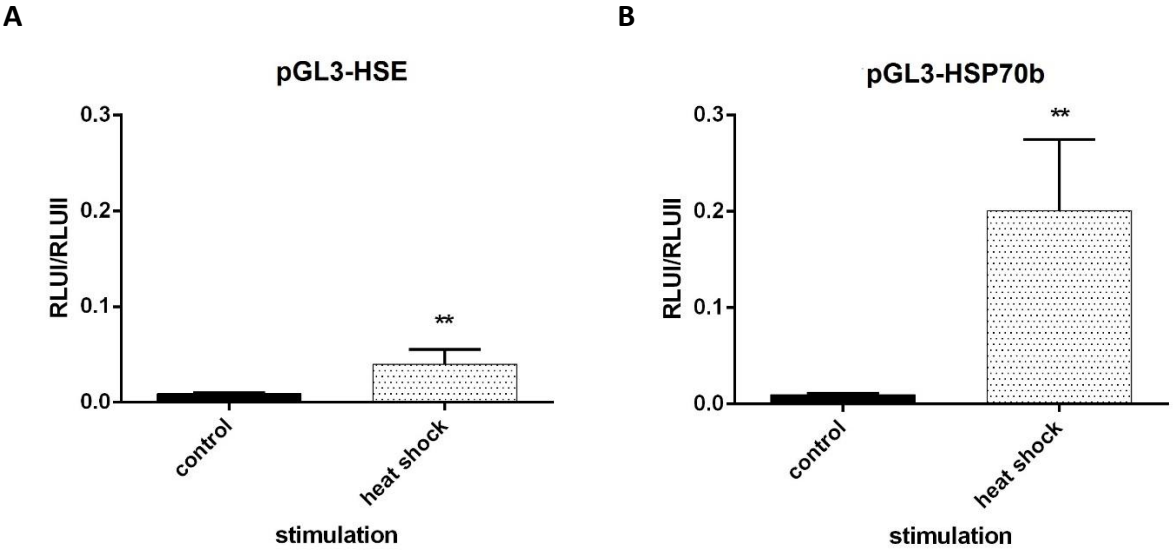

Figure 21: *In vitro* stimulation of heat shock response. Cells (L87) were seeded out in 96-well plates on day 1. On day 2, with 80% confluence, transient transfection was performed by using lipofectamy according to protocol. 6 hours after transfection, culture media was exchanged and cells were incubated for 24 hours at 37°C. On day 3, cells were subjected to heat shock for 30 minutes by using a 42°C water bath. Cells were subsequently returned to the 37°C incubator and incubated for another 24 hours, before being analyzed for luciferase activity. The experiment was repeated several times. Statistical analysis was performed by applying the Mann-Whitney-U-Test. **(A)** The heat shock responsive promoter HSE only carried a threefold increase in luciferase activity after the 30 minute exposure to 42°C. P=0.0079. **(B)** By contrast, the endogenous HSP70b promoter carried a ten-fold increase in luciferase activity after 30 minute exposure to 42°C. P=0.0079

3.3.3 Integrating *Sleeping Beauty* into the backbone: pcDNA-ITR-HSP70b-Cherry/Gaussia/TK

As a last step in the characterization of these new potential tools for the generation of MSC-based therapy procedures, the HSP70b promoter was adopted for use with the Sleeping Beauty-modified Multisite Gateway® Pro Plus system. The HSP70b endogenous promoter was amplified by PCR with

compatible ends for subcloning into the vector system. The primers were designed to generate the necessary attB sites on both ends, for the BP reaction. The resulting entry clone is shown in figure 22-A on the following page. The entry clone pENTR221-HSP70b was then paired with the entry clone pENTR221-Cherry (see figure 9-B on page 49) in an LR reaction with the destination vector pcDNA6.2PLITRBlasti-Dest, which contained the sleeping beauty transposition sites in the backbone. The resulting expression vector pcDNA-ITR-HSP70b-Cherry thus carried the endogenous HSP70b promoter in front of the mCherry red fluorescent protein as well as the sleeping beauty transposition sites and a blasticidin resistance gene in the backbone (see figure 22-B) Correct integration of the PCR amplicon in the entry clone as well as the two entry clones in the expression vector was verified by performing restriction digests and sequencing performed by GATC (data not shown).

The next step will be to stably transfect MSC with this plasmid and perform control studies. However, these future experiments could not be included in this study due to a lack of time. The system is now under study in the Nelson/Spitzweg labs of the Medizinische Klinik und Poliklinik IV in the context of a Sander Stiftung grant.

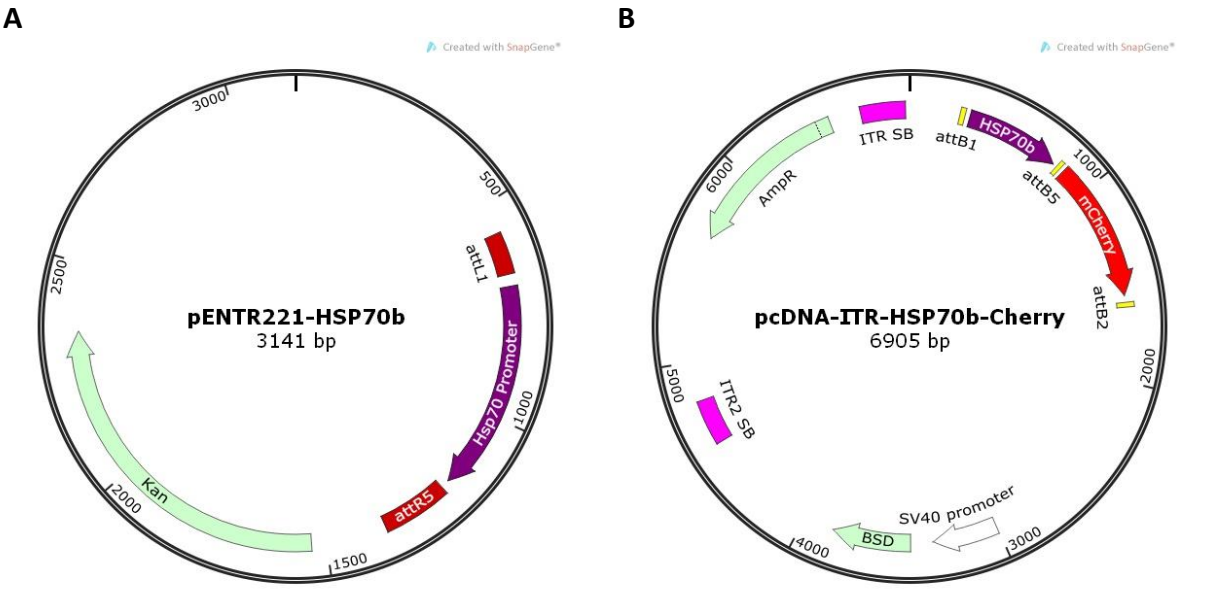

Figure 22: Plasmid maps of pENTR221-HSP70b and pcDNA-ITR-HSP70b-Cherry. (A) pENTR221-HSP70b is an entry clone that contains the attL1 and attR5 sites (red) flanking the HSP70b-promoter (purple). **(B)** pcDNA-ITR-HSP70b-Cherry is the expression vector resulting from recombination of pcDNA6.2PLITRBlasti-Dest with the entry clones pENTR221-HSP70b and pENTR221-Cherry during the LR reaction. Sleeping beauty transposition sites are marked in pink, att recombination sites are marked in yellow.

4 Discussion

4.1 Genetically engineered MSC are suitable agents in targeted therapy

Malignant diseases range among the top three causes of death worldwide. In Germany, 51% of men and 43% of women will suffer from malignant disease during the course of their life, and one in four men or one in five women will die from cancer (Robert-Koch-Institut 2013). With very few patients eligible for curative surgery, cancer therapy still widely relies on chemo- and radiation therapy. Both are systemic therapies with significant detrimental effects on healthy tissue. Therefore, the need for individualized, tumor-targeted therapies has become more and more pressing.

The concept of using MSC as targeted vehicles in tumor therapy is based on their potential to migrate towards injured and malignant tissue. However, the scientific community remains at odds over the potential effects of the application of MSC on tumor progression (Klopp 2011). But it is now established that engineering MSC to carry therapeutic agents or express therapeutic genes can render them effective weapons in cancer therapy (Hagenhoff 2016). Studeny *et al* used adenoviral transduction to infect MSC with adenoviruses carrying a construct that maintains β-interferon under the control of a constitutively active promoter, the cytomegalovirus (CMV). Successfully infected MSC then expressed high levels of β-interferon, a strongly anti-proliferative cytokine. They were injected intravenously via the tail vein in mice bearing metastatic melanomas. This served to significantly prolong survival. Interestingly, this could be achieved without toxic serum-levels of β-interferon, which constitutes an insurmountable obstacle in systemic interferon therapy of solid tumors (Studeny 2002, Studeny 2004). In a similar approach relying on a different cytokine, interleukin-2, Nakamura *et al* used MSC infected with adenoviruses expressing the immune-regulator in glioma-bearing rats. Again, survival could successfully be prolonged (Nakamura 2004). Other research groups focused on using genetically engineered MSC to activate prodrugs within the tumor. Miletic *et al,* for instance, used a rat glioma model and injected HSV-TK-expressing MSC subcutaneously into the vicinity or into the tumor itself and detected a therapeutic effect by positron emission tomography (Miletic 2007). Herpes simplex virus thymidine kinase (HSV-TK) can activate previously administered ganciclovir and is deemed a suicide gene that kills surrounding cells in a bystander effect, as outlined in chapter 1.1. Another prodrug that has been used in this way is 5-Fluorocytosine, with cytosine-deaminase as the equivalent to HSV-TK. Kucerova *et al* chose this approach in their study of the therapeutic efficacy of adipose tissue-derived MSC that were

retrovirus-transduced with yeast cytosine deaminase and administered intravenously in colon cancer-bearing mice. 5-Fluorocytosine is far less toxic than its famous relative 5-Fluoruracil, a potent yet highly toxic cytostatic drug. Upon application of 5-Fluorocytosine, it was converted to 5-Fluoruracil by MSC-expressed cytosine deaminase. As a result, significant growth inhibition in the absence of relevant side effects was recorded (Kucerova 2007). TRAIL (TNF-α related apoptosis inducing ligand) is a cytokine that is able to specifically induce apoptosis in the majority of tumor cells, while most normal tissues do not possess adequate receptors (LeBlanc 2003). Shah *et al* have engineered a recombinant form of TRAIL, named S-TRAIL, that can be secreted instead of being incorporated in the plasma membrane, thus increasing tissue concentrations (Shah 2004). S-TRAIL-expressing MSC were either implanted in mice simultaneously with glioma cells or added later on in the vicinity of existing tumors. Mice that received TRAIL-MSC survived significantly longer than the control animals (Sasportas 2009)

All of these studies exploited the homing capacities of MSC in an effort to create new therapeutic approaches aimed at increased specificity and efficacy combined with reduced toxicity. Our group has looked at ways to further refine these strategies by using the tumor microenvironment to induce the expression of therapeutic transgenes in engineered MSC. The aforementioned concepts all have one thing in common: They rely on constitutively expressed therapeutic genes. Our goal was to equip these therapeutic genes with a promoter that becomes activated once the MSC have reached the tumor. This serves to protect the MSC from their dangerous cargo until they have reached the tumor; and helps reduce undesirable side effects of MSCs that traffic to non-tumor tissues.

One approach for stalling tumor growth is to target the tumor microenvironment, also referred to as tumor stroma. The proliferation of tumor cells relies on neovascularization. MSC, which have infiltrated the stroma help contribute to the establishment of new vessel growth, a process that is regulated by angiopoietin-1, a vascular growth factor, and Tie-2, its receptor. Our group was able to show that MSC, engineered to express a red fluorescent protein under the control of a Tie-2 promoter, start to express Tie-2 once they have reached the tumor stroma, receive an angiopoietin signal and differentiate into endothelial cells. Once the red fluorescent protein had been exchanged with HSV-TK, ganciclovir administration after MSC injection served to significantly reduce tumor growth and prolong survival in pancreatic and breast cancer mouse models (Conrad 2011).

Neovascularization is by no means tumor-specific, but instead tissue-specific. However, the combination of homing of MSC and targeting transgene expression at their destination is what makes this therapeutic approach so precise.

4.2 Tissue-specific targeting increases efficacy and reduces toxicity

4.2.1 Targeting the inflammatory tumor milieu: Rantes/CCL5

A refined targeting strategy used for MSC gene delivery by our group utilizes the inflammatory milieu within a tumor for upregulation of the therapeutic transgene. CCL5 (Rantes) is a chemokine that has been shown to play a role in tumor progression and metastasis. It is secreted both by tumor cells and by cells infiltrating the tumor stroma such as MSC (Karnoub 2007, Aldinucci 2014). Reports, reviewed by Aldinucci *et al* and Borsig *et al,* have described the role of CCL5 in tumor progression as that of a coordinator of the immune response, which induces the stroma to switch from a tumor-suppressive to a tumor-supportive environment. It does so mainly by attracting immune-modulating cells to the stroma, enhancing the motility of cancer cells and remodeling the ECM. All this leads to increased local invasiveness and promotes metastasis to distant organs (Aldinucci 2014, Borsig 2014). Zischek *et al* used a version of the endogenous human CCL5 promoter to drive either reporter or therapeutic transgene (HSV-TK) expression in stably transfected immortalized MSC. The *in vivo* model used for these studies made use of syngeneic mice bearing an orthotopic pancreatic carcinoma, which is characterized by a distinctive amount of dense stroma. Tumors of mice injected with MSC carrying the CCL5-reporter construct showed high expression of the reporter gene in tissue sections of the excised tumors. To test for efficacy of the CCL5-HSV-TK construct, tumor bearing mice were subjected to three cycles of MSC administration and – following a 72-hour lag intended for successful recruitment and transgene activation – received systemic ganciclovir injections on three consecutive days. This led to significant reduction of tumor growth and metastasis to peritoneum, spleen and liver. Importantly, reporter gene expression by MSC was detected in spleen, lymph nodes, thymus, skin and gut when under control of the constitutive CMV-promoter, but not when under the control of CCL5. This shows that while engineered MSC do infiltrate other non-malignant tissues , activation of the CCL5 promoter-driven transgene is largely restricted to malignant tissues (Zischek 2009, Hagenhoff 2016)

In a similar approach, Knoop *et al* used the same CCL5 promoter but driving the sodium iodide symporter (NIS) transgene. The NIS protein is normally expressed by follicular cells of the thyroid

gland and is responsible for iodide uptake by thyroid cancer cells. This biology has revolutionized radionuclide-based therapy for this tumor and made differentiated thyroid cancer one of the most curable of solid tumors. Typically, radioactive iodine ^{131}I is administered orally after total thyroidectomy and local lymphadenectomy. Therefore, radioiodine therapy serves the purpose of eradicating residual thyroid tissue and potential distant metastases (Spitzweg 2002). As was detailed earlier, NIS is expressed predominantly by follicular cells in the thyroid gland, but also to a much lesser extent in salivary glands, gastric mucosa, lactating mammary gland, choroid plexus and ciliary body of the eye (Hingorani 2010).

Knoop *et al* showed that MSC stably transfected with a construct carrying the NIS gene under the control of the CCL5 promoter can make solid malignancies accessible to radioiodine therapy. Mice bearing HCC tumor xenografts (Huh7 cell line) received three doses of CCL5-NIS-MSC at intervals of four days, and ^{131}I was administered 72 hours after the last injection of MSC. This served to significantly stall tumor growth macroscopically, which was confirmed in immunohistochemical analysis of tissue sections, where tumors treated with CCL5-NIS-MSC and ^{131}I showed less proliferation in the Ki67-index and lower vessel density (Knoop 2011, Knoop 2013). In a recently published paper, Knoop *et al* investigated the applicability of the CCL5-NIS-MSC system to target metastatic disease. To this end, a metastatic cancer mouse model was created by injecting the human colon cancer cell line LS174t cells into the spleen of mice and then performing a splenectomy two days later. Over these two days LS174t cell effectively “seed” the liver thus modeling tumor metastases. Treatment of tumor-bearing mice with CCL5-NIS-MSC and ^{131}I showed efficacy not only in preventing formation of new metastases, but also in reducing already existing metastases (Knoop 2015). An interesting aspect of these findings is that it potentially also opens up new ways of diagnosing metastatic disease, as apparently MSC not only home to major solid malignancies but also towards small areas of malignant growth, which may not be detectable by conventional imaging technologies currently in use in the diagnosis and treatment of thyroid cancer.

These studies show that the concept of MSC equipped with CCL5-driven therapeutic genes works well in animal models in the context of both pancreatic and hepatocellular carcinoma. The purpose of the present study was to better characterize the molecular mechanisms involved in activation of the CCL5 promoter within the tumor microenvironment. As was discussed earlier, CCL5 activation within a tumor is thought to derive from the intense cytokine crosstalk that occurs between cancer cells and non-malignant cells that defines an inflammatory/hypoxic milieu, with production of TNF-

α, TGF-β, γ-IFN and IL-1β. Together with the fact that MSC do not home to tumors because they are malignant, but rather because they resemble chronic inflammatory sites, this raises the question of possible side effects of CCL5-directed MSC therapy. As was pointed out earlier, Zischek *et al* demonstrated incorporation of transplanted MSC into non-malignant tissues, namely secondary lymphatic tissues, skin and mucosa (Zischek 2009). While activation of the CCL5-driven transgene expression was found to be largely limited to the tumor environment, it remains to be seen how, for instance, skin and mucosa that have been impaired or damaged by therapy prior to MSC treatment could influence transgene expression. This may be especially important with regards to gastrointestinal mucosa, which as a highly replicative tissue suffers greatly from radiation and chemotherapy. The pathophysiology of gastrointestinal mucositis represents one of the main non-hematologic side effects of anti-cancer therapy (Sonis *et al*). Increased serum levels of TNF-α and IL-1β correlate with the extent of mucositis in patients undergoing chemotherapy. Therefore, gastrointestinal mucosa that is affected by a multitude of aggressive treatment regimens the patients received before might pose a risk in terms of possible side effects as the RANTES promoter-driven transgene may be activated in this inflammatory milieu.

4.2.2 Targeting the hypoxic tumor microenvironment: HIF-1α

CCL5 up-regulation is a cellular stress response. A rapidly growing tumor that develops ahead of its vasculature contains areas of severe hypoxia. One of the aims of this study was to find out whether CCL5 activation in MSC that have infiltrated the tumor stroma, as was demonstrated by Zischek *et al*, is caused by tumor hypoxia. Our results show that this is not the case. However, the idea of targeting tumor hypoxia is appealing, seeing as it correlates with increased invasiveness and poor prognosis. The transcription factor HIF-1α is a central player in cellular response to hypoxia. It is enhanced in a range of different tumors, depending on oxygen levels within the tumor stroma, but can also be activated independently of oxygen levels (as detailed in chapter 1.2.2).

To evaluate whether a transgene controlled by a HIF-responsive promoter (consisting of six HIF-responsive elements (HRE) and a minimal TK promoter) would show efficacy in engineered MSC-based tumor therapy, it was necessary to demonstrate that MSC enhance HIF-1α expression in the same way as their malignant counterparts, once they have infiltrated the tumor stroma. After all, bone marrow-derived MSC usually reside within the hypoxic confines of the hollow bones. Our results showed an approximately ten-fold induction of HIF-1 in MSC exposed to severe hypoxia (2% O_2) or the hypoxia-mimicking chelator cobalt chloride *in vitro*. The HCC-Huh7 spheroid model

provided an opportunity to study functional expression of HIF-1 in more physiologic circumstances. The engineered MSC where shown to invade the spheroids and to induce expression of HIF-1α-driven reporter transgene in the hypoxic center of the experimental tumor.

In vivo validation studies were subsequently performed in collaboration with Müller *et al* using the same promoter (Mueller 2016). The results demonstrate that MSC engineered with HIF-NIS injected into mice bearing HCC xenografts successfully express the transgene once they have infiltrated the tumor stroma (Mueller 2016). The study was performed on subcutaneous as well as orthotopic Huh7 xenografts. Both models showed strong radioiodine uptake, though a 2-fold increase was measured in orthotopic xenografts compared to subcutaneous. This was reproduced in a second set of experiments applying a therapeutic regime consisting of repeated MSC-HIF-NIS administrations and ^{131}I-injections. While mice bearing the subcutaneous xenografts showed no significant reduced tumor growth or prolonged survival as compared to the control group, radioiodine uptake in orthotopic xenografts was sufficient to stall tumor growth and improve survival (Mueller 2016). The study demonstrates that the concept of using tumor hypoxia for MSC-based targeted therapy is a valid approach. It is assumed that an endogenous hypoxia-sensitive promoter may offer better induction and more robust expression levels. Downstream gene targets of HIF-1 such as VEGF, for instance, may hold more promise and are currently under investigation in the Nelson lab.

This approach was inspired by the observation that rapidly growing primary tumors develop areas of severe hypoxia. In a wide range of tumors, up-regulation of HIF-1α correlates with poor prognosis. An interesting aspect of radiation biology was highlighted by Harada *et al* in a study on tumor hypoxia in colon carcinoma: It showed that tumor cells furthest away from oxygen-providing blood vessels, that were in hypoxic regions but were not expressing HIF-1 before radiation, acquired HIF-1 activity after radiation, which enabled them to migrate towards blood vessels in order to access oxygen. This is interpreted as one of the mechanisms underlying tumor recurrence after initially successful radiation therapy (Harada 2012). Deeply hypoxic tumor cells are able to survive radiation due to HIF-1-unrelated effects, but HIF-1 up-regulation after radiation may enhance tumor aggressiveness. MSC engineered to express a suicide gene under the control of a hypoxia-responsive promoter, applied together with radiation therapy, could help overcome this obstacle.

In mouse models, the CCL5-TK- and CCL5-NIS-MSC have been shown to have a therapeutic effect in primary tumors of pancreatic and hepatocellular origin as well as metastatic disease. The size of metastatic filiae can range from microscopically small colonies to vast solid tumors that are as big as

or even bigger than the primary tumor. However, oxygen shortage is more a question of growth speed than of the actual size of the tumor. Therefore, the grade of hypoxia in metastases presumably varies. On the other hand, several reports have described loss of tumor suppressor gene expression as well as gain of oncogenes can be sufficient to up-regulate HIF-expression (chapter 1.2.2). Whether a hypoxia-driven construct in MSC is as functional in metastatic disease as its CCL5-driven counterpart remains to be demonstrated.

Analogous to the potential side effects of a CCL5-driven therapeutic transgene in MSC, the extra-tumoral activation of a hypoxia-sensitive construct is mainly a question of precursory tissue damage through previous treatment regimens. Lymphatic tissue like spleen and lymph nodes, but also lung have been shown to be potential targets of circulating MSC, even though it is assumed that the micro-vasculature in these organs is responsible for extravasation of MSC rather than a directed chemotactic response. However, the extensive micro-vasculature in these tissues also maintains a steady flow of oxygen, therefore, hypoxic activation of the transgene is unlikely to occur. Chronic inflammation, for example of the gastrointestinal mucosa, is a common complication of chemotherapy, and could potentially cause unwelcome side effects in therapy with CCL5-MSC. By contrast, these effects are unlikely to induce a HIF-responsive promoter in MSC. Inflammation is associated with increased perfusion, and HIF-1 is not known as being involved in the inflammatory response. As described in chapter 1.1, patients suffering from myocardial infarction or cerebral ischemia have benefited to some extent from treatment with MSC. Therefore, patients presenting with a history of coronary artery disease, peripheral ischemic disease or transient cerebral ischemic attacks, might not be suitable candidates for this therapeutic approach.

4.2.3 Enhancing control of transgene activation through external activation: HSP70b

A vector system that would allow the induced expression of a therapeutic gene by MSC in response to external stimulation is an interesting idea. Hyperthermia is currently under investigation as an adjunct therapy to existing therapeutic regimes. Hyperthermia increases local perfusion and thus drug availability. Patients undergoing radiation therapy benefit from the increased oxygenation that enhances the local effect (chapter 1.2.2), while intratumoral drug delivery is more efficient in patients receiving chemotherapy (Wust 2002). Several studies have also highlighted the immunomodulating effects of hyperthermia. As described in chapter 1.2.3, extracellular HSP70 functions as a molecular chaperone in presenting tumor antigens to dendritic cells and leukocyte recruitment to the tumor microenvironment is enhanced by fever-range hyperthermia (Fisher 2011,

Jolesch 2011). Using heat-responsive promoters to drive therapeutic transgenes in response to regional hyperthermia would allow a tumor-specific induction of the transgene. Any potential beneficial effect of hypothermia on malignant growth, as previously demonstrated, could be added to the effect achieved through the therapeutic transgene (Haen 2011). Our results show that the endogenous HSP70b promoter is much stronger induced in MSC exposed to hypothermia, as compared to the synthetic heat-shock responsive promoter.

4.3 Clinical applicability: Individualized therapy

4.3.1 MSC

MSC can be harvested and isolated using a straightforward procedure involving a bone marrow aspirate, preferably from the iliac crest. After spinning down and washing the aspirate, MSC are isolated as they are the only cells that strongly attach to the plastic surface of a culture vessel (Beyer Nardi 2006). Subsequently, the identity of MSC can be confirmed by their pattern of cell surface markers, as described in chapter 1.1. After a lag phase of about 3-5 days in culture, cells begin to spread out and, with the first passage, can be transfected with the desired construct. The MSC can be harvested from the patient as part of an autologous transfer. If, however, the clinical condition of the patient does not allow bone marrow aspiration, the MSC can potentially be harvested from a donor. As explained in chapter 1.1, MSC do not provoke an immunogenic reaction, due to their lack of major histocompatibility complex MHC II.

Recently, Niess *et al* published the first study protocol that describes a phase I/II clinical trial with the aforementioned CCL5-TK construct incorporated into autologous MSC. The treatment regimen allows for three intravenous administrations of the engineered MSC in the space of 21 days, each followed by ganciclovir applications on three consecutive days, starting 48 hours later. This is hoped to provide sufficient time for the MSC to invade the tumor stroma and for the ganciclovir to reach its target cells (Niess 2015). The purpose of this clinical trial is to examine possible side effects of the therapeutic approach and to determine its safety. One of the questions that remain to be answered concerns the fate of MSC that are not being destroyed in the course of ganciclovir treatment, possibly because they do not activate the transgene. It is unclear whether they can persist within the patient, travel along with the blood stream or possibly settle down elsewhere, for example in the bone marrow.

4.3.2 Tumors

One particular strength of this potential therapeutic approach is its versatility. The goal of individualized cancer therapy is to increase specificity of treatment while simultaneously reducing side effects. The technique of engineering MSC with tumor-specific therapeutic genes opens up new possibilities to customize tumor therapy. As the comparison of three targeting strategies in this study showed, each promoter that has been used showed its potential in different circumstances.

The Rantes/CCL5-promoter has been studied by our group in pancreatic carcinoma, breast cancer, metastatic carcinoma and hepatocellular carcinoma models. In each model, it was demonstrated that a therapeutic gene, whether it was herpes simplex thymidine kinase or NIS, was expressed by MSC within the tumor when driven by the CCL5-promoter. Those could include difficult-to-treat tumors such as malignant melanoma, a skin cancer that metastasizes early and thus renders many patients in a palliative treatment situation at the time of diagnosis. The primary tumor is often very small (Thompson 2005). Hypothetically, the CCL5-MSC could not only be used as a therapeutic tool in this scenario, but also potentially as a diagnostic means to detect micro-metastases that are under the radar of positron emission tomography, because they are too small to register a significant increase in metabolism (e.g. by using the NIS theranostic gene).

On the other hand, tumors that show extensive growth at the primary side but tend to metastasize late may be potential indicators for the use of MSC engineered with a hypoxia-driven transgene. In this setting, the MSC could be used to stall tumor growth, or even to downstage the primary tumor to allow for a complete resection. As was detailed in chapter 1.3, hepatocellular carcinoma is a tumor not prone to chemo- or radiation therapy, with resection or liver transplantation being the only curative options. Many patients suffering from this disease are listed for liver transplantation, but organs are scarce and thus patients often die from the effects of the progressing tumor before receiving a suitable organ. Engineered MSC could potentially provide a valid treatment option to prolong the time span wherein patients are suitable candidates for organ transplantation.

Clinical applicability of HSP70b-MSC largely depends on the exact location of the primary tumor. Site-specific application of hyperthermia has been the focus of extensive research and several clinical trials so far, as reviewed by Wust *et al* (Wust 2002). For superficial tumors, like lymph node metastases, melanoma or breast cancer, local hyperthermia can be created by applying a micro- or radiowave-emitting electromagnetic device directly to the skin. Tumors that are accessible via implantation of heat-inducing devices are typically located in the head and neck region (esophageal

cancer or even glioblastoma) as well as the rectum and pelvis (prostate or cervical cancer). The abdomen can be subjected to regional hyperthermia by installing a ring of multiple applicators around the patient that are able to increase the temperature quite specifically in deep-seated tumor regions. The only feasible approach in patients presenting with metastatic disease is whole-body hyperthermia, which can be established by situating the patient in a closed, potentially moisture-saturated environment, and inducing heat with infrared radiators, for example. However, close monitoring and extensive patient care is necessary to keep potential side effects at bay, which occur at extreme body temperatures around 42°. The patient needs to be deeply sedated, rehydrated and under strong analgesia. Possible side effects include cardiac failure, coagulation disorders and local skin burn as well as edema due to fluid over-compensation (Wust 2002). Therefore, the feasibility of a therapeutic approach including heat-inducible transgenes delivered to the tumor by MSC strongly depends on the site of the tumor and the existence of distant metastasis. Whole-body hyperthermia, which would be necessary for transgene activation in metastatic disease, is associated with an extensive effort in clinical management and undermines the tumor-specificity of the approach.

To conclude, engineering mesenchymal stem cells with therapeutic transgenes targeting the tumor stroma is an exciting approach in the development of individualized cancer therapy. Future research by our group will focus on refining the existing targeting techniques and discovering new aspects of the tumor microenvironment that can serve as a target.

5 Addendum

5.1 Table of figures

5.2 Abbreviations

µg	micrograms
µl	microliters
µM	micro-molar
AIF	apoptosis-inducing factor
APAF-1	apoptotic protease activating factor
APS	ammoniumpersulfate
ATP	adenosine triphosphate
bp	base pairs
Bsd	blasticidin
C	celsius
$CaCl_2$	calcium chloride
CAF	cancer-associated fibroblast
CD	cluster of differentiation
CIP	calf intestine phosphatase
cm^2	square centimeters
CMFDA	5-chloromethylfluorescein diacetate
CMTMR	chloromethylbenzoylaminotetramethylrhodamine
CMV	cytomegalovirus
$CoCl_2$	cobalt chloride
DAPI	4',6-diamidino-2-phenylindole
DMEM	Dulbecco's Modified Eagle Medium
DNA	deoxyribonucleic acid
E.coli	Escherichia coli
ECL	enhanced chemiluminescence
ECM	extracellular matrix
EDTA	enhanced chemiluminescence
EGF	epithelial growth factor
EGTA	ethylene glycol tetraacetic acid
ELISA	enzyme linked immunosorbent assay
EMT	epithelial-mesenchymal transition
FACS	fluorescence activated cell scanning
FAP	fibroblast-activating protein
FCS	fetal calf serum
Fe	Ferrum
FGF-2	fibroblast growth factor-2
FSP	fibroblast-specific protein
GvHD	graft-versus-host-disease
HBV	hepatitis B virus
HCC	hepatocellular carcinoma
HCl	hydrochloride
HCV	hepatitis C virus
HGF	hepatic growth factor
HIF	hypoxia-inducible factor
HLA-DR	human leukocyte antigen – antigen D related
HRE	heat-responsive elements
HSP	heat shock protein

HSV	herpes simplex virus
IFN	interferon
IgG	immunoglobulin G
IL	interleukin
ITR	indirect terminal repeats
kDa	kilo-Dalton
LB	lysogeny broth
LDHA	lactate dehydrogenase A
MCT-4	monocarboxylate transporter 4
MHC	major histocompatibility complex
min/'	minutes
ml	milliliter
mM	micromolar
mmol	millimole
MMP	matrix metalloproteinase
MSC	mesenchymal stem cell
MT1-MMP	membrane type 1 metalloprotease
ng	nanogram
NIS	sodium iodide symporter
nm	nanometer
O_2	oxygen
OCT	optimal cutting temperature
PBS	phosphate buffered saline
PCR	polymerase chain reaction
PDGF	platelet-derived growth factor
PDK	pyruvate dehydrogenase kinase
PHD-2	prolyl hydroxylase domain-containing protein 2
polyHEMA	Polyhydroxyethylmethacrylate
RANTES	regulated on activation, normal T cell expressed and secreted
rpm	rounds per minute
RPMI	Roswell Park Memorial Institute
SDF-1	stroma-derived factor 1
SDS	sodium dodecyl sulfate
sec/''	seconds
SMA	smooth muscle actin
TACE	transcatheter arterial chemoembolization
TAF	tumor-associated fibroblast
TBST	tris-buffered saline and tween 20
TGF	transforming growth factor
TK	thymidine kinase
TNF	tumor necrosis factor
TRAIL	TNF-related apoptosis-inducing ligand
TRIS	tris(hydroxymethyl)aminomethane
U	units
UV	ultraviolet
V	volts
VEGF	vascular endothelial growth factor
vHL	von Hippel-Landau

WHO	world health organization
x	times

6 References

Aldinucci, D. and A. Colombatti (2014). "The inflammatory chemokine CCL5 and cancer progression." *Mediators of Inflammation*.

Au, P., J. Tam, et al. (2008). "Bone marrow derived mesenchymal stem cells facilitate engineering of long-lasting functional vasculature." *Blood* **111**(9): 4551-4558.

Baffy, G., E.M. Brunt, et al. (2012). "Hepatocellular carcinoma in non-alcoholic fatty liver disease: an emerging menace." *Journal of Hepatology* **56**(6): 1384-1391.

Bao, Q., Y. Zhao et al. (2012). "Mesenchymal stem sell-based tumor-targeted gene therapy in gastrointestinal cancer." *Stem Cells And Development* **21**(13): 2355-2365.

Barcellos-de-Souza, P., V. Gori et al. (2013). "Tumor microenvironment: Bone-marrow mesenchymal stem cells as key players." *Biochimica et Biophysica Acta* **1836**(2): 321-335.

Beckermann, B. M., G. Kallifatidis et al. (2008). "VEGF expression by mesenchymal stem cells contributes to angiogenesis in pancreatic carcinoma." *British Journal Of Cancer* **99**(4): 622-631.

Behrouzkia, Z., Z. Joveini et al. (2016). "Hyperthermia: How Can It Be Used?" *Oman Medical Journal* **31**(2): 89-97.

Bellot, G., R. Garcia-Medina, et al. (2009). "Hypoxia-induced autophagy is mediated through hypoxia-inducible factor induction of BNIP3 and BNIP3L via their BH3 domains." *Molecular and Cellular Biology* **29**(10): 2570-2581.

Beyer Nardi, N. and L. da Silva Mereilles (2006). "Mesenchymal stem cells: isolation, in vitro expansion and characterization." *Handbook of Experimental Pharmacology* **174**: 249-282.

Borczuk, A. C., N. Papanikolaou, et al. (2008). "Lung adenocarcinoma invasion in TGFbetaRII-deficient cells is mediated by CCL5/RANTES." *Oncogene* **27**(4): 557-564.

Borsig, L., M.J. Wolf, et al. (2014). "Inflammatory chemokines and metastasis - tracing the accessory." *Oncogene* **33**(25): 3217-3224.

Bremnes, R. M., T. Donnen, et al. (2011). "The role of tumor stroma in cancer progression and prognosis: emphasis on carcinoma-associated fibroblasts and non-small cell lung cancer." *Journal of Thoracic Oncology* **6**(1): 209-217.

Bressac, B., M. Kew, et al. (1991). "Selective G to T mutations of p53 gene in hepatocellular carcinoma from southern Africa." *Nature* **350**(6317): 429-431.

Brown, L. F., A.J. Guidi, et al. (1999). "Vascular stroma formation in carcinoma in situ, invasive carcinoma, and metastatic carcinoma of the breast." *Clinical Cancer Research* **5**(5): 1041-1056.

Bruix, J., M. Sala, et al. (2004). "Chemoembolization for hepatocellular carcinoma." *Gastroenterology* **127**(5): 179-188.

Bruix, J. and M. Sherman (2005). "Management of hepatocellular carcinoma." *Hepatology* **42**(5): 1208-1236.

Calon, A., D.V. Tauriello, et al. (2014). "TGF-beta in CAF-mediated tumor growth and metastasis." *Seminars in Cancer Biology*.

Campbell, J. S., S.D. Hughes, et al. (2005). "Platelet-derived growth factor C induces liver fibrosis, steatosis, and hepatocellular carcinoma." *Proceedings of the National Academy of Sciences of the United States of America* **102**(9): 3389-3394.

Carmeliet, P. and R. K. Jain (2011). "Principles and mechanisms of vessel normalization for cancer and other angiogenic diseases." *Nature Reviews. Drug Discovery* **10**(6): 417-427.

Casazza, A., G. Di Gonza, et al. (2014). "Tumor stroma: A complexity dictated by the hypoxic tumor microenvironment." *Oncogene* **33**(14): 1743-1754.

Ceradini, D. J., A.R. Kulkarni, et al. (2004). "Progenitor cell trafficking is regulated by hypoxic gradients through HIF-1 induction of SDF-1." *Nature Medicine* **10**(8): 858-864.

Chamberlain, G., J. Fox, et al. (2007). "Concise review: Mesenchymal stem cells: Their phenotype, differentiation capacity, immunological features, and potential for homing." *Stem Cells*(25): 2739-2749.

Chan, J. L., K.C. Tang, et al. (2006). "Antigen-presenting property of mesenchymal stem cells occurs during a narrow window at low levels of interferon-gamma." *Blood* **107**(12): 4817-4824.

Conrad, C., Y. Hüsemann, et al. (2011). "Linking transgene expression of engineered mesenchymal stem cells and angiopoietin-1-induced differentiation to target cancer angiogenesis." *Annals of Surgery* **253**(3): 6.

Corcione, A., F. Benvenuto, et al. (2006). "Human mesenchymal stem cells modulate B-cell function." *Blood* **107**(1): 367-372.

De Boeck, A., A. Hendrix et al. (2013). "Differential secretome analysis of cancer-associated fibroblasts and bone marrow-derived precursors to identify microenvironmental regulators of colon cancer progression." *Proteomics* **13**(2): 379-388.

Dembinski, J. L., S.M. Wilson, et al. (2013). "Tumor stroma engraftment of gene-modified mesenchymal stem cells as anti-tumor therapy against ovarian cancer." *Cytotherapy* **15**(1): 20-42.

Desmouliere, A., M. Redard, et al. (1995). "Apoptosis mediates the decrease in cellularity during the transition between granulation tissue and scar." *The American Journal of Pathology* **146**(1): 56-66.

Dvorak, H. F. (1986). "Tumors: Wounds that do not heal. Similarities between tumor stroma generation and wound healing. ." *New England Journal of Medicine* **315**(26): 1650-1659.

El-Serag, H. B. (2011). "Hepatocellular carcinoma." *New England Journal of Medicine* **365**(12): 1118-1127.

El-Serag, H. B. (2012). "Epidemiology of Viral Hepatitis and Hepatocellular Carcinoma." *Gastroenterology* **142**(6): 1264-1273.

Endo, M., M. Nishita, et al. (2014). "Insight into the role of Wnt5a-induced signaling in normal and cancer cells." *International Review of Cell and Molecular Biology* **314**: 117-148.

Farazi, P. A. and R. A. DePinho (2006). "Hepatocellular carcinoma pathogenesis: from genes to environment." *Nature Reviews Cancer* **6**(9): 674-687.

Fattovich, G., T. Stroffolini, et al. (2004). "Hepatocellular carcinoma in cirrhosis: incidence and risk factors." *Gastroenterology* **127**(5): 35-50.

Feder, M. E. (1999). "Heat-shock proteins, molecular chaperones, and the stress response: evolutionary and ecological physiology." *Annual Review of Physiology* **61**: 243-282.

Fisher, D. T., Q. Chen, et al. (2011). "IL-6 trans-signaling licenses mouse and human tumor microvascular gateways for trafficking of cytotoxic T-cells." *The Journal of Clinical Investigation* **121**(10): 3846-3859.

Forsythe, J. A., B.H. Jiang, et al. (1996). "Activation of vascular endothelial growth factor gene transcription by hypoxia-inducible factor 1." *Molecular and Cellular Biology* **16**(9): 4604-4613.

Franko, A. J. (1986). "Misonidazole and other hypoxia markers: metabolism and applications." *International Journal of Radiation Oncology, Biology, Physics* **12**(7): 1195-1202.

Garrido, C., M. Brunet (2006). "Heat shock proteins 27 and 70: anti-apoptotic proteins with tumorigenic properties." *Cell Cycle* **5**(22): 2592-2601.

Garrido, C., S. Gurbuxani, et al. (2001). "Heat shock proteins: endogenous modulators of apoptotic cell death." *Biochemical and Biophysical Research Communications* **286**(3): 433-442.

Gnecchi, M., Z. Zhang, et al. (2008). "Paracrine mechanisms in adult stem cell signaling and therapy." *Circulation Research* **103**(11): 1204-1219.

Goldberg, M. A., S.P. Dunning, et al. (1988). "Regulation of the erythropoietin gene: evidence that the oxygen sensor is a heme protein." *Science* **242**(4884): 1412-1415.

Haen, S. P., P.L. Pereira, et al. (2011). "More than just tumor destruction: immunomodulation by thermal ablation of cancer." *Clinical & Developmental Immunology*.

Hagenhoff, A., C.J. Bruns, et al. (2016). "Harnessing mesenchymal stem cell homing as an anticancer therapy." *Expert Opinion On Biological Therapy* **16**(9): 1079-1092.

Hall, B., J.L. Dembinski, et al. (2007). "Mesenchymal stem cells in cancer: Tumor-associated fibroblasts and cell-based delivery vehicles." *International Journal of Hematology* **86**(1): 8-16.

Hämmerling, G. J. and R. Ganss (2006). "Vascular integration of endothelial progenitors during multistep tumor progression." *Cell Cycle* **5**(5): 509-511.

Harada, H., M. Inoue et al. (2012). "Cancer cells that survive radiation therapy acquire HIF-1 activity and translocate towards tumor blood vessels." *Nature Communications*: 12.

Harrison, L. B., M. Chadha et al. (2002). "Impact of tumor hypoxia and anemia on radiation therapy outcomes." *The Oncologist* **7**(6): 492-508.

Hernandez-Gea, V., S. Toffanin, et al. (2013). "Role of the microenvironment in the pathogenesis and treatment of hepatocellular carcinoma." *Gastroenterology* **144**(3): 512-527.

Hingorani, M., C. Spitzweg, et al. (2010). "The biology of the sodium iodide symporter and its potential for targeted gene delivery." *Current Cancer Drug Targets* **10**(2): 242-267.

Hofstetter, C. P., E.J. Schwarz, et al. (2002). "Marrow stromal cells form guiding strands in the injured spinal cord and promote recovery." *Proceedings of the National Academy of Sciences of the United States of America.* **99**(4): 2199-2204.

Imai, T., A. Horiuchi, et al. (2003). "Hypoxia attenuates the expression of E-cadherin via up-regulation of SNAIL in ovarian carcinoma cells." *American Journal of Pathology* **163**(4): 1437-1447.

Issels, R. D., L.H. Lindner, et al. (2010). "Neo-adjuvant chemotherapy alone or with regional hyperthermia for localised high-risk soft-tissue sarcoma: a randomised phase 3 multicentre study." *The Lancet. Oncology* **11**(6): 561-570.

Jaeckel, C., M.S. Nogueira, et al. (2016). "A vector platform for the rapid and efficient engineering of stable complex transgenes." *Scientific Reports* **6**(34365).

Jego, G., A. Hazoumé, et al. (2010). "Targeting heat shock proteins in cancer." *Cancer Letters* **332**(2): 275-285.

Jolesch, A., K. Elmer, et al. (2011). "Hsp70, a messenger from hyperthermia for the immune system." *European Journal of Cell Biology* **91**(1): 48-52.

Karnoub, A. E., A.B. Dash, et al. (2007). "Mesenchymal stem cells within tumor stroma promote breast cancer metastasis." *Nature* **449**(7162): 557-563.

Kerbel, R. S. (2008). "Tumor angiogenesis." *New England Journal of Medicine* **358**(19): 2039-2049.

Kidd, S., E. Spaeth, et al. (2012). "Origins of the tumor microenvironment: Quantitative assessment of adipose-derived and bone marrow-derived stroma." *PLoS One* **7**(2).

Kim, J. W., I. Tchernyshyov, et al. (2006). "HIF-1-mediated expression of pyruvate dehydrogenase kinase: a metabolic switch required for cellular adaptation to hypoxia." *Cellular Metabolism* **3**(3): 177-185.

Klopp, A. H., A. Gupta, et al. (2011). "Concise review: Dissecting a discrepancy in literature: Do mesenchymal stem cells support or suppress tumor growth?" *Stem Cells* **29**(1): 11-19.

Klopp, A. H., L. Lacerda, et al. (2010). "Mesenchymal stem cells promote mammosphere formation and decrease E-cadherin in normal and malignant breast cells." *PLoS One* **5**(8).

Knoop, K., M. Kolokythas, et al. (2011). "Image-guided, tumor stroma-targeted ^{131}I therapy of hepatocellular cancer after systemic mesenchymal stem cell-mediated NIS gene delivery." *Molecular Therapy* **19**(9): 10.

Knoop, K., N. Schwenk, et al. (2013). "Stromal targeting of sodium iodide symporter using mesenchymal stem cells allows enhanced imaging and therapy of hepatocellular carcinoma." *Human Gene Therapy* **24**(3): 11.

Knoop, K., N. Schwenk, et al. (2015). "Mesenchymal stem cell-mediated, tumor stroma-targeted radioiodine therapy of metastatic colon cancer using the sodium iodide symporter as theranostic gene." *Journal of Nuclear Medicine* **56**(4): 600-606.

Krampera, M., S. Glennie, et al. (2003). "Bone marrow-derived mesenchymal stem cells inhibit the response of naive and memory antigen-specific T cells to their cognate peptide." *Blood* **101**(9): 3722-3729.

Krishnamachary, B., S. Berg-Dixon, et al. (2003). "Regulation of colon carcinoma cell invasion by hypoxia-inducible factor 1." *Cancer Research* **63**(5): 1138-1143.

Kucerova, L., V. Altanerova, et al. (2007). "Adipose tissue-derived human mesenchymal stem cells mediated prodrug cancer gene therapy." *Cancer Research* **67**(13): 6304-6313.

Laemmli, U. K. (1970). "Cleavage of structural proteins during the assembly of the head of bacteriophage T4." *Nature* **227**(5259): 680-685.

Lazennec, G. and C. Jorgensen (2008). "Concise review: Adult multipotent stromal cells and cancer: risk or benefit?" *Stem Cells* **26**(6): 1387-1394.

Le Blanc, K., F. Frassoni, et al. (2008). "Mesenchymal stem cells for treatment of steroid-resistant, severe, acute graft-versus-host disease: a phase II study." *Lancet* **371**(9624): 1579-1586.

Le Blanc, K., I. Rasmusson, et al. (2004). "Treatment of severe acute graft-versus-host disease with third party haploidentical mesenchymal stem cells." *Lancet* **363**(9419): 1439-1441.

Le Blanc, K. and O. Ringdén (2005). "Immunobiology of mesenchymal stem cells and future use in hematopoietic stem cell transplantation." *Biology of Blood and Marrow Transplantation* **11**(5): 321-334.

LeBlanc, H. N. and A. Ashkenazi (2003). "Apo2L/TRAIL and its death and decoy receptors." *Cell Death and Differentiation* **10**(1): 66-75.

Lindquist, S., E.A. Craig (1988). "The heat shock proteins." *Annual Review of Genetics* **22**(631-677).

Llovet, J. M., M.I. Real, et al. (2002). "Arterial embolisation or chemoembolisation versus symptomatic treatment in patients with unresectable hepatocellular carcinoma: a randomised controlled trial." *Lancet* **359**(9319): 1734-1739.

Llovet, J. M., S. Ricci, et al. (2008). "Sorafenib in advanced hepatocellular carcinoma." *New England Journal of Medicine* **359**(4): 378-390.

Lu, X. and Y. Kang (2010). "Hypoxia and hypoxia-inducible factors: Master regulators of metastasis." *Clinical Cancer Research* **16**(24): 5928-5935.

Luboshits, G., S. Shina, et al. (1999). "Elevated expression of the CC chemokine regulated on activation, normal T cell expressed and secreted (RANTES) in advanced breast carcinoma." *Cancer Research* **59**(18): 4681-4687.

Mansilla, E., G.H. Marin, et al. (2005). "Human mesenchymal stem cells are tolerized by mice and improve skin and spinal cord injuries." *Transplantation Proceedings* **37**(1): 292-294.

Martinez-Outschoorn, U. E., C. Trimmer, et al. (2010). "Autophagy in cancer associated fibroblasts promotes tumor cell survival: Role of hypoxia, HIF1 induction and NFκB activation in the tumor stromal microenvironment." *Cell Cycle* **9**(17): 3515-3533.

Maxson, S., E.A. Lopez, et al. (2012). "Concise review: Role of mesenchymal stem cells in wound repair." *Stem Cells Translational Medicine* **1**(2): 142-149.

Miletic, H., Y. Fischer, et al. (2007). "Bystander killing of malignant glioma by bone marrow-derived tumor-infiltrating progenitor cells expressing a suicide gene." *Molecular Therapy* **15**(7): 1373-1381.

Mueller, A. M., K.A. Schmohl, et al. (2016). "Hypoxia-targeted 131I therapy of hepatocellular cancer after systemic mesenchymal stem cell-mediated sodium iodide symporter gene delivery." *Oncotarget* **7**(34): 54795-54810.

Multhoff, G. (2007). "Heat shock protein 70 (Hsp70): membrane location, export and immunological relevance." *Methods* **43**(3): 229-237.

Muñoz-Nájar, U. M., K.M. Neurath, et al. (2006). "Hypoxia stimulates breast carcinoma cell invasion through MT1-MMP and MMP-2 activation." *Oncogene* **25**(16): 2379-2392.

Nakajima, E. C. and B. van Houten (2013). "Metabolic symbiosis in cancer: refocusing the Warburg lens." *Molecular Carcinogenesis* **52**(5): 329-337.

Nakamura, K., Y. Ito, et al. (2004). "Antitumor effect of genetically engineered mesenchymal stem cells in a rat glioma model." *Gene Therapy* **11**(14): 1155-1164.

Nelson, P. J., H.T. Kim, et al. (1993). "Genomic organization and transcriptional regulation of the RANTES chemokine gene." *Journal of Immunology* **151**(5): 2601-2612.

Niess, H., C. Jobst, et al. (2015). "Treatment of advanced gastrointestinal tumors with genetically modified autologous mesenchymal stromal cells (TREAT-ME1): study protocol of a phase I/II clinical trial." *BMC Cancer* **15**(237).

Niwa, Y., H. Akamatsu, et al. (2001). "Correlation of tissue and plasma RANTES levels with disease course in patients with breast or cervical cancer." *Clinical Cancer Research* **7**(2): 285-289.

Noessner, E., R. Gastpar, et al. (2002). "Tumor-derived heat shock protein 70 peptide complexes are cross-presented by human dendritic cells." *Journal of Immunology* **169**(10): 5424-5432.

Oei, A. L., L.E. Vriend, et al. (2015). "Effects of hyperthermia on DNA repair pathways: one treatment to inhibit them all." *Radiation Oncology* **10**(165).

Papandreou, I., R.A. Calms, et al. (2006). "HIF-1 mediates adaptation to hypoxia by actively downregulating mitochondrial oxygen consumption." *Cellular Metabolism* **3**(3): 187-197.

Quante, M., S.P. Tu, et al. (2011). "Bone marrow-derived myofibroblasts contribute to the mesenchymal stem cell niche and promote tumor growth." *Cancer Cell* **19**(2): 257-272.

Rastegar, F., D. Shenaq, et al. (2010). "Mesenchymal stem cells: Molecular characteristics and clinical applications." *World Journal of Stem Cells* **2**(4): 67-80.

Ritossa, F. (1962). "A new puffing pattern induced by temperature and DNP in *Drosophila*." *Experimentia* **18**: 571-573.

Robert-Koch-Institut (2013). Krebs in Deutschland 2009/2010. . Berlin, Robert Koch-Institut (Hrsg) und die Gesellschaft der epidemiologischen Krebsregister in Deutschland e.V.

Rome, C., F. Couillaud, et al. (2005). "Spatial and temporal control of expression of therapeutic genes using heat shock protein promoters." *Methods* **35**(2): 188-198.

Sabat, R., G. Grütz, et al. (2010). "Biology of interleukin-10." *Cytokine & Growth Factor Reviews* **21**(5): 331-344.

Sasportas, L. S., R. Kasmieh, et al. (2009). "Assessment of therapeutic efficacy and fate of engineered human mesenchymal stem cells for cancer therapy." *Proceedings of the National Academy of Sciences of the United States of America* **106**(12): 4822-4827.

Schmitt, E., M. Gehrmann, et al. (2007). "Intracellular and extracellular functions of heat shock proteins: repercussions in cancer therapy." *Journal of Leukocyte Biology* **81**(1): 15-27.

Seifert, G., V. Budach, et al. (2016). "Regional hyperthermia combined with chemotherapy in paediatric, adolescent and young adult patients: current and future perspectives." *Radiation Oncology* **11**(65).

Semenza, G. L. (2009). "Defining the role of hypoxia-inducible factor 1 in cancer biology and therapeutics." *Oncogene* **29**(5): 625-634.

Semenza, G. L. (2012). "Hypoxia-inducible factors in physiology and medicine." *Cell* **148**(3): 399-408.

Semenza, G. L. (2013). "HIF-1 mediates metabolic responses to intratumoral hypoxia and oncogenic mutations." *The Journal of Clinical Investigation* **123**(9): 3664-3671.

Semenza, G. L., B.H. Jiang, et al. (1996). "Hypoxia response elements in the aldolase A, enolase 1, and lactate dehydrogenase A gene promoters contain essential binding sites for hypoxia-inducible factor 1." *Journal of Biological Chemistry* **271**(51): 32529-32537.

Semenza, G. L., M.K. Nejfelt, et al. (1991). "Hypoxia-inducible nuclear factors bind to an enhancer element located 3' to the human erythropoietin gene." *Proceedings of the National Academy of Sciences of the United States of America* **88**(13): 5680-5684.

Shah, K., C.H. Tung, et al. (2004). "Inducible release of TRAIL fusion proteins from a proapoptotic form for tumor therapy." *Cancer Research* **64**(9): 3236-3242.

Sheng, H., Y. Wang, et al. (2008). "A critical role of IFNγ in priming MSC-mediated suppression of T cell proliferation through up-regulation of B7-H1." *Cell Research* **18**(8): 846-857.

Shinagawa, K., Y. Kitadai et al. (2010). "Mesenchymal stem cells enhance growth and metastasis of colon cancer." *International Journal of Cancer* **127**(10): 2323-2333.

Shinagawa, K., Y. Kitadai et al. (2012). "Stroma-directed imatinib therapy impairs the tumor-promoting effect of bone marrow-derived mesenchymal stem cells in an orthotopic transplantation model of colon cancer." *International Journal of Cancer* **132**(4): 813-823.

Shinojima, N., A. Hossain, et al. (2012). "TGF-beta mediates homing of bone marrow-derived human mesenchymal stem cells to glioma stem cells." *Cancer Research* **73**(7): 2333-2344.

Silzle, T., G.J. Randolph, et al. (2004). "The fibroblast: Sentinel cell and local immune modulator in tumor tissue." *International Journal of Cancer* **108**(2): 173-180.

Sivasubramaniyan, K., D. Lehnen, et al. (2012). "Phenotypic and functional heterogeneity of human bone marrow- and amnion-derived MSC subsets." *Annals of the New York Academy of Sciences* **1266**: 94-106.

Soria, G. and A. Ben-Baruch (2008). "The inflammatory chemokines CCL2 and CCL5 in breast cancer." *Cancer Letters* **267**(2): 271-285.

Spaeth, E. L., J.L. Dembinski et al. (2009). "Mesenchymal Stem Cell Transition to Tumor-Associated Fibroblasts Contributes to Fibrovascular Network Expansion and Tumor Progression." *PLoS One* **4**(4).

Spitzweg, C. and J. C. Morris (2002). "The sodium iodide symporter: its pathophysiological and therapeutic implications." *Clinical Endocrinology* **57**(5): 559-574.

Spring, H., T. Schüler, et al. (2005). "Chemokines direct endothelial progenitors into tumor neovessels." *Proceedings of the National Academy of Sciences of the United States of America* **102**(50): 18111-18116.

Srivastava, P. (2002). "Interaction of heat shock proteins with peptides and antigen presenting cells: chaperoning of the innate and adaptive immune responses." *Annual Review of Immunology* **20**: 395-425.

Studeny, M., F.C. Marini, et al. (2002). "Bone-marrow derived mesenchymal stem cells as vehicels for interferon-beta delivery into tumors." *Cancer Research* **62**(13): 3603-3608.

Studeny, M., F.C. Marini, et al. (2004). "Mesenchymal stem cells: Potential precursors for tumor stroma and target-delivery vehicles for anticancer agents." *Journal of the National Cancer Institute* **96**(21): 1593-1603.

Thompson, J. F., R.A. Scolyer, et al. (2005). "Cutaneous Melanoma." *Lancet* **365**(9460): 687-701.

Thorgeirsson, S. S. and J. W. Grisham (2002). "Molecular pathogenesis of human hepatocellular carcinoma." *Nature Genetics* **31**(4): 339-346.

Towbin, H., T. Staehelin, et al. (1979). "Electrophoretic transfer of proteins from polyacrylamide gels to nitrocellulose sheets: procedure and some applications." *Proceedings of the National Academy of Sciences of the United States of America* **76**(9): 4350-4354.

Van Dillen, I. J., N.H. Mulder, et al. (2002). "Influence of the bystander effect on HSV-tk/GCV gene therapy. A review." *Current Gene Therapy* **2**(3): 307-322.

Villanueva, A. and J. M. Llovet (2011). "Targeted Therapies for Hepatocellular Carcinoma." *Gastroenterology* **140**(5): 1410-1426.

von Luettichau, I., M. Notohamiprodjo, et al. (2005). "Human adult CD34- progenitor cells functionally express the chemokine receptors CCR1, CCR4, CCR7, CXCR5, and CCR10 but not CXCR4." *Stem Cells And Development* **14**(3): 329-336.

Von Luettichau, I., P.J. Nelson et al. (1996). "Rantes chemokine expression in diseased and normal human tissues." *Cytokine* **8**(1): 10.

Voronov, E., D.S. Shouval, et al. (2003). "IL-1 is required for tumor invasiveness and angiogenesis." *Proceedings of the National Academy of Sciences of the United States of America* **100**(5): 2645-2650.

Wang, G. L. and G. L. Semenza (1993). "Characterization of hypoxia-inducible factor 1 and regulation of DNA binding activity by hypoxia." *The Journal of Biological Chemistry* **268**(29): 21513-21518.

Wernicke, C. M., T.G.P. Grunewald, et al. (2011). "Mesenchymal stromal cells for the treatment of steroid-refractory GvHD: a review of the literature and two pediatric cases." *International Archives of Medicine* **4**(27).

WHO (2014). World Cancer Report 2014, International Agency for Research on Cancer (IARC).

Wust, P., B. Hildebrandt, et al. (2002). "Hyperthermia in combined treatment of cancer." *The Lancet. Oncology* **3**(8): 487-497.

Yaal-Hahoshen, N., S. Shina, et al. (2006). "The chemokine CCL5 as a potential prognostic factor predicting disease progression in stage II breast cancer patients." *Cancer Research* **12**(15): 4474-4480.

Yagi, H., A. Soto-Gutierrez, et al. (2010). "Mesenchymal stem cells: Mechanisms of immunomodulation and homing." *Cell Transplantation* **19**(6): 667-679.

Yang, M. H., M.Z. Wu, et al. (2008). "Direct regulation of TWIST by HIF-1alpha promotes metastasis." *Nature Cell Biology* **10**(3): 295-305.

Zhang, H., M.Bosch-Marce, et al. (2008). "Mitochondrial autophagy is an HIF-1-dependent adaptive metabolic response to hypoxia." *Journal of Biological Chemistry* **283**(16): 10892-10903.

Zischek, C., H. Niess, et al. (2009). "Targeting tumor stroma using engineered mesenchymal stem cells reduces the growth of pancreatic carcinoma." *Annals of Surgery* **250**(5): 7.

7 Acknowledgments

Many people have contributed in one way or other to the completion of this thesis. First and foremost, I want to thank my supervisor Prof. Dr. Peter J. Nelson for providing me with this opportunity, guiding me through the project and keeping up my spirit. I consider myself very fortunate to have found not only a supervisor but also a mentor who has taught me lessons in scientific enthusiasm and resilience.

I also want to thank PD Dr. Dr. med. Irene Teichert-von Luettichau for bringing me onto this project and for being a constant source of advice throughout my career.

I also want to thank the reviewers of this thesis for their time and effort.

Many collaborators of the Nelson laboratory have contributed to the success of this thesis. I want to thank Andrea Müller, Kerstin Knoop and Christine Spitzweg for the close cooperation, Josef Mysliwietz of the Helmholtz-Zentrum Großhadern for sorting the cells, as well as Prof. Grässer and Prof. Ogris for providing DNA plasmids essential to this project.

This thesis could never have been finished without the help of a great team of colleagues within the Nelson lab. Alexandra Wechselberger, Anke Fischer, Monika Hofstetter, Sylke Rohrer and Niklas Münchmeier have welcomed me into their team and shared their endless wisdom, humour and kindness with me. Carsten Jäckel and Nicole Salb have become valuable co-researchers over the years.

Outside the lab, my closest friends Regina, Barbara, Miriam, Franzi and Niklas have helped me take on this challenge, listened to me complaining about it and took my mind off things when necessary. Klement, thank you for helping me to find new motivation and strength.

Last but not least, I want to thank my parents Winfried and Cornelia as well as my brother Markus for always encouraging me to leave my comfort zone, supporting me when it gets tough and celebrating with me when I reach my goals.

Eidesstattliche Versicherung

Ich erkläre hiermit an Eides statt, dass ich die vorliegende Dissertation mit dem Thema „Engineered Mesenchymal Stem Cells In Tumor Therapy: A Comparison Of Three Targeting Strategies“ selbstständig verfasst, mich außer der angegebenen keiner weiteren Hilfmittel bedient und alle Erkenntnisse, die aus dem Schrifttum ganz oder annähernd übernommen sind, als solche kenntlich gemacht und nach ihrer Herkunft unter Bezeichnung der Fundstelle einzeln nachgewiesen habe.

Ich erkläre des Weiteren, dass die hier vorgelegte Dissertation nicht in gleicher oder ähnlicher Form bei einer anderen Stelle zur Erlangung eines akademischen Grades eingereicht wurde.

München, den 26.04.2018

_____

Hagenhoff, Anna Maria